Investigations on DNA methylation by Dnmt2

and

impact of tRNA modifications on TLR7 stimulation

Dissertation

zur Erlangung des Grades

„Doktor der Naturwissenschaften"

im Promotionsfach Pharmazie

am Fachbereich Chemie, Pharmazie und Geowissenschaften
der Johannes Gutenberg-Universität Mainz
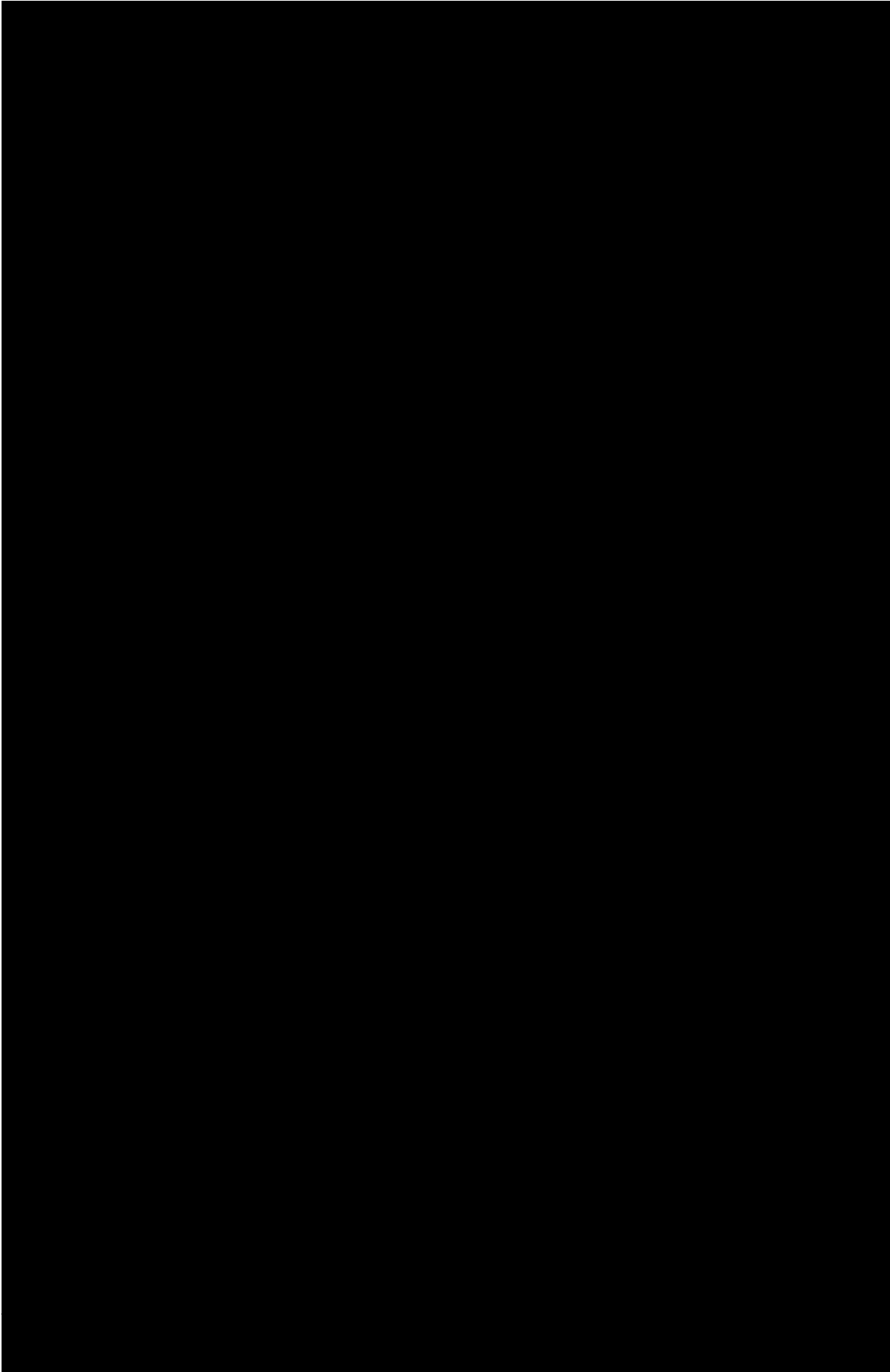
vorgelegt von

Steffen Kaiser

geb. in Mainz

Mainz, November 2015

Dekan: ██████████████████

1. Berichterstatter: ████████████████

2. Berichterstatter: ███████████████

Tag der mündlichen Prüfung: ████████

Abstract

The incorporation of modified nucleotides into ribonucleic acids (RNAs) is important for their structure and proper function. These modifications are inserted by distinct catalytic macromolecules one of them being Dnmt2. It methylates the Cytidine (C) at position 38 in tRNA to 5-methylcytidine (m^5C). Dnmt2 has been a paradigm in this respect, because all of its nearest neighbors in evolution are DNA-cytosine C5-methyltransferases and methylate DNA, while its (own) DNA methyltransferase activity is the subject of controversial reports with rates varying between zero and very weak. This work determines whether the biochemical potential for DNA methylation is present in the enzyme. It was discovered that DNA fragments, when presented as covalent RNA:DNA hybrids in the structural context of a tRNA, can be more efficiently methylated than the corresponding natural tRNA substrate. Additional minor deviations from a native tRNA structure that were seen to be tolerated by Dnmt2 were used for a stepwise development of a composite system of guide RNAs that enable the enzyme to perform cytidine methylation on single stranded DNA *in vitro*. Furthermore, a proof-of-principle is presented for utilizing the *S*-adenosyl methionine-analog cofactor SeAdoYn with Dnmt2 to search for new possible substrates in a SELEX-like approach.

In innate immunity, nucleic acids can function as pathogen associated molecular patterns (PAMPs) recognized by pattern recognition receptors (PRRs). The modification pattern of RNA is the discriminating factor for toll-like receptor 7 (TLR7) to distinguish between self and non-self RNA of invading pathogens. It was found that a 2'-O-methylated guanosine (Gm) at position18, naturally occurring at this position in some tRNAs, antagonizes recognition by TLR7. In the second part of this work it is pointed out, that recognition extends to the next downstream nucleotide and the effectively recognized molecular detail is actually a methylated dinucleotide. The immune silencing effect of the ribose methylation is most pronounced if the dinucleotide motif is composed of purin nucleobases whereas pyrimidines diminish the effect. Similar results were obtained when the Gm modification was transposed into other tRNA domains. Point mutations abolishing base pairings important for a proper tertiary structure had no effect on the immune stimulatory potential of a Gm modified tRNA. Taken together these results suggest a processive type of RNA inspection by TLR7.

Zusammenfassung

Der Einbau modifizierter Nukleotide in Ribonukleinsäuren (RNAs) ist wichtig für deren richtige Struktur und Funktion. Diese Modifikationen werden von bestimmten katalytisch aktiven Makromolekülen eingebaut. Ein solches Enzym ist Dnmt2. Von ihm wird das Cytidin (C) an Position 38 in tRNA zu 5-Methylcytidin (m^5C) methyliert. Dnmt2 war diesbezüglich eine Besonderheit, da alle näheren evolutionären Verwandten DNA-Cytosin C5-Methyltransferasen sind und dementsprechend DNA methylieren. Die DNA-Methyltransferaseaktivität von Dnmt2 ist dagegen Thema kontroverser Berichte und schwankt zwischen sehr gering und nicht vorhanden. In dieser Arbeit wird untersucht, ob Dnmt2 biochemisch dazu in der Lage ist DNA zu methylieren. Die Ergebnisse zeigen, dass DNA, wenn sie kovalent in RNA:DNA Hybriden im strukturellen Kontext einer tRNA vorliegt, von Dnmt2 methyliert werden kann. Außerdem wurden weitere kleinere Abweichungen von einer nativen tRNA entdeckt, die von Dnmt2 toleriert werden und dazu genutzt um Schritt für Schritt ein System zu entwickeln, um mit Hilfe von Guide RNAs ein eigenständiges DNA Molekül mit Dnmt2 *in vitro* zu methylieren. Desweiteren wird gezeigt, wie der *S*-Adenosylmethionin analoge Cofaktor SeAdoYn benutzt werden könnte um in einem SELEX-artigen Ansatz neue Dnmt2 Substrate zu entdecken.

Im angeborenen Immunsystem können Nukleinsäuren als pathogen-assoziierte molekulare Muster (PAMPs) fungieren, die von so genannten Pattern Recognition Rezeptoren (PRRs) erkannt werden. TLR7 nutzt das Modifizierungsmuster einer RNA um zwischen körpereigenen RNAs und den RNAs von pathogenen Organismen zu unterscheiden. Ein 2'-O-methyliertes Guanosin (Gm), das in einigen tRNAs an Position 18 vorkommt, sorgt dafür, dass die tRNA zu einem TLR7 Antagonisten wird. Im zweiten Teil dieser Arbeit wird gezeigt, dass das auf das 2'-O-methylierte folgende Nukleotid auch für die Erkennung wichtig ist und das von TLR7 erkannte molekulare Detail in Wirklichkeit ein methyliertes Dinukleotid ist. Der immununterdrückende Effekt ist am stärksten ausgeprägt, wenn das Dinukleotid Motiv aus Purin Basen besteht, während für Pyrimidine der Effekt abgeschwächt bis gar nicht vorhanden ist. Die Ergebnisse behalten auch ihre Gültigkeit, wenn die Modifikation in andere tRNA Domänen transplantiert wird. Punktmutationen, die die Ausbildung der Tertiärstruktur unterbinden, hatten keinen Einfluss auf die Stärke der Immunstimulation. Die Ergebnisse sprechen daher für eine abtastende RNA Untersuchung durch TLR7.

Table of contents

List of figures

Abbreviations

bp	base pair
DC	dendritic cell
dm^{5}C	2'-deoxy-5-methylcytidine
DNA	deoxyribonucleic acid
DNase	deoxyribonuclease
Dnmt2	DNA methyltransferase 2
DOTAP	1,2-dioleoyl-3-trimethylammonium-propane
ds	double stranded
Gm	2'-O-methylguanosine
IFN	interferon
IL	interleukin
IVT	*in vitro* transcript
m^{5}C	5-methylcytidine
nt	nucleotides
PAGE	polyacrylamid gel electrophoresis
PAMP	pathogen-associated molecular pattern
pDC	plasmacytoid dendritic cell
PNK	polynucleotide kinase
PRR	pattern-recognition receptor
Q	queuosine
RgD	RNA-guided DNA methylation
RNA	ribonucleic acid
SAM	*S*-adenosyl methionine
SELEX	systematic evolution of ligands by exponential enrichment
ss	single stranded
TLC	thin-layer chromatography
TLR7	Toll-like receptor 7
TrmH	tRNA (G18) 2'-O-methyltransferase
tRNA	transfer RNA
yW	wybutosine
Ψ	pseudouridine

1 Introduction

1.1 Transfer RNA (tRNA)

Transfer RNAs (tRNAs) are the adapters in protein biosynthesis (1) linking the transcribed genomic code with the translated cellular machinery of enzymes. Different tRNA species that incorporate the same amino acid in protein biosynthesis are called isoacceptors. Each tRNA isoacceptor transports a distinct amino acid, defined by the tRNAs anticodon to the ribosome. Here, the anticodon hybridizes to the reverse complementary codon of the messenger RNA (mRNA), which ensures the right amino acid sequence of the translated protein.

The secondary structure of a tRNA (Figure 1A) is commonly described as a cloverleaf (2) with three stem and three loop regions and a variable region. In addition, the acceptor stem contains the conserved 3' single stranded N-C-C-A$_{OH}$ overhang, where the correct amino acid is attached through esterification of the free 3'-hydroxyl group of the tRNA with the carboxyl group of the amino acid. The charging of the tRNA is catalyzed by aminoacyl-tRNA-synthetases.
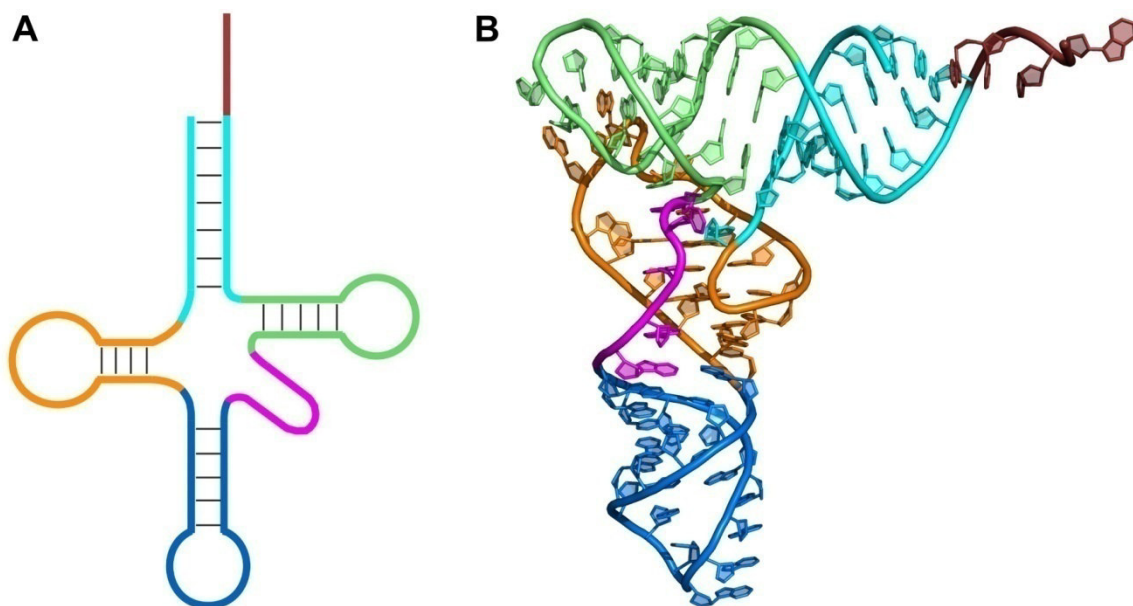
Figure 1: Secondary and tertiary structure of cytosolic tRNA. **A)** Cloverleaf. **B)** L-shaped 3D structure. The different colors highlight the acceptor stem (cyan) with the 3' overhang (ruby), the D-stem-loop (orange), the anticodon stem-loop (blue), the variable loop (magenta) and the TΨC-stem-loop (green).

However, the cloverleaf is only a simplified representation of the tRNA. In fact, the functional tertiary structure of the tRNA is more complicated since it is folded in an L-shape (Figure 1B).

In order to achieve this complicated structure, tRNAs have a large diversity of chemical modifications in their building blocks. The D-arm is rich in the modified nucleotides dihydrouridine (D), while ribothymidin (rT) and pseudouridine (Ψ) (Figure 2) are commonly found in the TΨC-arm. As these modifications are commonly found in all tRNAs, in all trees the life, they were used to name these loop regions of the tRNA. The L-shape is coined with two helical branches of similar size in perpendicular orientation to each other (3). One branch is formed by the amino acid acceptor stem stacked over the TΨC-arm and the other by a stack of the anticodon- and D-arms. In the tertiary structure the D-loop is close to the TΨC-loop. The loops are locked by interaction of G19 in the D-loop with C56 in the TΨC-loop and by interaction of G18 and Ψ55 (4).

The third arm, between the D and TΨC-arm, contains the anticodon, and is therefore called the anticodon loop. The D-, anticodon- and TΨC-arm are major pre-requisites of all tRNAs. Additionally, there is a variable region that can vary in size from four to twenty-four nucleotides.

1.2   Modified Nucleotides in tRNA

After transcription, tRNA contains only the four major ribonucleotides adenosine (A), cytidine (C), guanosine (G) and uridine (U). However, to achieve its functional L-shape, enzymes which post-transcriptionally introduce chemical modifications such as methylation, thiolation, and isomerization are needed. By now, over 150 chemically different modified nucleotides have been found in tRNA (5,6). These modifications occur at specific positions of the tRNA, like the above mentioned dihydrouridine and pseudouridine. Modified nucleotides are used to stabilize the tertiary structure of the molecule by different mechanisms. On the one hand they can stabilize the folding by unconventional base pairings or by the introduction of other small structural changes. They can also prevent base pairing and thereby avoid misfolding of the tRNA. Modifications alter the conformational preferences of a nucleotide, which has an effect on the overall thermostability of the whole tRNA (7-9). While some modifications serve a major role in structural stabilization, modifications

near or within the anticodon are utilized for modulating the anticodon-codon binding. In eukaryotes, for example Wybutosine (yW) (Figure 2) and its derivatives, have only been found directly adjacent to the anticodon (position 37) in tRNA^{Phe} (3).

While yW has only been observed in eukaryotes, archaeosine (G+) only in archaea and 5-methoxyuridine only in bacteria (Figure 2), other modifications like pseudouridine, inosine and 5-methylcytidine can be found in all three domains of life. As some modifications are unique to certain domains of life, this might also be a mechanism the innate immune system uses to distinguish between self and non-self RNA.

In a cell, tRNA is the highest modified subtype of RNA with the modified nucleotides being at well defined position in its sequence. In addition, tRNA occurs non-protein-bound in the cytoplasm and is therefore free to interact with other macromolecules *e.g.* a given receptor. These features make it a promising candidate to investigate the impact of modifications on the immunostimulatory potential of RNAs.
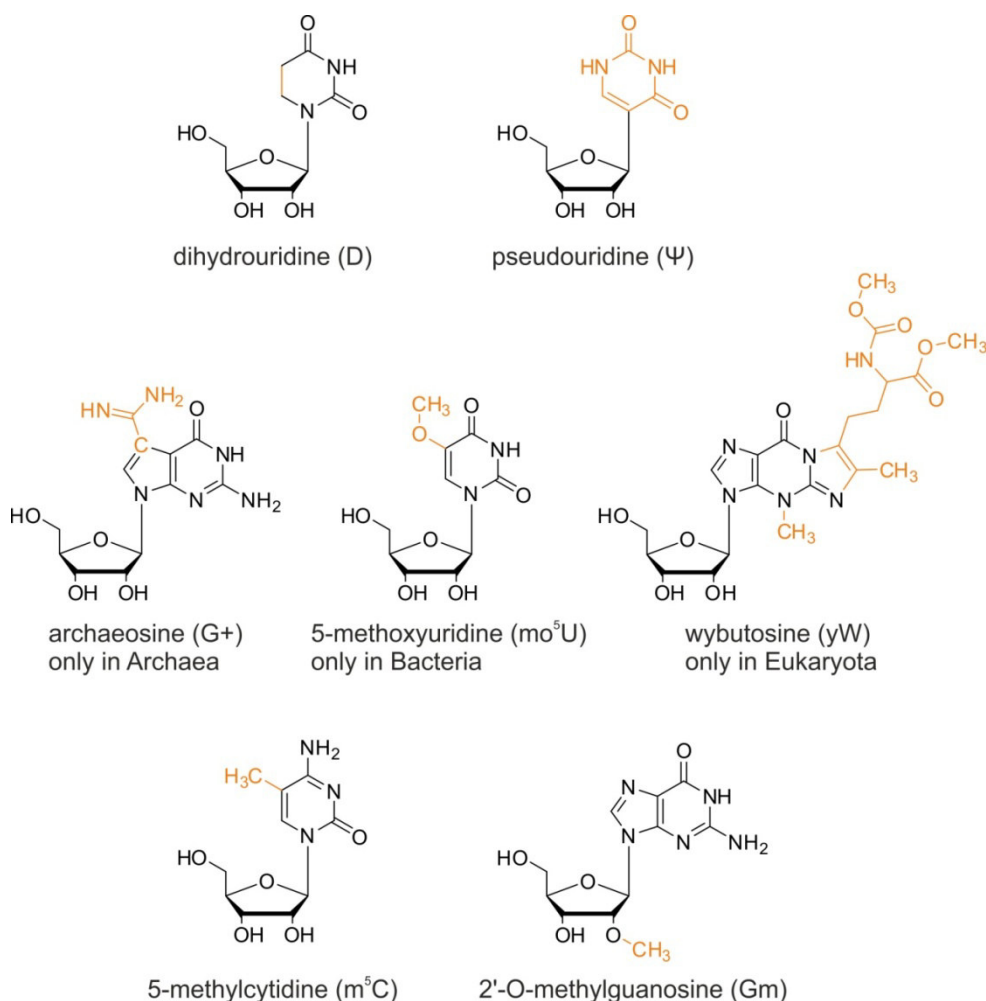
Figure 2: Examples of modified nucleosides found in tRNA.

1.3 Examples of RNA Modifying Enzymes

1.3.1 Dnmt2

5-methylcytidine (m^5C) is one of the two dozen RNA modifications that are conserved in all domains of life. 5-methylcytosine is furthermore found not only in RNA, but also in DNA of eukaryotes and bacteria. It is biosynthetically introduced by methyltranserases which transfer a methylgroup from *S*-adenosyl methionine (Adomet or SAM) to position 5 of cytosine. DNA methyltransferase 2 (Dnmt2) was first identified due to its strong sequence conservation of catalytic DNA methyltransferase motifs (Figure 3), yet the N-terminal regulatory domain usually found in other eukaryotic DNA methyltransferases is absent in Dnmt2 (10). Dnmt2 is widely conserved in plants, fungi and animals (Figure 4) suggesting an important

function of this enzyme (11). However, no role for Dnmt2 in *de novo* or maintenance methylation of DNA could be found (12).
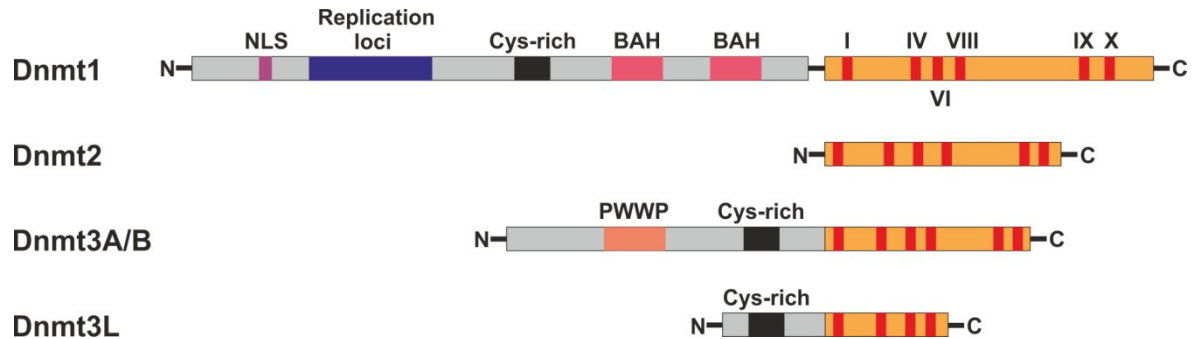
Figure 3: Scheme of mouse DNA m^{5}C methyltransferases. The six highly conserved motifs of the C-terminal methyltransferase domain (orange) are highlighted in red. Figure adapted from (11)

Until 2007 all Dnmt2 knockout organisms investigated, lacked an obvious phenotype and were viable and fertile (13) so that the biological function remained unknown. Additionally, the DNA methylation activity of Dnmt2 is only very weak at best and still a controversial subject (14,15) with sometimes opposing results, *e.g.* concerning the methylation of *Invader4* retroelements in *Drosophila melanogaster* (16,17). A major contribution to understand this enzyme's function was the discovery of Dnmt2's tRNA methylation activity on tRNA[Asp] in mouse, *Drosophila melanogaster* and *Arabidopsis thaliana* as its major substrate. Here, Dnmt2 methylates the cytidine at position 38 in the anticodon-loop (13). Furthermore, in zebrafish, a phenotype could be found for the first time after knockdown of Dnmt2, leading to reduced RNA methylation in the cytoplasm and significant differentiation defects in brain, liver and retina tissue (18).
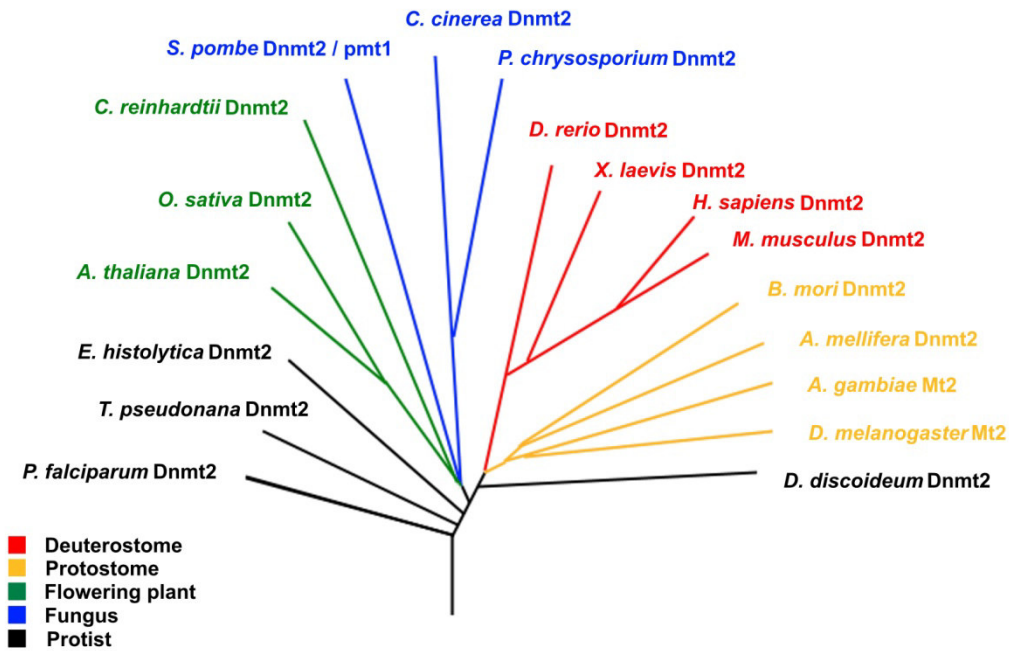
Figure 4: Occurrence of Dnmt2 in plants, fungi and animals. Figure adapted from (11).

An interesting characteristic of Dnmt2 is that it utilizes a DNA m^{5}C methyltransferase-like mechanism to methylate RNA (Figure 5) (19). A catalytic cysteine's S$^-$-group, located in the conserved motif IV attacks the C5 of the cytosine in a Michael addition reaction. This nucleophilic attack is facilitated by protonation of N3 by a glutamic acid residue in the conserved motif VI. The glutamate also stabilizes the covalent intermediate. In a next step, the now activated C5 position of the cytosine executes a nucleophilic attack on the methyl group of the cofactor *S*-adenosyl methionine.
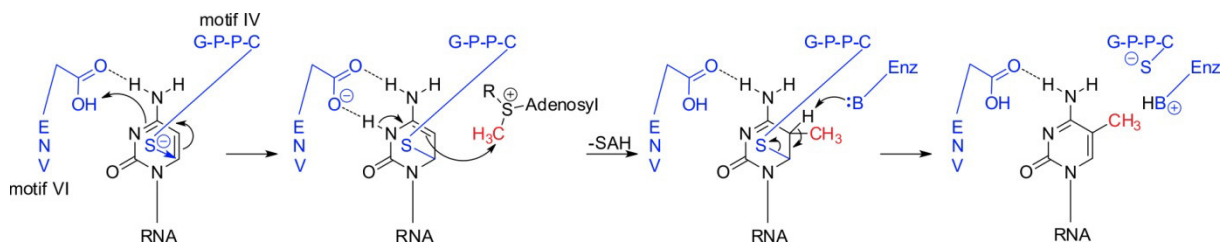
Figure 5: Scheme of the DNA m^{5}C methyltransferase-like mechanism utilized by Dnmt2 to methylate RNA. Figure adapted from (20).

In the last reaction step C5 is deprotonated by a basic residue of the enzyme, the cysteinyl group is eliminated and the nucleobase re-aromatized. RNA m^{5}C methylatransferases on the other hand, utilize a cysteine located in motif VI for the

attack on the cytidine and an aspartic acid from motif IV for stabilization of the intermediate (21).

To this day further substrates beside tRNA[Asp] have been identified, including tRNA[Val] and tRNA[Gly] in mouse (22), tRNA[Glu] in *Schizosaccharomyces pombe* (23), tRNA[Gly] and tRNA[Glu] in *Dictyostelium discoideum* (24), tRNA[Val], and tRNA[Gly] in *Drosophila melanogaster* (25,26), tRNA[Glu] in *Geobacter sulfurreducens* (27) and tRNA[Gly] in *Arabidopsis thaliana* (28). It could be shown that methylation by Dnmt2 protects tRNAs against stress-induced cleavage (26). In mice, although single-knockout mutants had no detectable effect, Dnmt2 and NSun2 double-knockout mice had a reduced protein synthesis, an underdevelopment phenotype and higher lethality, indicating Dnmt2's importance for tRNA stability, translational fidelity and cellular differentiation (22). Dnmt2 is most likely involved in other additional processes that remain unknown at the moment, especially concerning methylation of a specific DNA target. Until now, there has been no report of DNA methylation by Dnmt2 *in vitro*.

1.3.2 TrmH

tRNA (G18) 2'-O-methyltransferase (TrmH) catalyzes the reaction of a conserved guanosine at position 18 to 2'-O-methylguanosine in bacterial tRNAs (29). The cofactor *S*-adenosyl methionine is utilized as methyl donor. Gm18, located in the D-loop, interacts with a conserved pseudouridine at position 55 in the T-loop to stabilize the tertiary L-shaped structure. Organisms with TrmH include *E. coli* (29), *Thermus thermophilus* (30) and *Aquifex aeolicus* (31) but TrmH homologs are also found in eukaryotic organisms, for example Trm3p in *Saccharomyces cerevisiae* (32). TrmH enzymes are subdivided into two types. Type I TrmH, found *e.g.* in *Thermus thermophilus,* can modify all tRNA species, whereas Type II TrmH can only modify a certain subset of tRNA species. *E. coli*'s type II TrmH catalyzes Gm18 formation in 14 out of the 47 tRNA species present (33). It was shown, that Gm18 in *E. coli* tRNA[Tyr] is responsible and sufficient to antagonize recognition byTLR7 (34).

1.4 The Innate Immune system

The innate immune system is the first line of defense in host protection against invading microbial pathogens (35) and is mediated by phagocytes including macrophages and dendritic cells (DCs). It is evolutionarily conserved and recognizes invading microorganisms through germline-encoded pattern-recognition receptors (PRRS) (36). PRRs detect conserved microbial components called pathogen-associated molecular patterns (PAMPs). PAMPS are directed against essential components of the microorganism, which are needed for the pathogens survival. Therefore, they are difficult for the microorganism to alter (35) and are found in a wide variety of pathogens including bacteria, parasites, fungi, protozoa and viruses (37-40).

The immune system of vertebrates comprises a second branch of immunity, the acquired immunity. It is activated by the innate immune system and specialized immune cells recognize non-self structures. These specialized cells, namely B and T lymphocytes, utilize antigen receptors, such as immuno-globulines and T cell receptors (39). Acquired immunity shows a high specificity, developed by clonal selection from a vast repertoire of lymphocytes bearing antigen-specific receptors that are generated by gene rearrangement (35) and unlike the innate immunity, acquired immunity creates an immunological memory.

In contrast, the innate immune system has a limited number of germline-encoded PRRs that are non-clonal, expressed on all cells of a given type and independent of immunological memory (35).

1.4.1 Toll-like Receptors (TLRs)

The Toll receptor, after which the TLR family was named, was first identified as a gene product essential for dorsal-ventral patterning in *Drosophila* embryos after binding of its ligand Spätzle (41-43). Afterwards it was discovered, that in adult *Drosophila* the Toll/Dorsal signaling pathway is important for anti-fungal response (44) and one year later a mammalian homolog of Toll was found, now known as TLR4, which was shown to induce expression of genes involved in inflammatory response and to activate adaptive immunity (45).
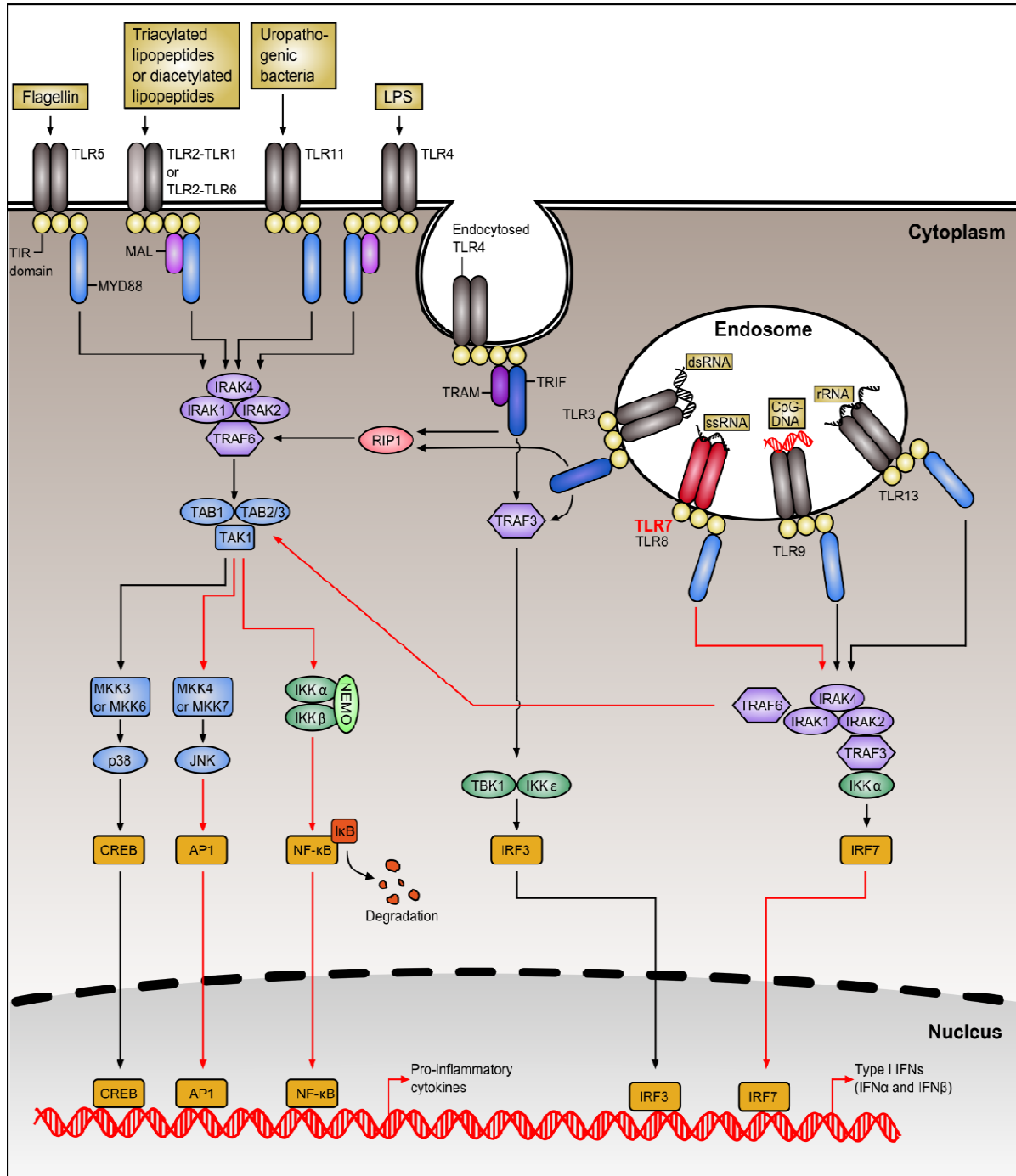
Figure 6: Toll-like receptors, their ligands and signaling pathways. TLR7 and its possible signaling cascades are highlighted in red. Upon ligand-induced dimerization (homo- or heterodimerization depending on the TLR) the TIR domains of the TLRs interact with the TIR domain of the adapter proteins MYD88 (and MAL) or TRIF (and TRAM). Further downstream signaling is mediated by IRAKs (IL-1R-associated kinases) and TRAFs (TNF receptor-associated factors) as well as TAK1 (transforming growth factor-β-activated kinase-1) and TABs (TAK1 binding proteins). TAK1 activates mitogen-activated protein kinases (MAPKs) that subsequently phosphorylate JNK (c-Jun N-terminal kinase) and p38 to activate the transcription factors AP-1 (Activator Protein 1) and/or CREB (cAMP responsive element-binding protein). Another important transcription factor activated by TAK1 is NF-κB (nuclear factor kappa-light-chain-enhancer of activated B cells). TAK1 activates the IκB kinase (IKK) complex (consisting of the catalytic components IKKα and IKKβ and the regulatory component NEMO) that phophorylates IκB (NF-κB inhibitor). Phosphorylated IκB is polyubiquitinated and degraded allowing NF-κB to move into the nucleus. Those transcription factors lead to the induction of pro-inflammatory cytokines. Interferon regulatory factors (IRFs) activated by IRAKs and TRAFs downstream of the endosomal-localized TLRs 3, 7, 9 and 13 or endocytosed TLR4, lead to the transcription of type 1 interferon genes. Figure adapted from (46).

By now the TLR family counts thirteen members, each one recognizing specific PAMPs derived from various pathogens like bacteria, fungi, protozoa and viruses. TLR1 – TLR10 are present in humans and mice, whereas TLR11, TLR12 and TLR13 have been lost from the human genome (47). Figure 6 gives an overview on TLRs and their substrates.

TLR2 is able to sense bacterial lipopeptides, peptidoglycan (PG) and lipoteichoic acid (LTA) from Gram-positive bacterial cell walls (35). Furthermore, TLR2 forms heterodimers with TLR1 or TLR6 (48). In a heterodimer together with TLR1 it recognizes triacylatedlipopeptides (49,50) and diacylatedlipopeptides in a TLR2-TLR6 heterodimer (51,52). TLR4 recognizes and binds bacterial lipopolysaccharide (LPS) (53-55) in cooperation with myeloid differentiation factor 2 (MD-2) (56-59). The flagellin protein, a component of bacterial flagella is recognized by TLR5 (60-63). Mouse TLR10 is not functional because of retrovirus insertion (47) and the ligand of human TLR10 is not known, yet. However, it could be shown, that human TLR10 is expressed by B cells and plasmacytoid dendritic cells and is able to homodimerize as well as heterodimerize with TLR1 or TLR2 (64). TLR11 recognizes components of uropathogenic bacteria (65). Additionally it can recognize the profilin-like molecule from *Toxoplasma gondii* in cooperation with TLR12 (66-68). Whereas TLRs 1, 2, 4, 5, 6, 11 and 12 are expressed on the cell surface, the ones recognizing nucleic acids, TLRs 3, 7, 8, 9 and 13, are located almost exclusively in intracellular compartments like endosomes (Figure 6) requiring the internalization of their ligands before signaling is possible (35). Double-stranded RNA (dsRNA), mainly derived from viruses, activates TLR3 (69-72). TLRs 7 and 8 on the other hand recognize single-stranded RNA (ssRNA) (73-78). TLR9 recognizes unmethylated CpG DNA (79-82) and mouse TLR13 is able to recognize bacterial 23S ribosomal RNA (83-85).

The TLRs are expressed on immune cells such as macrophages, DCs, B cells and neutrophils but also on non-immune cells like fibroblast cells, epithelial cells and keratinocytes (86).

TLRs are type I integral membrane glycoproteins. They consist of N-terminal extracellular leucine-rich repeats (LRRs), a membrane-spanning domain and a C-terminal cytoplasmic domain, which is homologous to that of the interleukin 1 receptor and therefore termed the Toll/IL-1R homology (TIR) domain (87,88). The LRR domains contain 19 to 25 tandem LRR motifs. Each LRR motif has a length of

24 to 29 amino acids comprising the motif XLXXLXLXX as well as other conserved amino acid residues (35).

1.4.2 Toll-like Receptor 7

TLR7 is expressed in human plasmacytoid dendritic cells (pDCs) along with TLR9 (89). As other TLRs are absent in pDCs, they do not respond to bacterial components such as LPS and peptidoglycan but only to nucleic acids. pDCs secrete large amounts of type I interferones, especially IFN-α, during virus infection (90,91) and are therefore also known as interferon-producing cells.

TLR7 is encoded by a gene located on the X chromosome which has a high homology to the TLR8 gene located on the same chromosome. It was discovered first, that TLR7 can recognize synthetic antiviral imidazoquinoline compounds (R848 (92,93), Imiquimod (92) as well as other synthetic guanine nucleoside analog compounds like loxoribine (94,95) which has antiviral and antitumor activities (Figure 7). They have structural similarities to guanosine nucleosides which led to the prediction, that TLR7 recognizes nucleic acid-like structures. For R848 and short RNAs it was shown that imidazoquinoline and RNA oligonucleotide sensing by TLR7 shares overall structure function principles (96). However, despite overlapping sensing areas, the recognition of each type of ligand seems to involve several unique residues not required for detection of the other ligand. It is known by now, that TLR7 actually recognizes guanosine- uridine-rich single-stranded RNA from viruses such as the human immunodeficiency virus, the vesicular stromatitis virus or the influenza virus (73-75). Additionally, nonviral synthetic poly-uridine RNA and some small interfering RNAs (siRNAs) are also recognized by TLR7 and lead to an activation of pDCs (73,76).

Upon binding of its single-stranded RNA substrate, TLR7 initiates a well studied response pathway, which is highlighted with red arrows in Figure 6. Recognition of PAMPs by TLR7 leads to a homodimerization of the receptor, thereby inducing conformational changes required for the recruitment of the adapter molecule MyD88 (myeloid differentiation primary response gene 88) to the TIR domain of TLR7. MyD88 contains a C-terminal TIR domain and an N-terminal death domain (39). It associates with the TLR through its TIR domain and recruits IRAK-4 (IL-1R-associated kinase 4) and IRAK-1 through homophilic interaction of the death

domains (35,39,97). IRAK-4 is activated and induces the phosphorylation and activation of IRAK-1 (98).

Imiquimod R848 (Resiquimod) Gardiquimod

Loxoribine Guanosine
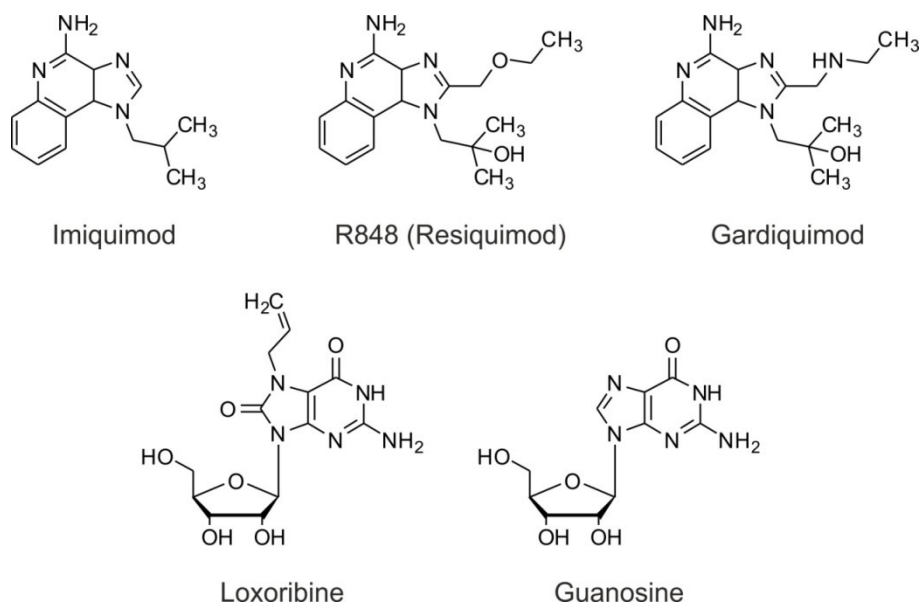
Figure 7: Structural formula of synthetic compounds that act as TLR7 agonists in comparison with guanosine.

Then TRAF6 (tumor-necrosis-factor-receptor-associated factor 6), a RING domain E3 ubiquitin ligase, associates with the phosphorylated IRAK-1 (99,100). TRAF6 promotes together with UBC13 (ubiquitin-conjugating enzyme 13) and UEV1A (ubiquitin-conjugating enzyme E2 variant 1) the Lys63-linked polyubiquitination of itself and NEMO (NF-κB essential modifier/IKKγ) (99,101,102). Polyubiquitinated TRAF6 recruits a protein kinase complex (101) containing TAK1 (transforming growth factor-β-activated kinase-1), a MAPKKK (103), and the TAK1 binding proteins (TABs) TAB1 and TAB2 or TAB3 (104-107) which leads to the activation of two distinct pathways.

On one hand, TAK1 activates the mitogen-activated protein kinase (MAPK) pathway by phophorylating MKK3 and MKK6, which subsequently phosphorylate c-Jun N-terminal kinases and p38 to activate the transcription factor AP-1 (ATF2-c-Jun) (97). On the other hand, TAK1 activates the IKK (IκB kinase) complex, involving two catalytic components IKKα and IKKβ and a regulatory component NEMO, by phosphorylation of IKKβ (108). The IKK complex leads to the phophorylation of specific serine residues of IκB (NF-κB inhibitor). Phosphorylated IκB is polyubiquinated and degraded by the 26S proteasome, allowing NF-κB (nuclear

factor kappa-light-chain-enhancer of activated B cells) to move into the nucleus (109). Both pathways lead to the induction of inflammatory cytokines.

To cause type I interferon induction, in particular that of IFN-α, a complex comprised of MyD88, IRAK-4, IRAK-1, TRAF6 and IRF7 (interferon regulatory factor 7) is formed and recruited to the TLR (110,111). IRF7 is phosphorylated in the C-terminal region by IRAK-1 (112) and IKKα (113). TRAF6 mediated ubiquitination is also required for IRF7 activation (111). Another involved molecule is TRAF3. It binds to a MyD88-IRAK1-IRF7 complex and pDCs from TRAF3-deficent mice have defects in IFN-α production (114,115). Phosphorylated IRF7 dimerizes and is translocated into the nucleus where it regulates the expression of type I interferons like IFN-α and IFN-β.

However, the decisive criteria RNA needs to have to activate TLR7 signaling are not yet known. One important strategy to distinguish between self and non-self RNA, besides the composition of the sequence, is the incorporation of modified nucleotides. As the number and complexity of nucleotide modifications correlates with the evolutionary level of the organism, eukaryotic RNA is in general more modified than bacterial or viral RNA. Thereby, it is a possibility to differentiate between self or non-self origin (116,117) by modification status and complexity. As a matter of fact it has been shown that the incorporation of modified nucleosides such as 5-methylcytidine (m^5C), N6-methyladenosine (m^6A), 5-methyluridine (m^5U), 2-thiouridine (s^2U) or pseudouridine (Ψ) into *in vitro* transcripts led to an absence of TLR signaling (117). The incorporation of 2'-O-methylated nucleotides into siRNA also led to suppression of immunostimulation (118-121). However, the exact identity, location and sequence context of TLR7 silencing/activating modifications remained unstudied.

2 Objectives of this work

Modifications are important for structure and function of RNAs. By now more than 150 naturally occurring RNA modifications have been discovered. Understanding the characteristics and heritage of the enzyme inserting a particular modification into RNA helps understanding the function of the modification itself. Dnmt2, showing a strong sequence homology to bacterial and eukaryotic DNA m^{5}C methyltransferases, efficiently methylates tRNA at C38. However, its DNA methyltransferase activity is very weak at best and neither could a distinct DNA substrate be identified nor was DNA methylation detectable *in vitro*. Dnmt2 is an interesting example that shows how comparative genomics can be misleading. In this work it was investigated if Dnmt2 is biochemically able to methylate DNA and to which extend alterations from the structure of its canonical substrate, a tRNA, are tolerated by the enzyme. In an additional set of experiments if was explored if synthetic SAM-analog molecules could be used as cofactor of Dnmt2 to label tRNA and search for further Dnmt2 substrate.

While the function of most nucleic acid modifications remains unclear, their effect on host-pathogen interactions is similarly important. The incorporation of modified nucleotides into RNA is a significant feature which enables the immune system of the host organism to distinguish between self RNA and non-self RNA of invading pathogens. As tRNA is the highest modified subtype of RNA and the modifications are also at specific positions, it is a good choice for investigating TLR7 mediated immune response and getting insights how exactly RNA is recognized and bound to the receptor. In the second part of this work I present a systematic approach to identify TLR7 modulating tRNA modifications, studies to assess the effect of their location and furthermore outline the importance of their sequence context.

3 Results

3.1 DNA methylation by DNA methyltranferase 2 (Dnmt2)

3.1.1 General procedure to assess Dnmt2 activity on DNA containing substrates

The main substrate of Dnmt2 is tRNA^{Asp}, whereas linear double-stranded DNA is a poor substrate at best. To see whether Dnmt2 has DNA methylation activity in addition to tRNA, different tRNA hybrids were synthesized by splinted ligation, substituting a stretch of 1 up to 17 ribonucleotides with deoxynucleotides. Therefore two (synthetic) RNA or RNA:DNA-hybrid fragments, corresponding in sequence to mouse/human tRNA^{Asp}, were annealed onto a reverse-complementary 52 nt-long DNA splint and ligated with T4 DNA ligase (Figure 8). After the ligation reaction the splint was digested with DNase I. In case of the RNA:DNA constructs containing stretches of more than three deoxynucleotides the DNase digestion was omitted, to avoid RNA:DNA construct digestion. Since the DNA splint and the full-length construct have a size difference of 23 nts, the ligation product was purified by denaturing PAGE. The qualification of those hybrid constructs as substrates for Dnmt2 was assessed in a tritium incorporation assay with ^{3}H-SAM.
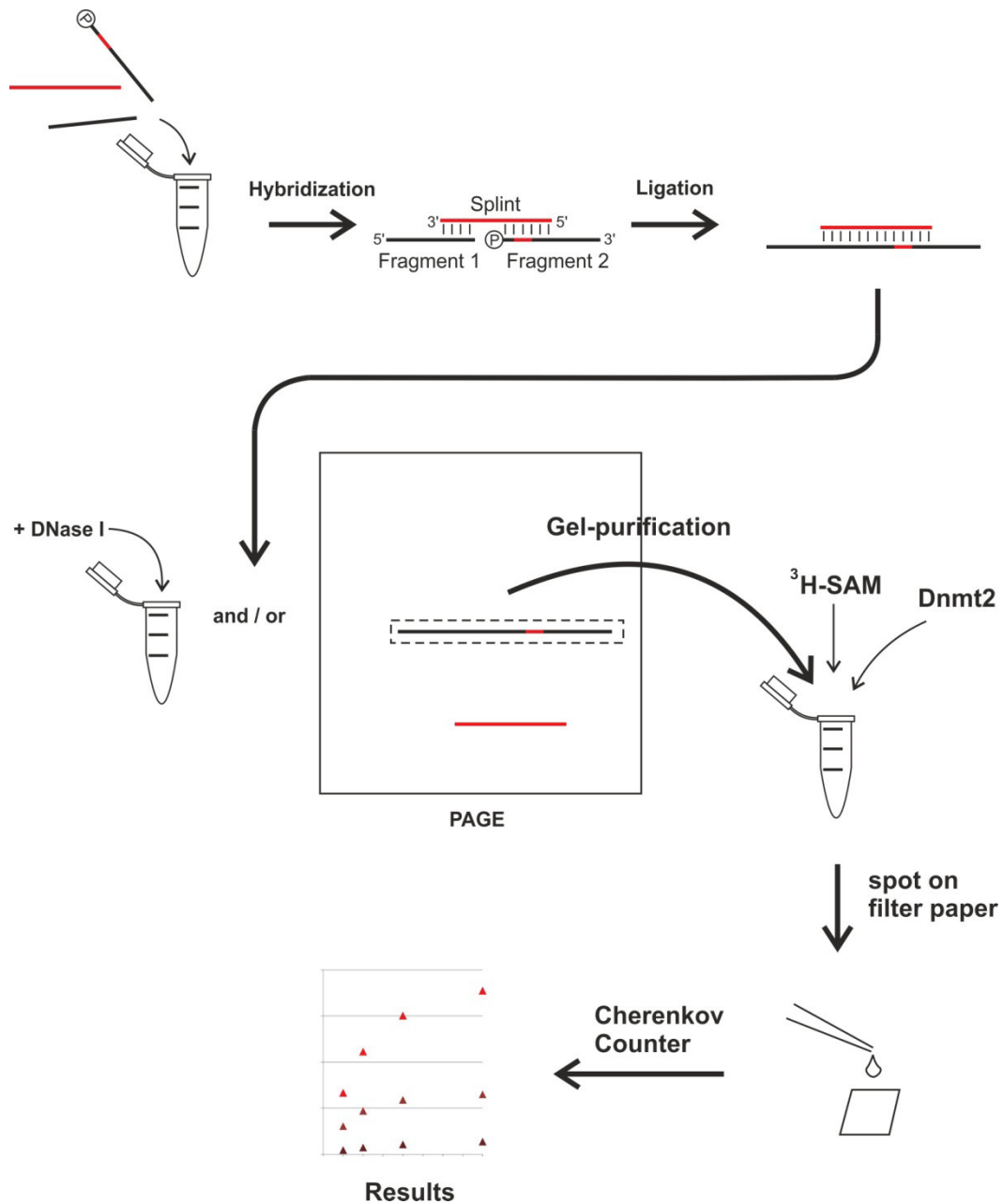
Figure 8: Schematic workflow to assess methylation activity of Dnmt2. Two synthetic RNA or RNA:DNA-hybrid fragments, corresponding in sequence to mouse/human tRNA[Asp], are annealed onto a reverse-complementary 52 nt-long DNA splint and ligated with T4 DNA ligase (requiring a free 3' OH and a 5' phosphate at the ligation site). The ligation product is purified by denaturing PAGE after digestion of the DNA splint by DNase I. If the hybrid RNA:DNA construct contains a stretch of more than three deoxynucleotides the DNase I digestion is omitted. The purified hybrid tRNA is tested in a tritium incorporation assay with Dnmt2 and ^{3}H-SAM. During the reaction, aliquots are taken and spotted on small filter papers. Finally the aliquots are analyzed by Cherenkov counting. DNA is represented in red, RNA in black.

3.1.2 Introduction of a DNA nucleotide at the target site of Dnmt2

In native tRNA^{Asp} the cytidine at position 38 is methylated by Dnmt2 yielding rm^{5}C. Therefore, in the first hybrid construct to be tested, only the single target nucleotide C38 was substituted with a dC38 and compared to the natural all-ribo tRNA^{Asp} (Figure 9).

As the main substrate of Dnmt2, the all-ribo tRNA^{Asp} showed a robust methylation. Surprisingly, the tRNA$^{Asp}_{dC38}$ was an even better substrate than the natural all-ribo tRNA^{Asp}. A hybrid containing dm^{5}C at position 38 was used as a negative control and no methyl group acceptor properties could be found for this construct in the tritium incorporation assay.
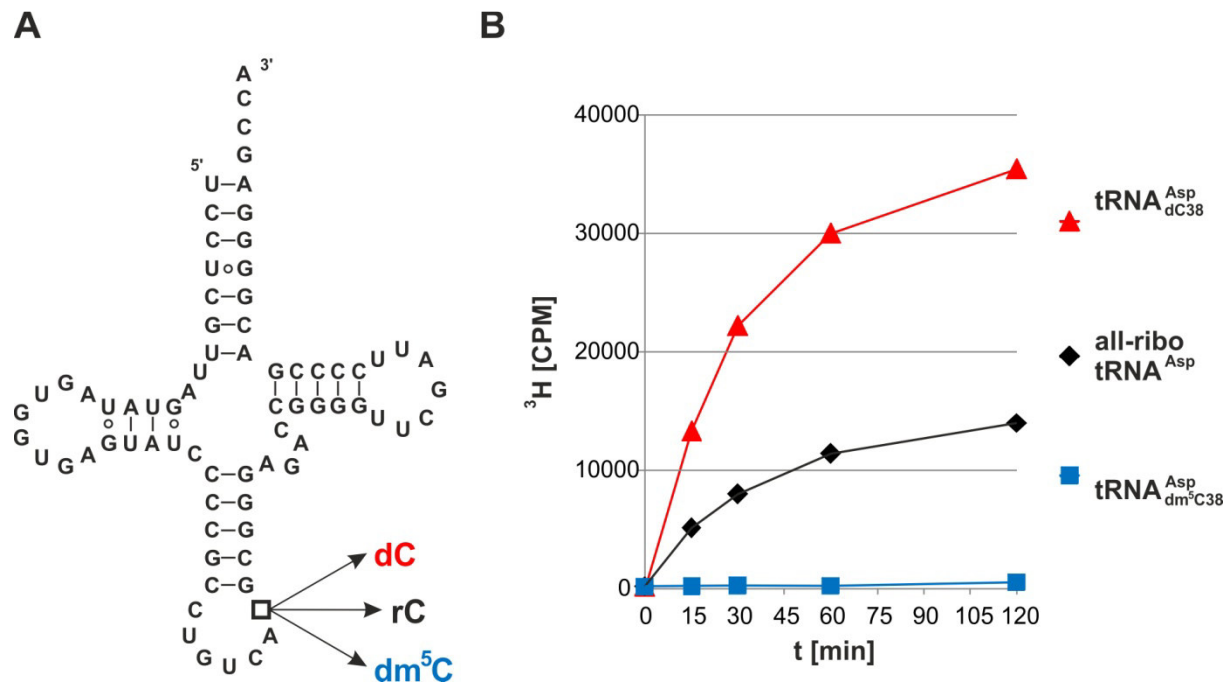
Figure 9: Dnmt2 methylates a tRNA containing a deoxycytidine at position 38. **A)** Cloverleaf structure of unmodified human cytosolic tRNA^{Asp}. Position 38 has been engineered to contain either rC, dC, or dm^{5}C. **B)** *In vitro* methylation measured by tritium incorporation from ^{3}H-SAM. One out of three experiments is shown. Average values and standard deviations are given in Figure 13.

To validate those results and confirm the structure of the methylated nucleotide, the experiment was repeated with non-radioactive SAM and purified constructs were analyzed by LC-MS/MS (Figure 10).
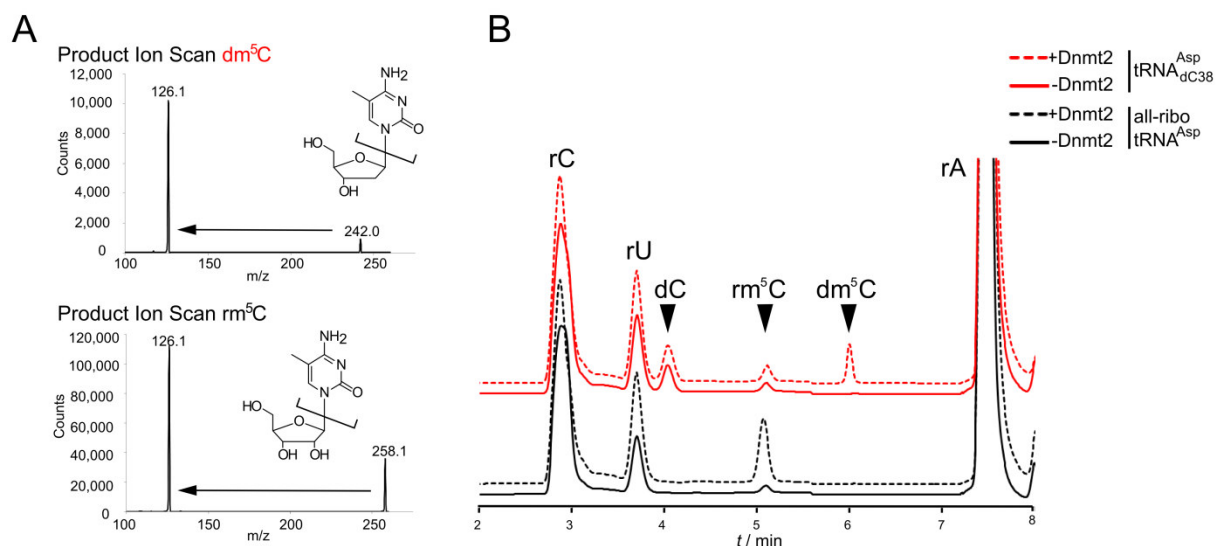
Figure 10: LC-MS/MS analysis of Dnmt2 methylating tRNA containing a deoxycytidine at position 38. **A)** Fragmentation patterns and mass transitions used for detection of rm5C and dm5C by LC-MS/MS. **B)** LC-MS/MS analysis of all-ribo tRNA^{Asp} and hybrid tRNA$^{Asp}_{dC38}$ before and after *in vitro* methylation by human Dnmt2.

Using fragmentation patterns from synthetic rm5C and dm5C, a multiple reaction monitoring (MRM) method with a limit of detection in the single digit femtomol range was established. This method allowed direct distinction between RNA and DNA methylation.

Both tRNAs, the all-ribo and the hybrid dC38, contained trace amounts of rm5C, that have already been present in the synthetic oligonucleotides that were used for ligation of the full length substrates (122), but a strong increase of rm5C in the all-ribo substrate is clearly detectable after incubation with Dnmt2. While no methylated deoxycytidine was present in the substrates before the reaction, analysis of material after the reaction revealed the presence of a new peak in the hybrid tRNA$^{Asp}_{dC38}$ that corresponds to dm5C in both retention time and fragmentation pattern (Figure 10B).

These results clearly show methylation of dC38, and prove that Dnmt2 can accept and turn over deoxynucleotides in its active site.

3.1.3   Reaction speed of all-ribo tRNA^{Asp} compared with tRNA$^{Asp}_{dC38}$

A more detailed analysis of the methylation data during the first 20 minutes of the reaction showed that it followed Michaelis-Menten kinetics (Figure 11). The apparent K_m values gained for all-ribo tRNA^{Asp} and tRNA$^{Asp}_{dC38}$ were quite similar (4.2 µM *vs.* 4.0 µM), while the k_{cat} value of the hybrid tRNA$^{Asp}_{dC38}$ was increased by a factor of

2.3. This indicates similar binding properties combined with an accelerated turnover as a consequence of the lack of the 2'-hydroxylgroup at position 38.
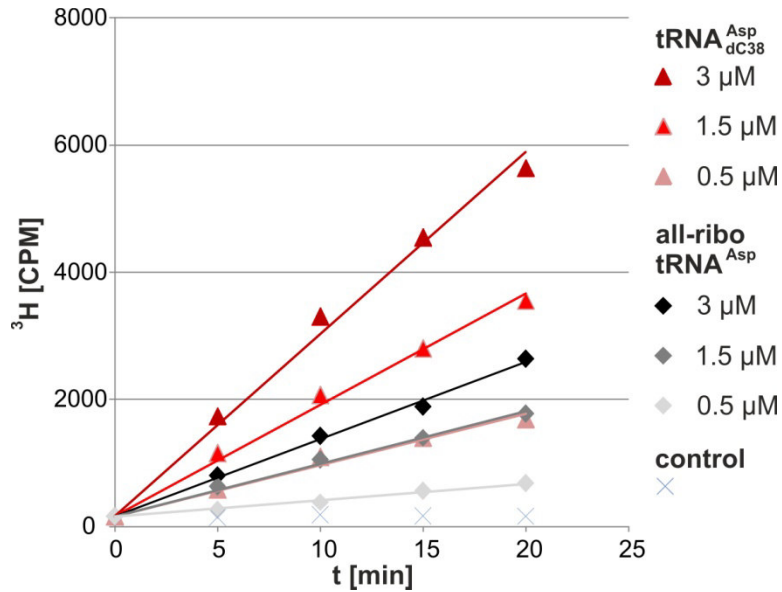
Figure 11: Methylation kinetics under Michaelis-Menten conditions of all-ribo tRNA^{Asp} and tRNA$^{Asp}_{dC38}$.

3.1.4 Increasing the DNA content in hybrid tRNA^{Asp}

In the hybrid constructs synthesized and tested next, the nucleotides flanking the target C38 were substituted as well, increasing the DNA stretch to three, five or ten deoxynucleotides, respectively (Figure 12).
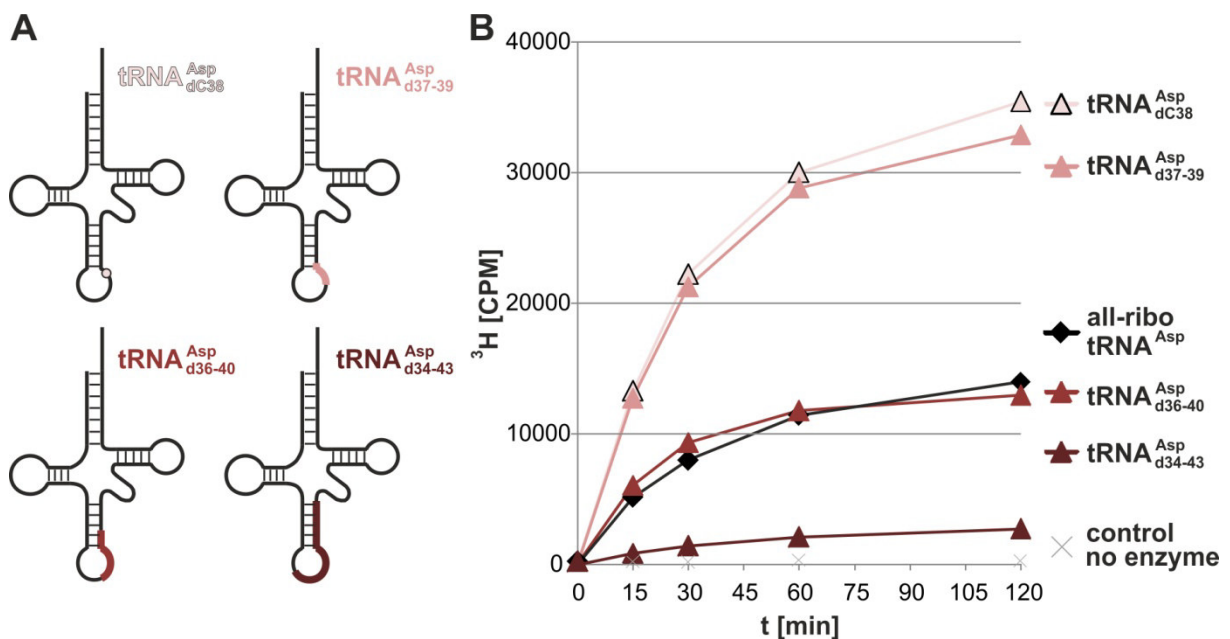
Figure 12: Methylation of hybrid tRNAs containing up to 10 deoxynucleotides by Dnmt2. **A)** Positions of DNA substitutions in the tRNA cloverleaf in hybrid tRNAs. **B)** Methylation of hybrid tRNAs of increasing DNA content. Average values and standard deviations are given in Figure 13.

The hybrid tRNA$^{Asp}_{d37\text{-}39}$ showed methylation levels similar to the tRNA$^{Asp}_{dC38}$, clearly surpassing the all-ribo tRNA^{Asp}. Even hybrid tRNA$^{Asp}_{d36\text{-}40}$, containing a stretch of five deoxynucleotides, was still a substrate comparable to the all-ribo tRNA^{Asp}. However, as the DNA stretch was further extended to ten, thirteen or seventeen deoxynucleotides in hybrid tRNA$^{Asp}_{d34\text{-}43}$, the methylation activity was clearly decreased, though it was still readily detectable (compare Figure 16).
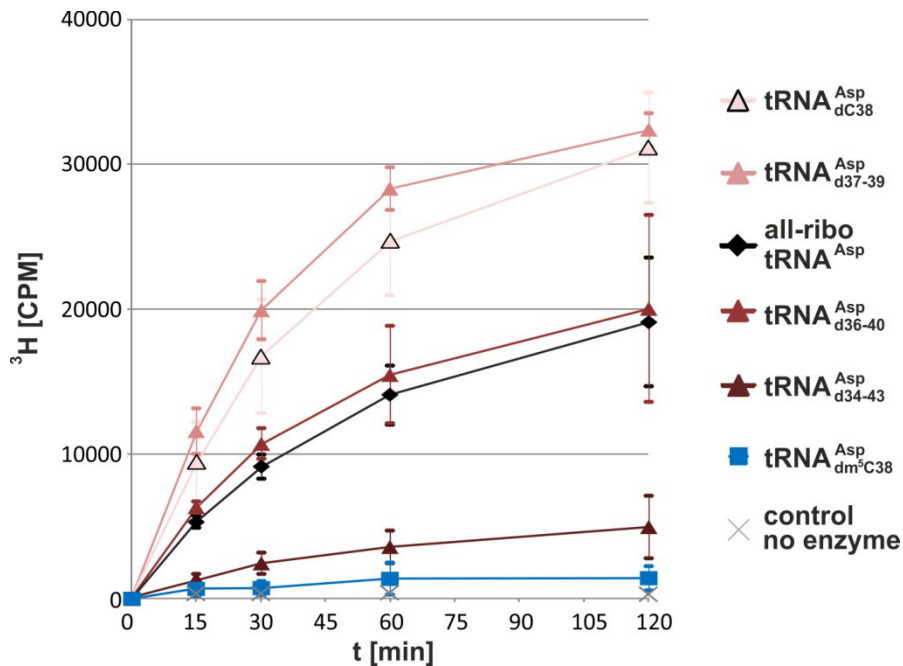
Figure 13: Average values and standard deviations of three tritium incorporation assays of all-ribo tRNA and various hybrid tRNAs.

3.1.5   Substitution of a whole stem-loop with deoxynucleotides

It was investigated how the replacement of a whole tRNA domain with DNA would affect methylation efficiency by Dnmt2. In those hybrid tRNAs either the hole D-, anticodon- or TΨC-stem-loop was composed entirely of deoxynucleotides (Figure 14). As in hybrid tRNA$^{Asp}_{d34\text{-}43}$ the 3' half of the anticodon was substituted with deoxynucleotides, a hybrid tRNA$^{Asp}_{27\text{-}33}$, in which the 5' half of the anticodon was comprised of DNA, was also synthesized to be compared to the others (Figure 14d).
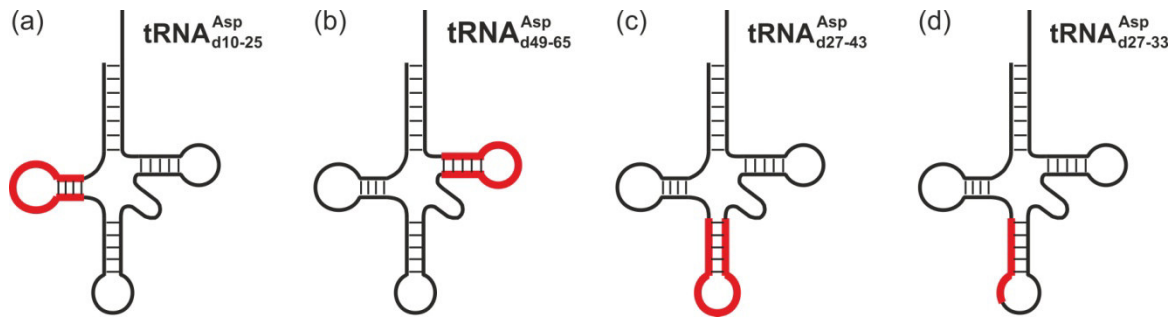
Figure 14: Positions of DNA substitutions (red) in the tRNA cloverleaf in hybrid tRNAs with a DNA-stem-loop.

If the D- or TΨC-arm was comprised of DNA, no methylation activity could be detected (compare Figure 16). It is possible that the conformation of those hybrid tRNAs is changed in a way that they are no longer recognized by Dnmt2 as a substrate. Or that although they are still able to bind Dnmt2, they cannot undergo conformational changes anymore or have difficulties undergoing conformational changes necessary for entering the transition state/catalysis. The other two hybrid tRNAs still showed a slight methylation. Some of the DNA substitutions are in regions that have been shown to be important for the enzyme-tRNA interaction (Figure 15, (123)). The lack of the 2' OH-group could play a role here, if an interaction was based on those OH-groups. Besides, 2'-OH groups are involved in tRNA tertiary folding. Likewise it is possible, that a whole domain comprised of DNA adopts a deoxyribose C2'-endo conformation. This C2'-endo-pucker would significantly influence the overall 3D structure. A stem composed of DNA might be more likely to have a certain B-helix character, compared to the usual RNA A-helix. In the case of Figure 14a) and Figure 14b), the D-loop could no longer interact with the T-loop (orange and green highlighted parts in Figure 15B) rendering an L-shaped tertiary structure less likely.
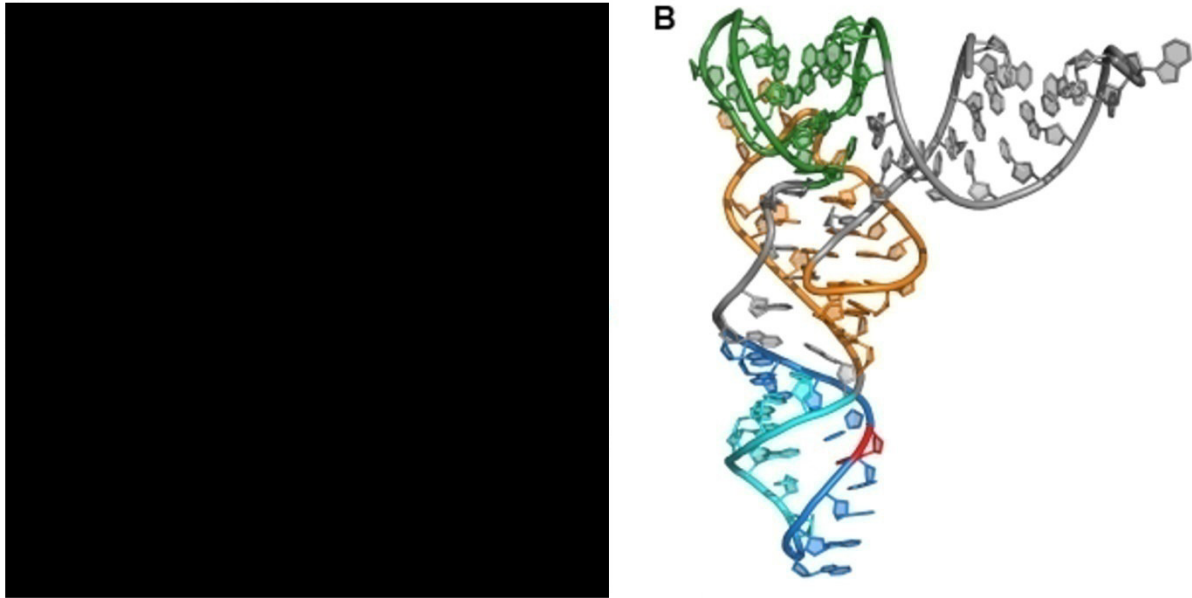
Figure 15: Interaction of Dnmt2 with tRNA^Asp. **A)** Binding model of Dnmt2 with a manually placed tRNA^Asp such that the target base is able to approach the binding pocket. Cofactor product S-adenosyl-L-homocysteine is shown in dark blue, the target nucleotide in purple. Residues highlighted in red have been shown to be important for the Dnmt2-tRNA interaction and mutations in one of those residues reduced the catalytic activity to less than 25% (123). The arrows (colors correspond to the region in B) indicate important locations of interaction that would have to interact with DNA in the hybrid tRNAs. Figure adapted from (123).**B)** tRNA 3D structure. Nucleotides 10-15 (orange), 27-33 (cyan), 34-43 (blue) and 49-65 (green) are highlighted. C38 is shown in red.

Figure 16 gives an overview of the relative methylation efficiencies of the hybrid tRNAs^Asp presented so far.

In conclusion, substitution of C38, or C38 and its neighboring nucleotides, with DNA surrogates leads to a higher methylation activity of Dnmt2 compared to its natural substrate, all-ribo tRNA^Asp. The further the DNA stretch is expanded, the more the activity is reduced. If a whole stem-loop is comprised of DNA the activity is either very small (in case of the deoxy-anticodon stem-loop) or completely abolished (D- or T-stem-loop).

Dnmt2 is biochemically able to methylate DNA and the catalysis reaction itself is even faster. However, the substrate must be presented in the structural context of a tRNA. If the DNA content in the hybrid tRNA constructs increases, the adopted tertiary structure distances itself more and more from its canonical 3D structure and at one point might no longer be recognized by Dnmt2 as a substrate.
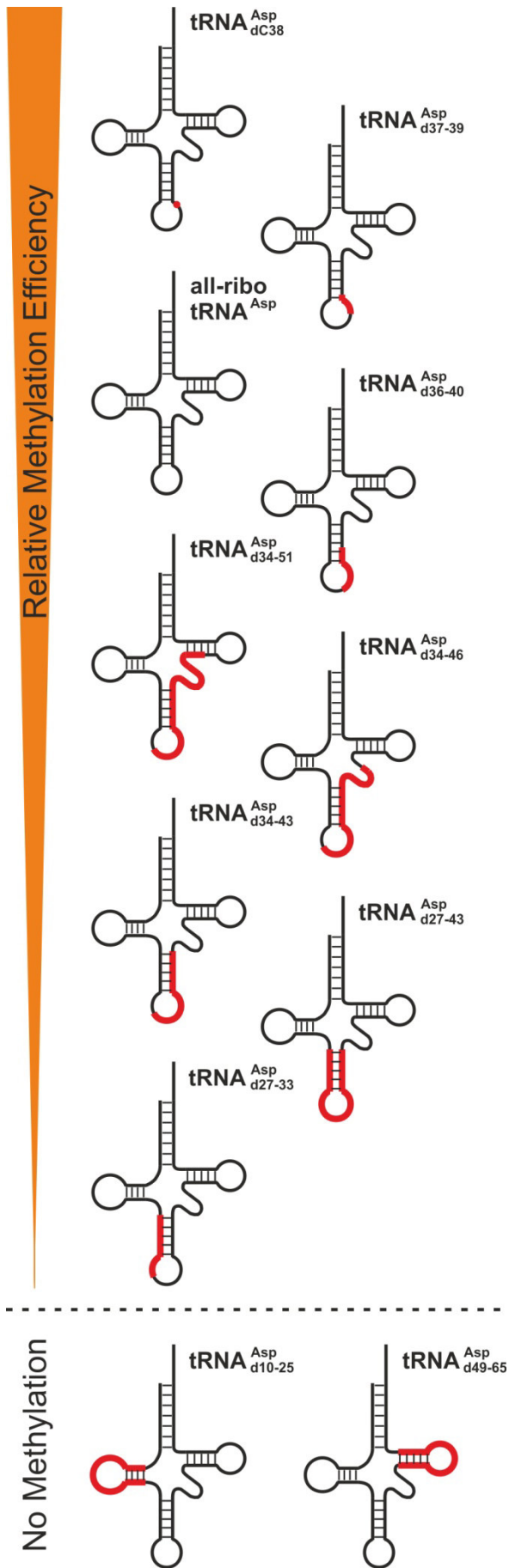
Figure 16: Relative methylation efficiency of the hybrid tRNAs^{Asp} compared to the all-ribo tRNA^{Asp}.

3.1.6 Exploration of various tRNA permutations on the Dnmt2 methylation efficiency

The number of deoxynucleotides in the hybrid tRNA could only be increased to a certain amount before the methylation reaction by Dnmt2 dropped significantly or was completely absent, most likely due to structural changes that brought the hybrid tRNA too far away from the canonical 3D structure. However, to explore, which exchanges are accepted by Dnmt2 and find possible DNA substrates, further changes were introduced into the tRNA. Therefore, the following study utilized tRNA constructs with deoxy-sequences, while introducing additional structural changes into all-ribo tRNA^{Asp} and hybrid tRNAs^{Asp}, *e.g.* a nick in the anticodon-loop or poly-cytidinylation. Figure 17 shows the results for all constructs in order of methylation efficiency.

If all-ribo tRNA^{Asp} and tRNA$^{Asp}_{dC38}$ contained a nick in the anticodon loop, their methylation (Figure 17j, 9g) activity was reduced compared to the corresponding tRNAs without a nick. However nicked tRNA$^{Asp}_{dC38}$ still showed higher methylation efficiency than nicked all-ribo tRNA^{Asp}, in line with the trend for the non-nicked ones.

If the four nucleotides between the nick and dC38 were substituted with four deoxycytidines (Figure 17b) the methylation rate was strongly improved, nearly reaching the all-ribo tRNA^{Asp} without nick. However, it was not possible to determine, whether the higher ^{3}H CPM count was due to a faster reaction rate, or if it was caused by more than one methylation per hybrid tRNA molecule.

Substitution of the following five nucleotides with their DNA surrogates lead to a construct (Figure 17c) that still performed well in the methylation reaction, as did another construct where additional five DNA nucleotides were added to the 5' end of the nick (Figure 17d) in the anticodon loop. Dnmt2 also tolerated the supplemental addition of five RNA nucleotides to the 3' end of the nick, reverse-complementary to the five DNA nucleotides added to the 5' end of the nick (Figure 17f), as well as the supplemental addition of RNA nucleotides to the 5' end of the tRNA (Figure 17k).

Interestingly, both the constructs with an anticodon stem-loop composed of deoxy-nucleotides (Figure 14c) and the one where only the 5' half of anticodon stem-loop was substituted with DNA (Figure 14d), showed an about 4-fold increase in their methylation efficiency when the nick was present in the anticodon loop Figure 17e) and h), respectively. The nick possibly relieves the constraints induced by the non-

RNA like helix formation by the DNA C3 endo pucker (B-shape), which allows improved recognition and methylation by Dnmt2.

Two hairpin-like constructs (Figure 17n, 9o) composed entirely of deoxynucleotides with a sequence derived from tRNA^{Asp} without the D- and T-stem-loop were tested as kinds of minimal substrates. They were no longer a substrate of Dnmt2.

In summary, the presented results show, that Dnmt2 methylates DNA and also tolerates various minor structural changes. However, changes strongly influencing the tRNA shape abolish methylation by Dnmt2.
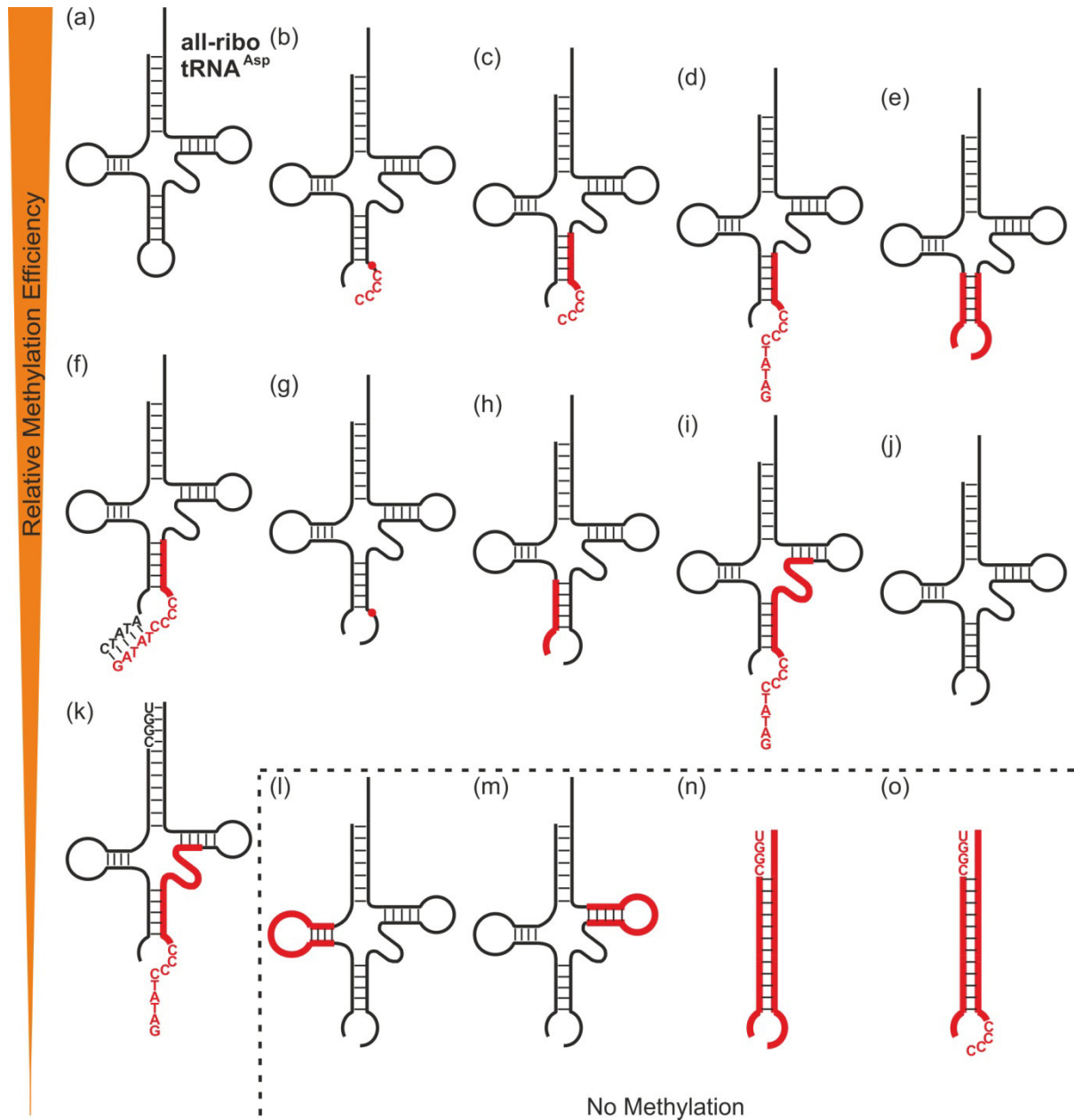
Figure 17: Overview of hybrid constructs tested and their structural alterations shown in the order of relative methylation efficiency from (b) to (k) compared to the more active all-ribo tRNA^Asp (a). Constructs (l) to (o) showed no methylation activity. Deviations from the nativetRNA^Asp sequence are presented in capital letters, DNA is highlighted in red.

3.1.7 RNA guided DNA methylation

With the knowledge gained from the hybrid constructs tested in the tritium incorporation assay it was now investigated if Dnmt2 could also methylate a molecule exclusively composed of deoxynucleotides. To present this DNA molecule in a tRNA like shape, it must be hybridized with RNA, the RNA guide. The resulting (unligated) construct is referred to as RNA guided DNA (short RgD).

For the first approaches the tRNA was divided into three parts, two composed of RNA and one of DNA. In addition, the 3' CCA end was ligated to the 5' end of the tRNA by splinted ligation (Figure 18) to bring the RNA into the right spatial arrangement before the DNA molecule hybridizes with it. However 3'/5' ligated constructs showed no activity in the tritium incorporation assay.
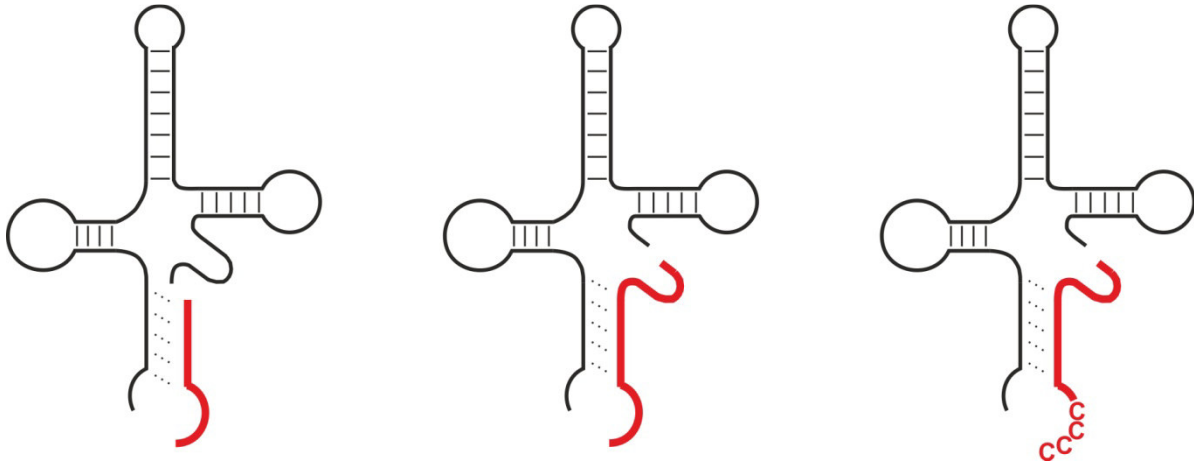
Figure 18: First approaches for a construct with a DNA molecule hybridized to an RNA. Deviations from the normal tRNA^{Asp} sequence are presented in capital letters, DNA is highlighted in red.

Consequently in a new set-up the RNA molecules were not 3'/5' ligated and a longer DNA oligonucleotide was chosen to achieve base pairing with both RNA guides (Figure 19a). This construct was not methylated by Dnmt2, either. However, the main concern for RgD approaches is the hybridization of three oligonucleotides to a tRNA-like structure. To increase the likelihood of the correct base-pairings, two sets of alterations were made. In the first set, additional nucleotides were added at the 5' or 3' end (Figure 19b, 11c) of the first ribonucleotide (the one corresponding to the 5' half of the tRNA) to render more base pairings possible. The second set comprised additional permutations of two G-C pairs with A-T and A-U in the T-stem to decrease the probability of an unwanted hybridization pattern, as both the T-stem and the anticodon-stem are composed of five G-C basepairs (Figure 19d, 11e, 11f).
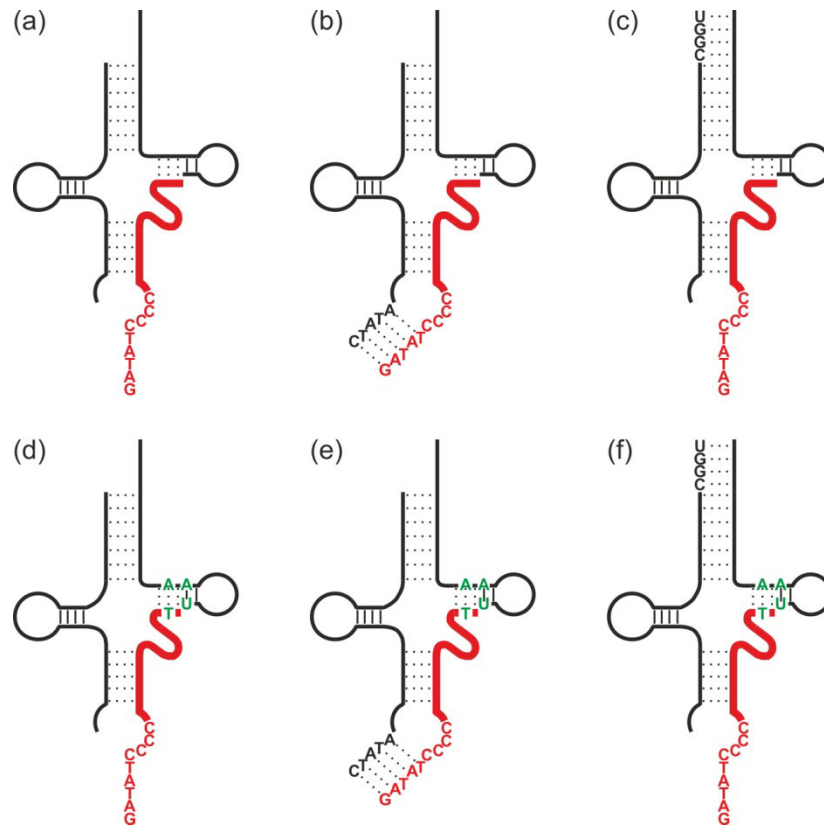
Figure 19: Constructs tested in the tritium incorporation assay composed of a deoxynucleotide (red) hybridized with two ribonucleotides. The sequence is derived from tRNA^{Asp}, deviations are given in capital letters. The green letters are permutations of two of five G-C base pairs in the T-stem to decrease the probability of undesired base pairings, as the anticodon-stem also contains five G-C base pairs.

The first experiment focused on the influence of the oligonucleotide–hybridization–order for both sets of constructs. 2 possible hybridization orders can be imagined: (a) the DNA oligonucleotide is hybridized with the "5' RNA oligonucleotide" of the tRNA first and the "3' RNA oligonucleotide" is added afterwards or (b) the DNA oligonucleotide is hybridized with the "3' RNA oligonucleotide" first and the "5' RNA oligonucleotide" is added second.

For both sets of constructs and both hybridization strategies, only one case (Figure 19c) produced a small signal in the tritium incorporation assay and only if the DNA was hybridized with the "3' RNA fragment" first and the other "5'-RNA" oligonucleotide was added afterwards (strategy b). To confirm this reproducible result, despite the low signal intensity, the signal-to-noise ratio (SNR) needed improvement. As a goal, the common SNR > 3 to reliably qualify a signal was chosen.

This goal was achieved with an increased ratio of ^{3}H-SAM to non-radioactive SAM, a 25% increase in reaction volume and doubling of the concentrations for all oligonucleotides and Dnmt2, respectively.

Two timepoints after reaction start (15 and 120 minutes) were chosen, an aliquot spotted on a whatman filter paper and measured with the Cherenkov counter. The results (Figure 20) show a distinct ^{3}H signal for the hybridized construct (red bars), clearly above the background levels (grey bars). **These results demonstrate the capability of Dnmt2 to methylate a short DNA oligonucleotide with the help of RNAs acting as a guide.**
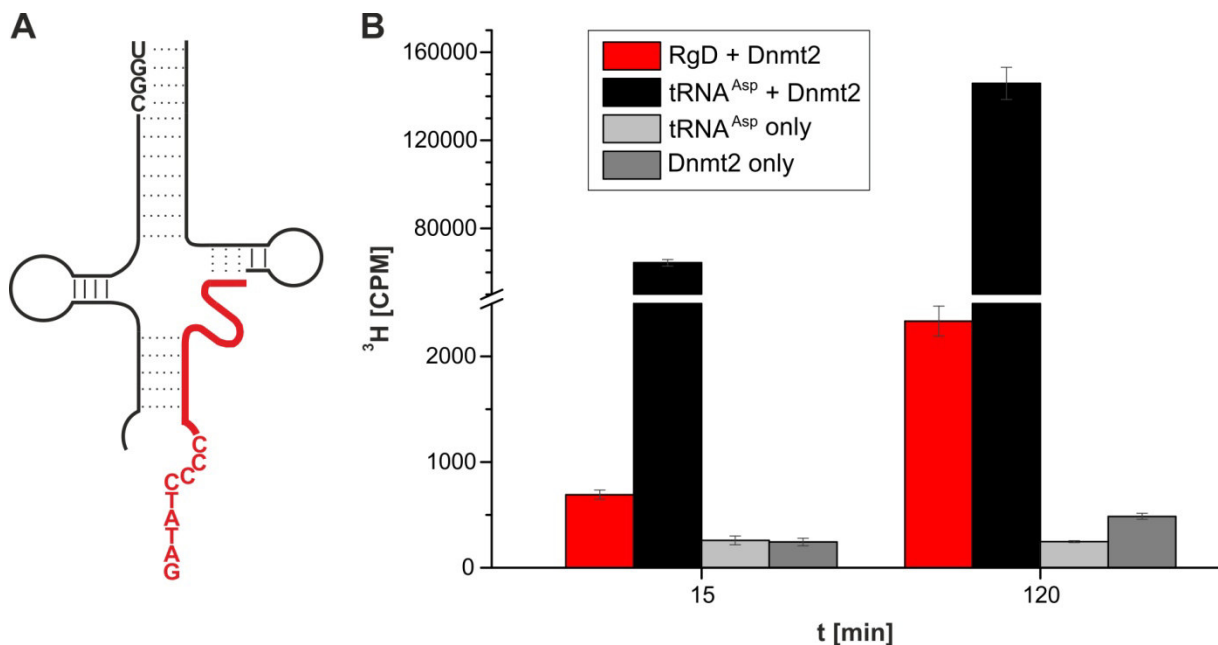
Figure 20: Methylation of an RNA-guided DNA oligonucleotide by Dnmt2. (**A**) Structure of the hybridized construct. DNA is shown in red. (**B**) Average values and standard deviations of three tritium incorporation assays are shown. (Note: The small signal increase in the Dnmt2 sample without nucleic acids is most likely due to a small fraction of tRNA present with the enzyme, as it is (nearly) impossible to separate a strong tRNA-binding enzyme like Dnmt2 completely from all RNA without losing the enzyme's activity.)

To distinguish possible RNA methylation from the assumed DNA methylation, the remaining ^{3}H-labeled samples were analyzed by 2D TLC. After purification by precipitation and size exclusion, the samples were hydrolyzed, mixed with commercially (non-^{3}H-labeled) nucleosides and spotted on a cellulose plate (Figure 21A).
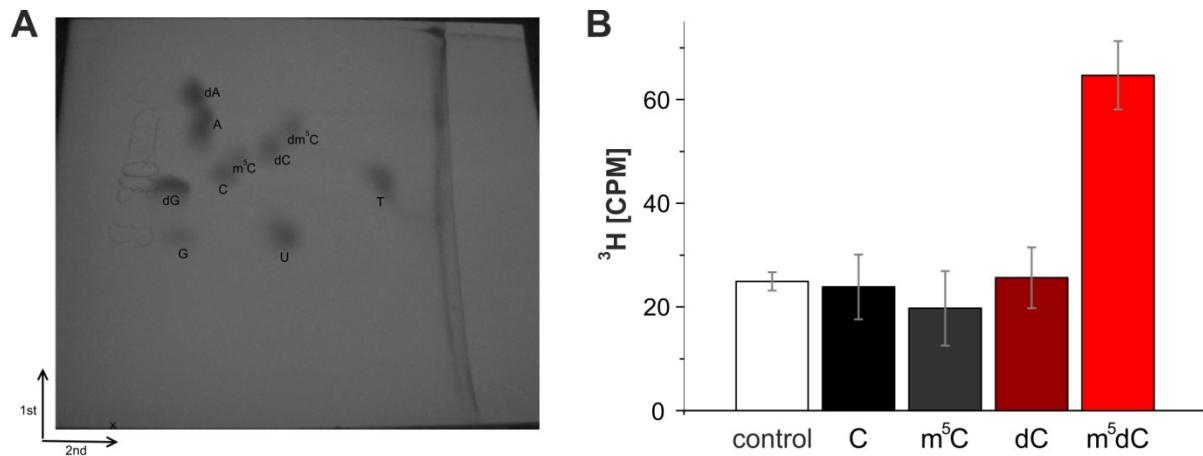
Figure 21: TLC analysis of RNA guided DNA methylation. **A)** Two-dimensional thin-layer chromatography of nucleosides on a 10 cm x 10 cm cellulose TLC plate. Solvent of the first dimension is isobutyric acid : concentrated ammonia : H_2O (50 : 1.1 : 28.9 [v : v : v]), solvent of the second dimension is isopropanol : concentrated HCl : H_2O (68 : 18 : 14 [v : v : v]). The starting point is marked with X. **B)** Methylation of an RNA-guided DNA oligonucleotide by Dnmt2. The oligonucleotides have been hydrolyzed to nucleosides after the tritium incorporation assay, separated by 2D thin-layer chromatography and analyzed with the Cherenkov counter. Tritium could only be detected in the dm^5C spot. Average values and standard deviations of three experiments are shown. Control corresponds to background signal of the TLC plate.

Position of the nucleosides were visualized with a 254 nm UV lamp and marked. The cellulose of each nucleoside spot was transferred carefully into a 1.5 ml Eppendorf tube with a scalpel and the nucleosides extracted three times with water. Finally, ^3H activity of each TLC spot was measured with the Cherenkov counter (Figure 21B).

A clear Tritium signal was only detected in the dm^5C spot. In the other TLC eluted spots, the number of counts corresponded to the usual background values.

Those results confirm the methylation of a short DNA oligonucleotide by Dnmt2, in the structural context of tRNA.

3.1.8 Encountered Problems with the methylation of the RgD and approaches to solve them

As mentioned in the last chapter, the tritium signal detected after the methylation reaction of the RgD and Dnmt2 was just above the background signal. Here, I present several additional, but compared to TLC less successful, approaches to improve the assay conditions to get a stronger signal with a SNR greater than three.

a) Increase of the ratio of tritium-labeled SAM to unlabeled SAM: The underlying idea here is the increased likelihood of tritium-labeled methylgroup incorporation into the DNA oligonucleotide when the methylation reaction takes place. This measure did indeed improve the signal, but not to a sufficient extent as the greater quantity of radioactivity in the reaction did increase the background level, too.

b) Loss of small oligonucleotides during the assay: Another consideration was loss of this rather short oligonucleotide during precipitation with trichloroacetic acid on a whatman filter paper. Therefore, the filter papers were exchanged with diethylaminoethyl (DEAE) cellulose filter papers. The positively charged DEAE groups strongly interact with negatively charged nucleic acids and allow a precipitation of very small oligonucleotides. The use of DEAE cellulose did not improve the strength of the ^{3}H-signal in the assay and it was concluded, that the small signal was due to a small methylation level and not the effect of an insufficient precipitation.

c) Increase of starting volume: The reaction volume was now increased to 50 µl, allowing greater aliquots to be spotted on the filter papers. However, the limiting factor is the given size of the filter paper, as it cannot soak up more than approximately 14 µl. If the size of the filter paper was increased it would have to be crumpled to fit into the scintillation vials, falsifying the measurement.

d) Increase of reactant concentrations: Consequently, as the volume could not be increased in a significant amount, the concentration of the reaction partners had to be increased. Concentration of Dnmt2 and the oligonucleotides was doubled and tested in the tritium incorporation assay, leading to a sufficiently strong CPM signal.

e) Analysis of the reaction on a urea gel: It had to be further investigated if the tritium labeled methylgroup was really transferred onto the DNA oligonucleotide and not onto one of the two ribo-oligonucleotides. Therefore, the reaction with the doubled concentration was repeated and in addition the volume was increased by 25%. This allowed measurements of the aliquots with the Cherenkov counter on the one hand and yielded enough material for a $LiClO_4$ precipitation on the other hand. After separation of the oligonucleotides on a urea gel and drying of the gel, the method of choice would be to expose an X-ray film or storage phosphor screen with the radioactive gel, to see which oligonucleotide band contains the tritium label. However, an X-ray film, as well as a storage phosphor screen, exposed with a serial dilution of ^{3}H-SAM on a filter paper for up to five weeks, showed that at least 100000 CPM ^{3}H are needed for detection. Since the RgD signal was always below 1000 CPM, it would not be detectable by these methods. Therefore, after running a urea gel the bands containing the oligonucleotides and several additional gel slices as controls were excised and eluted. The eluted nucleic acids were measured with the Cherenkov counter. Here, the encountered problem was a high background radiation, especially in the lower half of the gel, preventing identification of the methylated oligonucleotide. Use of a size exclusion column (Microspin G-50) led to a reduced overall radioactivity but did not improve the SNR. In conclusion, the best method to identify the nucleobase methylated by Dnmt2 was digestion of the nucleic acids to nucleosides and analyzing them on a 2D TLC.

3.1.9 Alternative Cofactors for Dnmt2 and possible applications

As presented in the previous chapter, Dnmt2 has methylation activity for DNA. However, the methylation could only be shown in the presence of the two guide RNAs, which most probably force the DNA in a distinct 2 dimensional structure. With the goal to find the natural DNA substrate(s) of Dnmt2, a new technique for detection and enrichment of thus alkylated DNA was developed.

The synthetic SAM-analog molecules AdoEnYn (Figure 22a, (124)) and SeAdoYn (Figure 22b, (125,126)) have been evaluated as cofactors of Dnmt2. They were a gift

from Prof. Dr. Elmar Weinhold (RWTH Aachen). AdoEnYn contains a pent-2-en-4-ynyl moiety, SeAdoYn a propargyl moiety, instead of the methyl group.
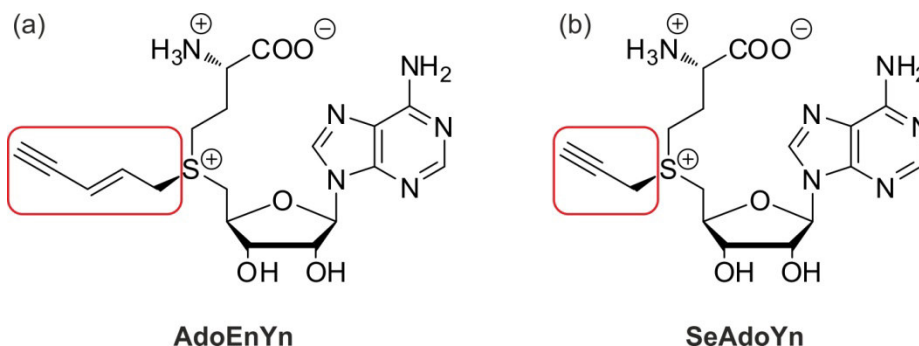
Figure 22: SAM-analog cofactors AdoEnYn (a) and SeAdoYn (b). The residue transferred during the enzymatic reaction is highlighted with a red box.

If the methyltransferase would tolerate the exchanged cofactor, it could be used to (site-specifically) tag the enzyme's target molecule with a reactive, bio-orthogonal terminal alkyne. The product of this enzymatic reaction can be further modified, with the azide of a fluorescent dye or a biotin, *via* the copper (I)-catalyzed azide alkyne [3+2] cycloadditon (CuAAC). Here, I want to present a summarized proof-of-principle on the applicability of the modified SAM-cofactors.

In this study, two mutant enzymes of Dnmt2 were tested beside the wild type enzyme, namely Dnmt2 N375A and Dnmt2 N375G. In those mutants an asparagine, inside the believed cofactor binding pocket, was substituted with a less voluminous alanine, or glycine respectively. These mutations will most likely reduce steric hindrance and accommodate the larger cofactors better. The already described reaction of Trm1p and *S. c.* tRNA[Phe] with AdoEnYn (124) was used as the positive control. After the enzymatic reaction, the tRNA was purified by phenol/chloroform extraction and subjected to a CuAAC click reaction with an Alexa 594 azide. Excess dye was removed with a DyeEx size-exclusion column before loading the tRNA on a denaturing gel, and analyzing it with the typhoon scanner.

Both, the Dnmt2 wild type and the N375G mutant, showed a fluorescent band with the SeAdoYn cofactor (Figure 23). As expected, no fluorescent signals were detectable in the controls without enzyme. This verifies that only those tRNAs that got

propargylated by Dnmt2 and SeAdoYn could be selectively tagged by the dye-azide in the CuAAC reaction.

In a separate experiment with AdoEnYn (not shown here), no fluorescent band could be detected after the reaction of Dnmt2 (neither wt, nor mutants) with tRNA^{Asp}, leading to the conclusion that Dnmt2 did not tolerate AdoEnYn, which could be due to the bigger size (C3 *vs.* C5). In contrast, Trm1p could use AdoEnYn but not SeAdoYn as cofactor. This finding might be explained by different interactions of the two enzymes' catalytic cores with the different sizes of the cofactors alkyle chains.

In contrast to both Dnmt2 wild type and the N375G mutant, Dnmt2 N375A showed no activity with either cofactor.

The presented experiments indicate a possible use of SeAdoYn in a SELEX-like approach to identify possible DNA and RNA substrates of Dnmt2.
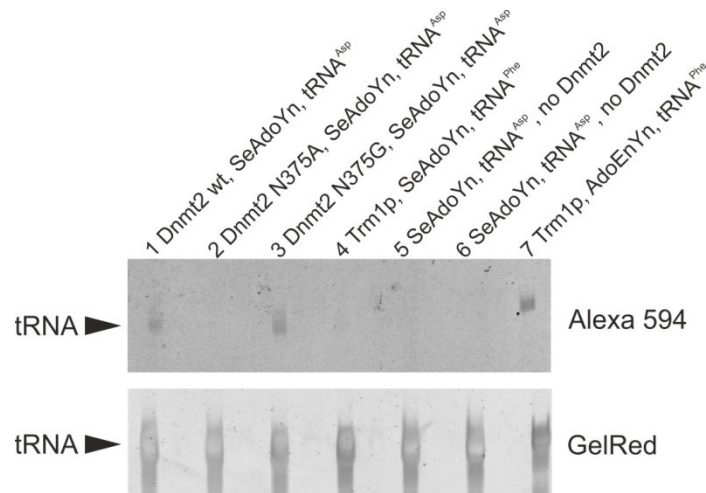
Figure 23: Dnmt2 and SeAdoYn. Dnmt2 wt and two mutants N375A and N375G were incubated with tRNA^{Asp} and SeAdoYn as cofactor. After the reaction the tRNAs were purified by phenol/chloroform extraction, labeled with a dye *via* CuAAC reaction, run on a gel after the excess dye had been removed with a spin filter and scanned for Alexa 594 with the typhoon scanner. Dnmt2 wt and Dnmt2 N375G were able to transfer a propargyl moiety from SeAdoYn to tRNA^{Asp} (lanes 1 and 3). Trm1p, AdoEnYn, tRNA^{Phe} (lane 7) served as positive control. Below gel stained with GelRed as loading control.

A necessary prerequisite for such an approach would be that different substrates lead to differently strong readout signals. To further investigate the feasibility of such an approach, a preliminary experiment, using Dnmt2 and SeAdoYn with three substrates of varying alkylation efficiency were compared. Here, *D. melanogaster*

tRNA^{Asp} was chosen as a good substrate, a *S. cerevisiae* tRNA^{Asp} mutant (U32→C, G37→A, U40→C) as a weak substrate and *E. coli* tRNA^{Tyr} as a non-substrate. Figure 24 shows the tRNAs structure, the mutations and the methylation efficiency found in a ^{3}H incorporation assay. After the enzymatic reaction, the tRNAs were purified by phenol/chloroform extraction and clicked with the TAMRA-Azide-Biotin, a trifunctional molecule, enabling visualization and affinity purification of the propargylated tRNAs. After the CuAAC reaction, excess dye was removed with a DyeEx spin filter, the samples run on a denaturing gel and scanned for the TAMRA-dye with the typhoon scanner. A strong band could be visualized for *D. melanogaster* tRNA^{Asp} (Figure 25, lane 1) whereas the mutant *S. cerevisiae* tRNA^{Asp}, as a weak Dnmt2 substrate, showed only a faint band (Figure 25, lane 2). No band was visible for *E. coli* tRNA^{Tyr} and the negative controls (Figure 25, lanes 3-7). These results demonstrate that it is not only possible to distinguish if a tRNA is substrate or not, but in addition, the efficiency of substrate methylation can be visualized.
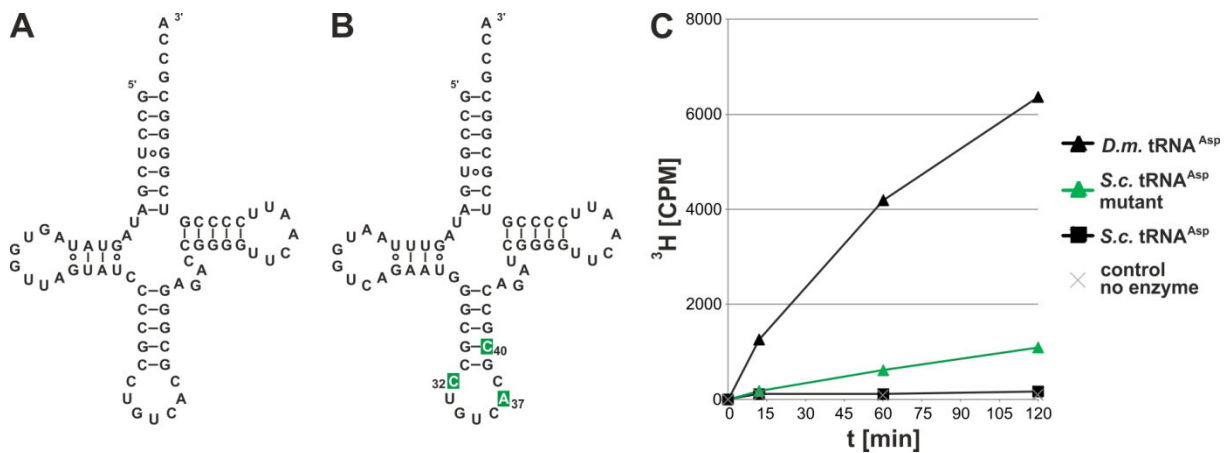
Figure 24: Three point mutations transform *S. cerevisiae* tRNA^{Asp} into a weak Dnmt2 substrate. **A)** Secondary structure of *D. melanogaster* tRNA^{Asp}. **B)** Secondary structure of yeast tRNA^{Asp}. Three point mutations have been inserted, U32→C, G37→A and U40→C (highlighted in green), for the anticodon stem-loop sequence to be more similar to a Dnmt2 tRNA substrate. **C)** *In vitro* methylation measured by tritium incorporation from ^{3}H-SAM. Whereas yeast tRNA^{Asp} is no Dnmt2 substrate, the introduction of three point mutations transformed it into is a weak Dnmt2 substrate compared to *D. melanogaster* tRNA^{Asp}.
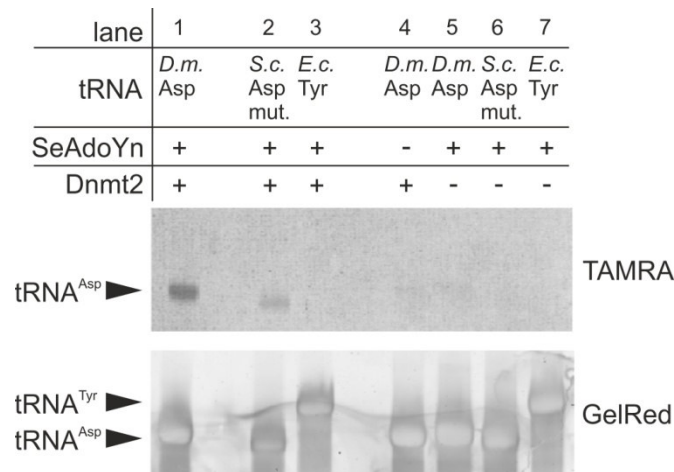
Figure 25: Reaction of Dnmt2 and SeAdoYn with different tRNAs. Dnmt2 was incubated with either *D. m.* tRNA^{Asp}, *S. c.* tRNA^{Asp} mutant (U32C, G37A, U40C) or *E. coli* tRNA^{Tyr} and SeAdoYn as cofactor. After the reaction the tRNAs were purified by phenol/chloroform extraction, clicked with TAMRA-Azide-Biotin *via* CuAAC reaction, run on a gel after the excess dye had been removed with a spin filter and scanned with the typhoon scanner. *D. m.* tRNA^{Asp} as a good Dnmt2 substrate showed a strong TAMRA dye signal (lane 1), the mutant *S. c.* tRNA^{Asp} as a weak Dnmt2 substrate showed only a weak band (lane 2). For *E. coli* tRNA^{Tyr}, that is no Dnmt2 substrate, no signal was obtained. The negative controls (lanes 4-7) showed no bands, too. Below gel stained with GelRed as loading control.

The presented results show the potential of SeAdoYn as a possible SELEX-tool candidate. Before using this modified SAM cofactor on a complex cell lysate, two degenerated tRNA pools (as indicated in Figure 26) have been prepared from degenerated DNA templates by *in vitro* transcription. Dnmt2 wild type and SeAdoYn will be used to identify Dnmt2 substrates in these tRNA pools to get more insights into the sequence requirements for a Dnmt2 substrate in RNA. This experiment is a work-in-progress and therefore no results are yet available.
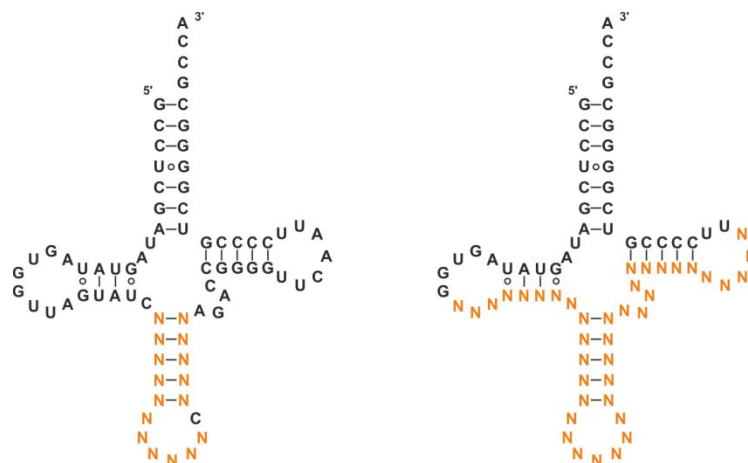
Figure 26: Degenerated tRNA pools. The degenerated transcripts were synthesized from degenerated DNA templates by *in vitro* transcription. The variable nucleobase positions are highlighted in orange.

3.2 TLR7 stimulation by modified tRNAs

3.2.1 General techniques used to investigate TLR7 stimulation by tRNA

TLR7, located in the endosome, is able to recognize single-stranded RNA of microbial pathogens as bacteria and viruses. It has been proposed, that naturally occurring nucleoside modifications in RNA are structural determinants involved in TLR7 discriminating self from foreign RNA. However, the exact structural motif(s) recognized remain(s) unknown.

tRNA was chosen to investigate TLR7 recognition and the impact of modifications on the immunostimulatory potential of RNA, as it represents the highest modified subtype of RNA and is located freely, non-protein-bound in the cytoplasm. Furthermore, the modifications are incorporated into tRNA at well-defined and known positions.

The immunostimulatory potential of a given RNA was quantified by measuring the amount of TLR7-mediated secretion of IFN-α, that was produced by human blood mononuclear cells (PBMCs), after transfection with DOTAP encapsulated tRNA (34). The PBMCs responsible for the IFN-α secretion were plasmacytoid dendritic cells. Depletion of pDCs from PBMCs abolished tRNA-mediated secretion of IFN-α. To take blood donor variance into consideration, experimental results were normalized to stimulation with the TLR9 ligand CpG2216. The immunostimulation experiments were performed in the lab of Prof. Dalpke in Heidelberg.

Native tRNAs containing modified nucleosides and *in vitro* transcripts (IVTs, Figure 27) that do not comprise any modification at all, were investigated, as well as tRNA hybrids made out of native tRNAs and IVTs by a molecular surgical approach (Figure 28). In addition, other differentially modified tRNA species, named modivariants, were synthesized by splinted ligation from synthetic ribo-oligonucleotides. The IVT's DNA template included a self-excising hammerhead ribozyme leader sequence (Figure 27) ensuring the absence of 5'-triphosphates that could activate RIG-I. The tRNA hybrids were synthesized in a two-step procedure (Figure 28). First the tRNA (native and/or IVT) is cleaved site-specifically by a DNAzyme, yielding RNA fragments with modifications from native tRNA, or the corresponding unmodified ones from IVT.

Afterwards the fragments are isolated by PAGE. The RNA cleavage activity of the DNAzyme leaves the 5' end of the cleavage site with a free OH-group and the 3' end with a cyclic phosphate. As T4 DNA ligase necessitates a 5' phosphate and 3' free OH-group, the fragments are made competent for ligation by T4 polynucleotide kinase (T4 PNK). T4 PNK possesses a 5' kinase and a 3' phosphatase activity. In the second step the fragments of native and IVT origin are cross-ligated in a splinted ligation, leading to tRNA hybrids with different sets of nucleotide modifications.
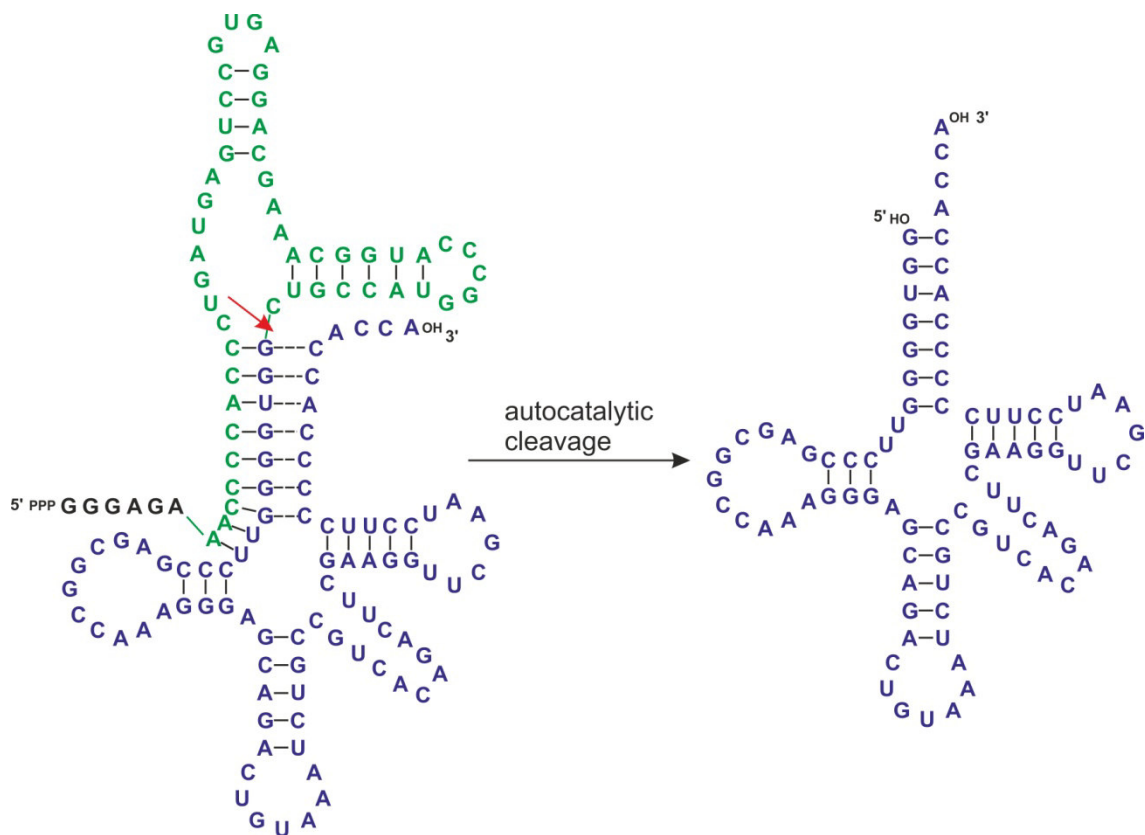
Figure 27: Hammerhead–tRNA product of the *in vitro* transcription. Under transcription reaction conditions the hammerhead ribozyme (green) autocatalyticly cleaves itself (and a strong T7 promotor shown in black letters) from the tRNA (blue), yielding the tRNA with a free 5' OH-group.
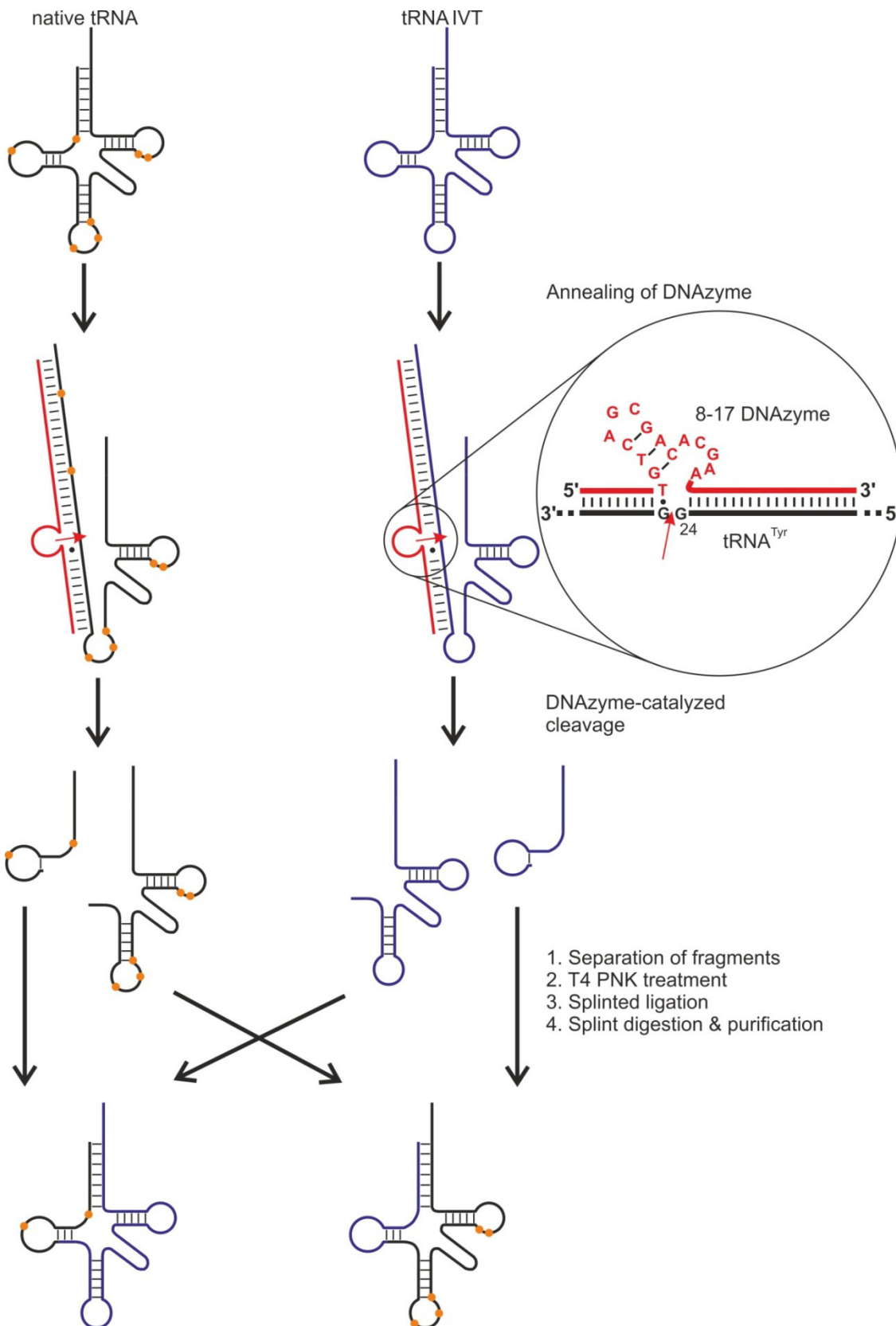
Figure 28: Molecular surgery to synthesize tRNA hybrids. A native and an *in vitro* transcribed tRNA are site-specifically cleaved by a DNAzyme. The sequences of the DNAzyme flanking the catalytic core are reverse complementary to the tRNA and are chosen to direct the activity to the desired position. The resulting RNA fragments are purified on a denaturing gel and cross-ligated with T4 DNA ligase in a splinted ligation to yield the tRNA hybrid. Detail of the catalytic core of the DNAzyme designed to cleave *E. coli* tRNA[Tyr] between G24 and G25 is shown in the black circle.

The modivariants synthesized from synthetic oligonucleotides by splinted ligation enable the analysis of single modifications at specific locations. Moreover, this method gives access to tRNAs with nucleotide modifications and/or point mutations at any desired site-specific location in any combination.

3.2.2 TLR7 stimulation of a whole tRNA can be suppressed by a single 2'-O-methylguanosine

In general, total tRNA of bacterial origin was more immunostimulative than total tRNA of eukaryotic origin. The same was true for single, native tRNA species tested. This is in line with the trend, that eukaryotic tRNA contains more modifications and more chemically complex modifications (*e.g.* yW) than bacterial tRNA (compare Figure 29). *In vitro* transcribed tRNAs on the other hand, containing no modified nucleotides, always showed a high immunostimulation whether they were of bacterial or eukaryotic origin.

This paragraph is a short overview of the work done during my diploma thesis and the preceding master theses of Stefanie Gehrig and Flavia Botschen. The preparation of the paper took place at the beginning of my thesis work and .the results are crucial for my later experiments. They are therefore presented here and not in the introduction section. For more details please refer to:

Identification of modifications in microbial, native tRNA that suppress immunostimulatory activity.

Gehrig S, Eberle ME, Botschen F, Rimbach K, Eberle F, Eigenbrod T, Kaiser S, Holmes WM, Erdmann VA, Sprinzl M, Bec G, Keith G, Dalpke AH, Helm M.

J. Exp. Med., 2012.
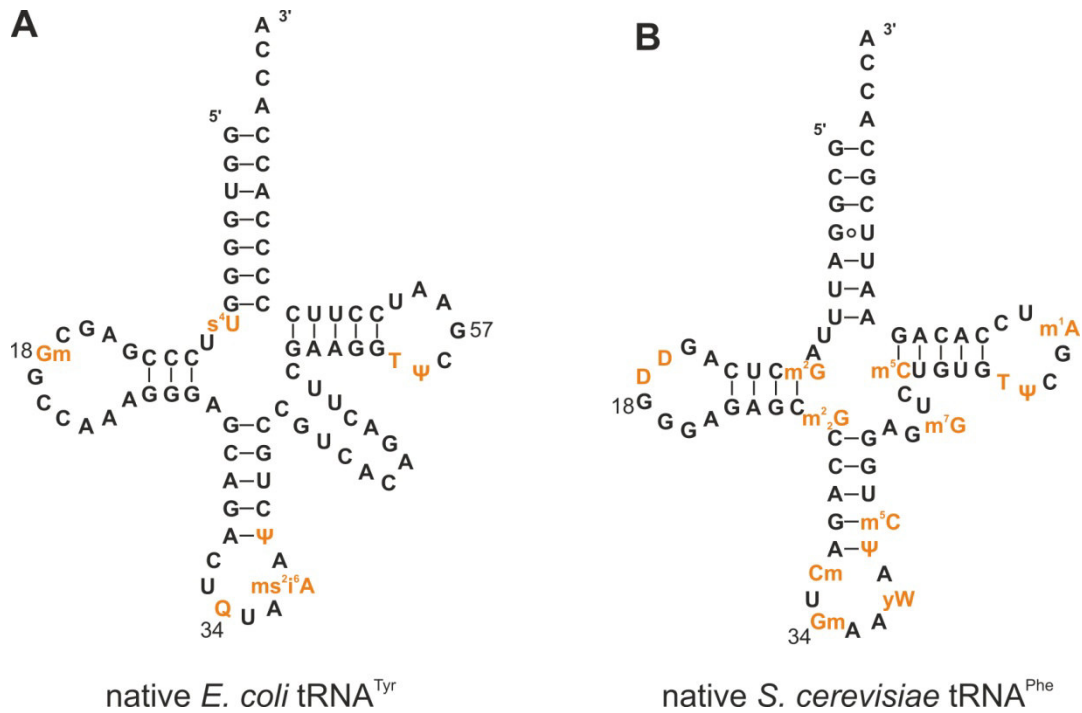
Figure 29: Examples of native tRNAs. **A)** Native *E. coli* tRNA^{Tyr} and the positions of its seven modified nucleotides highlighted in orange. **B)** Native *S. cerevisiae* tRNA^{Phe} as an example for a eukaryotic tRNA. It contains more modifications (fourteen compared to seven of *E. coli* tRNA^{Tyr}) and also chemically more complex ones like wybutosine. Abbreviations: s^{4}U: 4-thiouridine, Gm: 2'-O-methylguanosine, Q: queuosine, ms^{2}i^{6}A: 2-methylthio-N6-isopentenyladenoisine, Ψ: pseudouridine, T: 5-methyluridine/ribothymidine, m^{2}G: N2-methylguanosine, D: dihydrouridine, m$^2_2$G: N2,N2-dimethylguanosine, Cm: 2'-O-methylcytidine, yW: wybutosine, m^{5}C: 5-methylcytidine, m^{7}G: 7-methylguanosine, m^{1}A: 1-methyladenosine.

However, one bacterial tRNA, tRNA^{Tyr} from *E. coli* showed no significant immune stimulation, comparable to eukaryotic tRNAs. More striking, *E. coli* tRNA^{Tyr} was also able, if present with other immunostimulatory tRNA, to reduce or even suppress the immunostimulation of the otherwise stimulatory RNA (34), acting as a TLR7 antagonist. The reason for *E. coli* tRNA^{Tyr}'s lack of immune stimulation could be traced down to a 2'-O-Methylguanosine at position 18 in the D-loop. An *E. coli* tRNA^{Tyr} Gm18 modivariant synthesized by splinted ligation behaved identical to native *E. coli* tRNA^{Tyr} in the experiments, verifying that out of the seven modified nucleotides present in native *E. coli* tRNA^{Tyr} Gm18 was necessary and sufficient (34) to suppress immune stimulation.

S. cerevisiae tRNA^{Phe} was further investigated as an example of a eukaryotic tRNA. It contains fourteen modified nucleotides one of them being a Gm at position 34 in the anticodon loop. A modivariant with Gm34 as the only modification suppressed the immunostimulation, too. However, the reduced effect was not as strong as for the

fully-modified, native tRNA, implying that other modifications have an effect here as well on the immune stimulatory potential.

In molecular transplantation experiments the 2'-O-methylguanosine was incorporated into the scaffold of *E. coli* tRNA^{Tyr} at position 34 and in *S. cerevisiae* tRNA^{Phe} at position 18. In both cases the immune stimulation was significantly reduced compared to the unmodified IVT. It is noteworthy, that the Gm18 modivariants were less immunostimulatory than the corresponding Gm34 modivariant in both cases.

In an additional *E. coli* tRNA^{Tyr} modivariant the Gm was translocated to position 57 to assess the effect of Gm in the TΨC-loop. The immune stimulation was reduced comparable to *E. coli* tRNA^{Tyr} Gm34. Remarkably, the Gm19 modivariant in which the Gm was moved just one position in relation to its natural position led to a strong immune response comparable to the unmodified IVT. Gm19 had reproducibly no effect on immunostimulation of the tRNA. Those results (summarized in Figure 30) could imply that the position of the 2'-O-methylguanosine in the overall 3D structure of the tRNA plays an important role in TLR7 recognition.
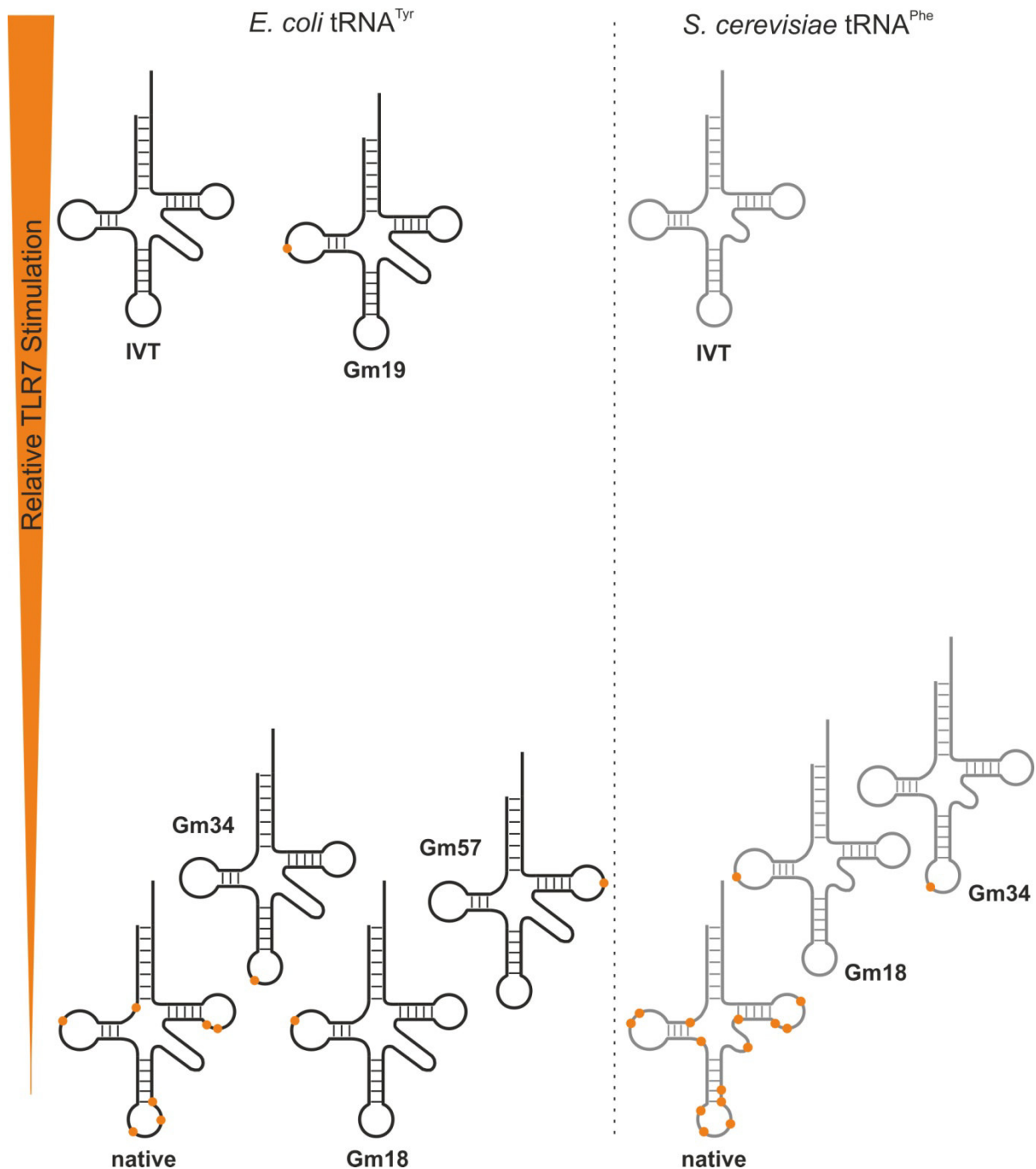
Figure 30: Overview of *E. coli* tRNA[Tyr] and *S. cerevisiae* tRNA[Phe] modivariants and their relative TLR7 stimulating potential in the immunoassay. Modified nucleotides in the cloverleaf are indicated with orange dots at their position.

3.2.3 Effect of point mutations in tRNA, at positions important for its tertiary structure, on TLR7 stimulation

If the position of Gm in the 3D structure is of importance for the immune stimulation mediated by TLR7, a change of this very structure should have a noticeable effect on

the amount of IFN-α measured in the experiments. Gm18 modivariants were synthesized that included one or more point mutations to abolish one, two or three base pairings necessary for the formation of the proper L-shaped 3D structure (Figure 31A and B; (127)).
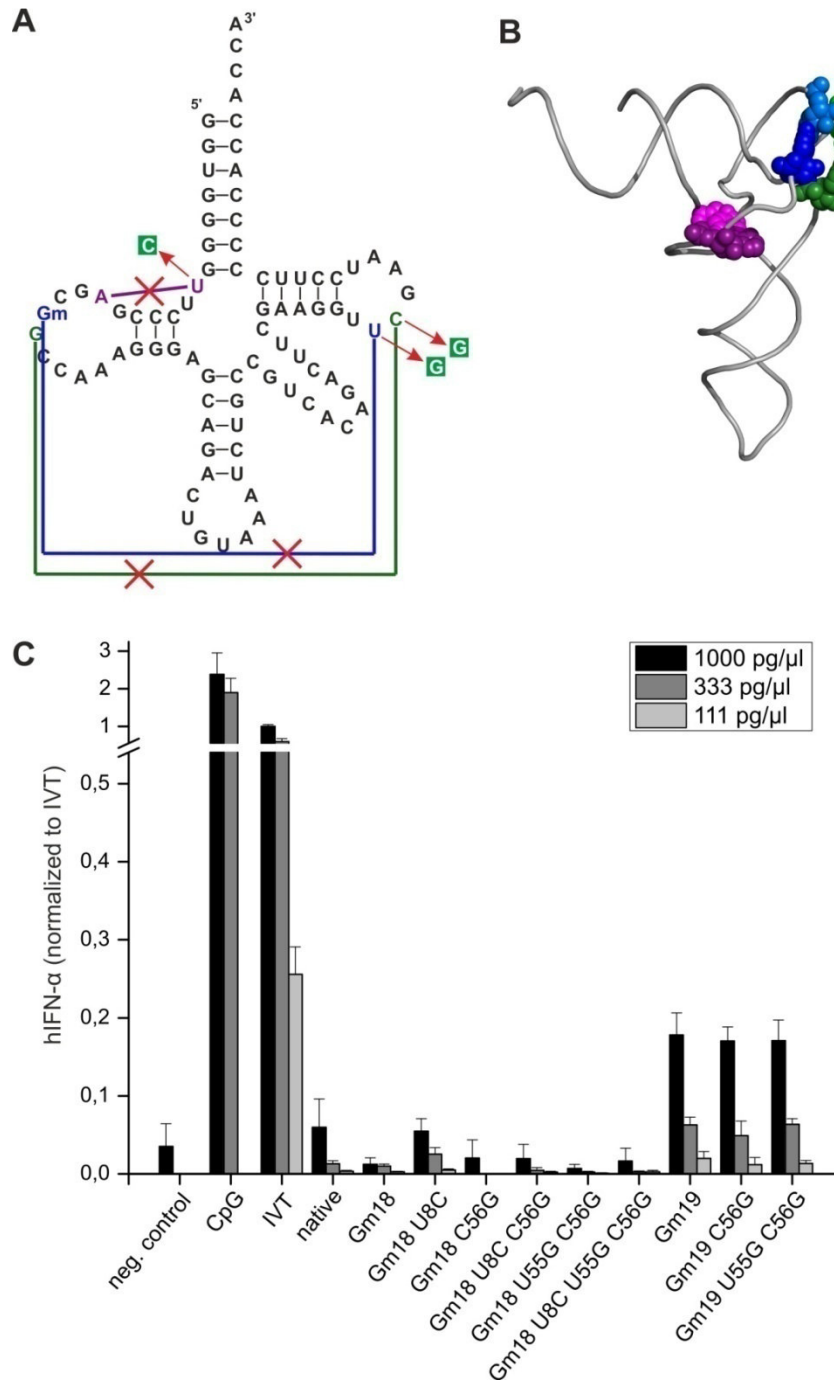
Figure 31: Effect of point mutations in tRNA on TLR7 stimulation. **A)** Base pairings important for the adoption of a proper L-shaped tertiary structure that were negated by point mutations. **B)** tRNA tertiary structure highlighting those three base pairings in the same color code. **C:** Effect of one, two or three point mutations that should have a strong impact on the tertiary structure, on the immune stimulatory potential of *E. coli* tRNA[Tyr] Gm18 or Gm19 modivariants as measured by IFN-α secretion. The results shown are from PBMCs of two different donors. IFN-α production from plasmacytoid dendritic cells was measured by ELISA and normalized to the unmodified tRNA transcript (IVT). The mutations had no effect on TLR7 stimulation. Gm18 modivariants were immunosilent independent of the point mutations present. Analog Gm19 modivariants were all stimulative.

As seen in Figure 31C, the mutations had no significant effect. All five Gm18 modivariants comprising point mutations tested, suppressed the immune stimulation comparable to the unmutated *E. coli* tRNA^{Tyr} Gm18. On the other hand Gm19 modivariants with those mutations were as immunostimulatory as the Gm19 modivariant without mutations. Those results indicate that the overall 3D structure of the tRNA might not be a determinant for TLR7 recognition. However, it should be noted, that it is not known how the tRNA 3D structure looks like under the acidic conditions inside the endosome and how much it differs from the canonical L-shape under physiological conditions.

3.2.4 Discovery of a dinucleotide motif responsible for silencing TLR7

In the next experiments the focus was set more on sequence than on 3D structure. The oligonucleotide MH490 comprising the 5' third of the *E. coli* tRNA^{Tyr} Gm18 modivariant including the modified nucleotide, was ligated with itself in an enzymatic reaction with T4 RNA ligase I (see sequence Figure 32B). The reaction mixture was run on a denaturing gel and bands corresponding in size to MH490 ligated two and four times with itself (referred to as 2x490 and 4x490 from here on) were cut out and the RNA was purified. The product RNAs contained two or four 2'-O-methylguanosines respectively in a similar sequence context, but without tRNA structure. The same procedure was repeated with oligonucleotide MH515 corresponding in sequence to MH490 but without any modification (product RNAs referred to as 2x515 and 4x515).

A
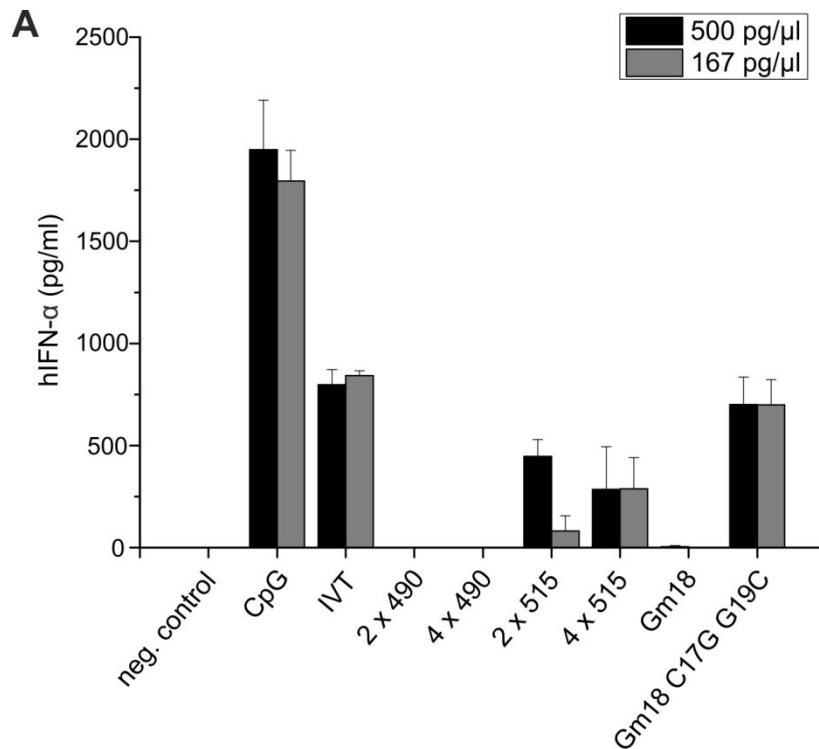
B MH 490: 5' GGUGGGGUUCCCGAGC**Gm**GCCAAAG 3'

2 x 490: 5' GGUGGGGUUCCCGAGC**Gm**GCCAAAGGGUGGGGUUCCCGAGC**Gm**GCCAAAG 3'

Figure 32: Investigating the effect of Gm in a similar sequence context that is not a tRNA and the effect of Gm18 in a tRNA^{Tyr} modivariant when its neighboring nucleotides are changed. **A)** The results shown are from PBMCs of one donor. IFN-α production from plasmacytoid dendritic cells was measured by ELISA. The two or four 2'-O-methylguanosines present in the 2x490 or 4x490 RNA were sufficient to completely abolish the immune stimulation whereas their unmodified counterparts 2x515 and 4x515 were stimulatory. Gm had a similar effect in RNAs that should structurally be distinct from tRNAs. The *E. coli* tRNA^{Tyr} Gm18 C17G G19C modivariant was the first Gm18 modivariant that was highly stimulative. **B)** Sequence of the oligo MH490 corresponding to the first 24 nt of *E. coli* tRNA^{Tyr} Gm18. 2x490 is MH490 ligated with itself. Hence 4x490 is composed four times of MH490. 2x515 and 4x515 correspond to the analog RNAs without modifications.

In the immunostimulation assay, the Gm containing RNAs 2x490 and 4x490 were not stimulative whereas the unmodified 2x515 and 4x515 RNAs led to a robust IFN-α secretion (Figure 32). These results show that 2'-O-Methylguanosine suppressed immune stimulation, when present in non-tRNA ribo-oligonucleotides of comparable size.

To investigate the impact of sequence changes in the context of tRNA, an *E. coli* tRNA^{Tyr} Gm18 modivariant was altered with point mutations (C17→G, G19→C) at the positions flanking the modified nucleotide. As the Gm19 modivariant was surprisingly high stimulative in contrast to Gm18 for example, it showed that even small changes could have a great effect on immunostimulation. Remarkably the Gm18 C17G G19C modivariant was suddenly a Gm18 construct nearly as stimulative as the IVT. Most

likely the Cytidin following is responsible for this effect. The Cytosine nucleobase is in close proximity to the 2'-OMe of the preceding Gm and might influence the interaction with the receptor. It is also striking that the only other Gm-containing modivariant that was stimulative so far was *E. coli* tRNA^{Tyr} Gm19 in which the Gm was followed by a C, too. To verify the hypothesis that Cytidine following a 2'-O-methylguanosine can negate the immune suppressive effect of Gm, an *E. coli* tRNA^{Tyr} Gm18 modivariant was tested with a C19 and an *E. coli* tRNA^{Tyr} Gm19 modivariant with a G20 instead of C20. Again the Gm18 modivariant was highly stimulative but the Gm19 C20G modivariant on the other hand was now immunosilent. A comprehensive experiment was designed comprising Gm18, Gm34 and Gm57 *E. coli* tRNA^{Tyr} modivariants in which the nucleotide at the position after the Gm was permutated to assess the effect of Gm at its natural occurring position and in the two other loops where it does not naturally occur in *E. coli* tRNA^{Tyr}. Additionally, the original 2'-O-methylgroup-bearing nucleotide was permutated as well, leading to *E. coli* tRNA^{Tyr} Am18, Um18 and Cm18 modivariants (Figure 33).

The results revealed, that the nucleobase of the 2'-O-Me bearing nucleotide is less important than the following downstream nucleobase. Gm, Am and Um followed 3' by a purin base led to an efficient silencing of TLR7 signaling (Figure 33A). Cm was an exception as the silencing effect was less efficient and showed a strong variation among the five donors. However, the ribose methylation at position 18 was not sufficient for silencing by itself but depended on a downstream neighboring purine (Figure 33B). In contrast, pyrimidines at the +1 position led to a reduced or even completely abolished immune suppression. The effect is milder for uridine and more pronounced for cytidine. It explains why *E. coli* tRNA^{Tyr} Gm18 was immunosilent whereas *E. coli* tRNA^{Tyr} Gm19 was highly stimulative. Exchange of C20 to G restored the silencing effect (Figure 33C). Consistent results were obtained for Gm and its downstream nucleobase when the modification was transplanted into the anticodon loop (Gm34, Figure 33D) or the T-loop (Gm57, Figure 33E).

In summary, the results imply a functional [DmR] motif (with D = all but C; R = purine), composed of a methylated ribose in a dinucleotide unit with a 3' purine, that suppresses TLR7 stimulation. Modivariants with a proper [DmR] motif were immune silent independent of the position of the motif in the tRNA.
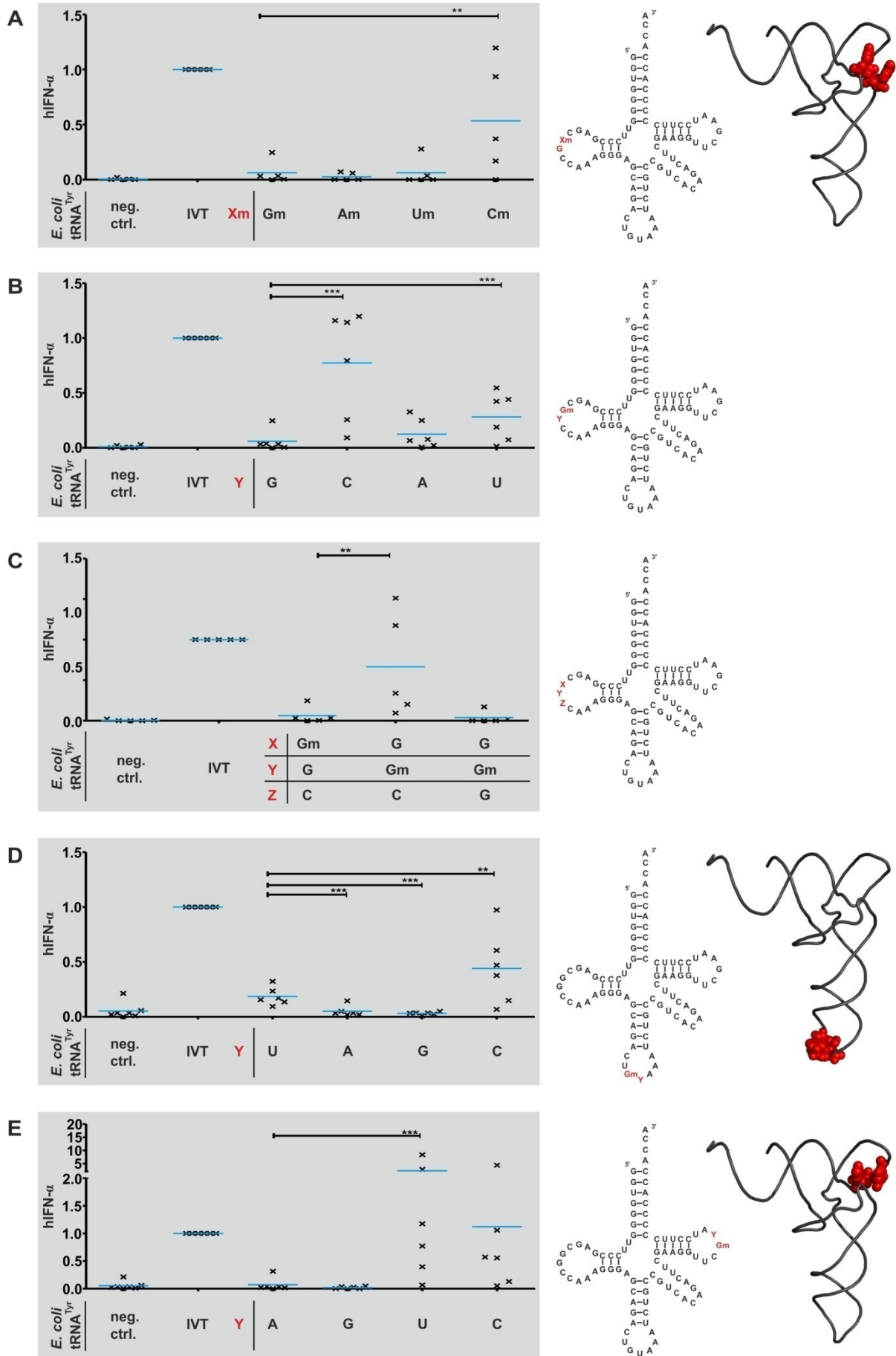
Figure 33: Effect and localization of the DmR dinucleotide motif responsible for TLR7 silencing by tRNA. PBMCs of five to six different donors were activated by transfection with 500 ng/ml tRNA (if not indicated otherwise). IFN-α production from plasmacytoid dendritic cells was measured by ELISA and was normalized to the unmodified tRNA transcript (IVT). Each dot in the figure represents one donor. To test for significance, Student's t -test was performed. (∗∗) P < 0.01, (∗∗∗) P < 0.001. **A)** Effect of permutation of nucleotide Xm18. **B)** Permutation of Y19. **C)** Transplantation of the motif by 1 nt downstream. **D)** Transplantation of the motif to the anticodon loop and permutation. **E)** Transplantation of the motif to the T-loop and permutation. Figure adapted from (128).

Moreover, a tRNA with an effective [DmR] motif is not only immunosilent, but can also suppress the immune stimulation as an antagonist when cotransfected with a stimulatory IVT (Figure 34).
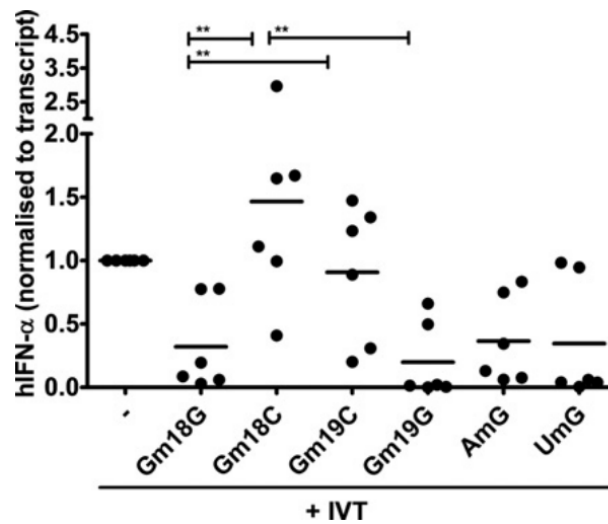
Figure 34: Immunosuppressing activity of selected RNA modivariants. 500 nanograms per milliliter of *in vitro* transcript (IVT) were cotransfected with or without ("- " label) 500 ng/ml tRNA modivariant to test for suppressive activity. IFN-α production was measured by ELISA and normalized to IVT alone ("- "). Each dot in the figure represents one donor. To test for significance, Student ' s t-test was performed. (∗∗) P < 0.01. Figure adapted from (128).

For more information about the work on suppression of TLR activation by 2'-O-methylated RNA please see:

A modified dinucleotide motif specifies tRNA recognition by TLR7.

<u>Steffen Kaiser</u>, Katharina Rimbach, Tatjana Eigenbrod, Alexander H. Dalpke and Mark Helm

RNA, 2014

2'-O-Methylation within Bacterial RNA Acts as Suppressor of TLR7/TLR8 Activation in Human Innate Immune Cells

Katharina Rimbach, <u>Steffen Kaiser</u>, Mark Helm, Alexander H. Dalpke and Tatjana Eigenbrod

J. Innate Immun., 2015

4 Summary and Discussion

DNA methylation by Dnmt2

Dnmt2 selectively methylates its tRNA substrates at the Cytidine at position 38 to 5-methylcytidine. However, Dnmt2's nearest neighbors in evolution are all DNA-cytosine C5-methyltransferases and methylate DNA. In this work it was assessed whether Dnmt2 is biochemically able to methylate DNA in addition to RNA. To this end short stretches of DNA were presented as substrate in the form of covalent chimeric molecules in the structural context of a tRNA by substituting RNA nucleotides with their corresponding deoxy-surrogates, starting with the single target nucleotide C38. Surprisingly $tRNA^{Asp}_{dC38}$ was more efficiently methylated than the natural all-ribo $tRNA^{Asp}$. The apparent K_m values were quite similar, the k_{cat} value on the other hand was clearly increased for $tRNA^{Asp}_{dC38}$. That means the lack of a single 2'-hydroxylgroup at position C38 led to a 2.3 times increased turnover while the binding properties were maintained. If the DNA stretch was increased from position 37 to 39 the hybrid tRNA was still a better substrate than the all-ribo tRNA and a stretch of five deoxynucleotides (position 36 to 40) was methylated comparable to the all-ribo tRNA. Only after the DNA content was increased even more, the methylation activity dropped, but Dnmt2 could still methylate tRNAs with a stretch of nearly 20 deoxynucleotides. Most likely the increasing content of deoxynucleotides leads to a more and more evident deviation from a proper tRNA tertiary structure, which depends, among other features, on the presence of A-form helices, until the hybrid tRNA can no longer be recognized by Dnmt2 as substrate.

It could be shown that Dnmt2 also tolerates other structural changes incorporated into the tRNA in addition to the deoxynucleotides like a nick in the anticodon loop, sequence changes to a small poly-C stretch and/or extension of the opened anticodon ends to the 3' and the 5' ends. All-ribo and dC38 $tRNA^{Asp}$ with a nick in the anticodon loop were methylated by Dnmt2, although to a much lesser extent than the corresponding tRNAs without the nick. Still the nicked $tRNA^{Asp}_{dC38}$ was clearly a better substrate than the nicked all-ribo tRNA and one nicked poly-C construct could even match the methylation efficiency of the all-ribo tRNA. In some cases, for example a tRNA with a whole anticodon stem loop composed of deoxynucleotides, the methylation rate was strongly increased after incorporation of the nick. Here it is

51

likely that the nick relieves the constraints induced by the non-RNA like helix formation by the DNA C3 endo pucker (B-shape), which allows improved recognition and methylation by Dnmt2.

As the 5'-tRNA half can be viewed as a guide RNA for the 3' RNA:DNA hybrid tRNA half the insights from the experiments were used for the development of an RNA-guided system for DNA methylation where the DNA part is no longer covalently linked to the RNA. With the RgD approach a standalone DNA oligonucleotide could be methylated by Dnmt2 *in vitro*.

The results show that Dnmt2 is definitely biochemically able to methylate DNA and, together with its strong sequence homology with DNA methyltransferases and the findings that it utilizes a DNA methyltransferase-like mechanism (129) to methylate tRNA, support the hypothesis that Dnmt2 had evolved from a DNA methyltransferase precursor that at some point switched its substrate specificity from DNA to RNA.

In a further set of experiments a proof of principle was shown for using the alternative cofactor SeAdoYn in a SELEX-like approach to screen for possible Dnmt2 substrate candidates in a degenerated pool of tRNAs. This may help to identify substrate preferences of Dnmt2 that can be used in search of further RNA and DNA substrates.

Impact of nucleotide modifications on TLR7 stimulation by tRNA

The innate immune system has evolved to be able to distinguish between self-RNA and non-self-RNA by sensing the nucleic acids as PAMPs with specialized PRR. For TLR7, sensing single-stranded RNA, modified nucleotides are a decisive factor to discriminate between self RNA and non-self RNA of invading pathogens. For tRNAs, the most abundant and most heavily modified subspecies of RNA, it could be shown that unmodified tRNAs trigger a strong TLR7 mediated immune response, as well as many tRNAs of bacterial origin that have less modifications and less chemically complex modifications than their eukaryotic counterparts. Although the major function of these modified nucleotides is to increase tRNA stability (9) and translational fidelity, they seem to have evolved a secondary function in immune recognition.

Different tRNAs, including native and *in vitro* transcribed tRNAs as well as modivariants synthesized by splint ligation from synthetic oligonucleotides, were

tested for their immune stimulatory potential on PBMCs derived from different blood donors. Surprisingly, bacterial *E. coli* tRNA^{Tyr} was immunosilent. Out of seven modified nucleotides present in native *E. coli* tRNA^{Tyr} a 2'-O-methylated guanosine (Gm) at position 18 in the D-loop could be identified as the reason for the lack of TLR7 stimulation (34). Moreover *E. coli* tRNA^{Tyr} could act as a TLR7 antagonist and suppress the immune response when present with otherwise stimulatory tRNA.

Continuing this work, different Gm bearing *E. coli* tRNA^{Tyr} modivariants were synthesized and analyzed for their immune stimulatory potential with regard to the localization of the modification. Additionally, up to three point mutations were introduced in some modivariants that abolished base pairings important for a proper tertiary structure. In the latter no effect could be found on TLR7 stimulation. *E. coli* tRNA^{Tyr} Gm18 was always immunosilent and *E. coli* tRNA^{Tyr} Gm19 was always immune stimulatory independent of the introduced mutations, indicating that the overall 3D structure of the tRNA might not be a determinant for TLR7 recognition. Focusing on the sequence context of the modified nucleoside it was discovered that the nucleotide following downstream of the 2'-O-methylated one is even more important (128). Modivariants bearing a Gm18, Am18 or Um18 were all completely immune silent when followed by a purine base. Cm18 was an exception as the silencing effect was not as efficient as for the other three and showed a high donor variance. The 2'-O-methylation is not sufficient by itself but necessitates a downstream purin to efficiently suppress immunostimulation as shown for Gm18 modivariants followed by a G (as in the wt) or an A. The effect is milder for a downstream U. Here the immune stimulation was clearly reduced but not completely ablated. A downstream C abrogated the immune silencing effect and these modivariants showed stimulation comparable to the unmodified IVT. Similar results were obtained when the Gm modification was transplanted into other tRNA domains where it does not naturally occur in *E. coli* tRNA^{Tyr} (anticodon- and T-loop). The strong immune stimulatory Gm19 modivariant tRNA could be transformed in a completely silent one by exchanging C20 with a G. These findings suggest a functional [DmR] motif (with D = all but C; R = purine), composed of a methylated ribose in a dinucleotide unit with a 3' purine, that suppresses TLR7 stimulation. A single [DmR] motif seems to be sufficient to completely ablate immune stimulation of a whole 85 nt long tRNA independent of its location. This could imply a processive type of RNA inspection by TLR7 scanning different regions for a dinucleotide motif.

5 Conclusion and Outlook

It was shown that Dnmt2 is biochemically able to methylate DNA and tolerates structural deviations from a tRNA to some degree. A small DNA oligonucleotide was methylated *in vitro* with help of two RNA molecules acting as guides. For a possible *in vivo* DNA target of Dnmt2 one may speculate that a partially single stranded DNA molecule with a deoxycytidine in a loop region could function as a Dnmt2 substrate, if there is some structural resemblance to a proper tRNA. It might even be possible that an RNA guided DNA methylation takes place. RNases like Angiogenin, an RNase A-like ribonuclease, have been shown to cleave tRNA in the anticodon loop (130). The 5' tRNA fragments resulting from this cleavage would be very similar to the one used as guide in the experiments with the hybridized constructs or the RgD approach.

Only recently it was shown in *Schizosaccharomyces pombe* that C38 methylation by the Dnmt2 homolog Pmt1 is dependent on the tRNA hypermodification queuosine (Q). It was discovered that the C38 methylation level was decreased *in vivo* by about 80% if the tRNA was not modified with a queuosine Q which is a naturally occurring modification of position 34 in tRNA^{Asp} (131). Although there are fewer modifications in DNA and especially no complex hypermodifications like queuosine known to date, this finding gives rise to the question if Dnmt2's ability to methylate DNA is only possible if another DNA modification is already present. Therefore, Dnmt2 DNA substrates might be found in organisms that incorporate other, possibly even yet unknown, DNA modifications.

In the second part of this work the impact of modified nucleotides on TLR7 recognition of tRNAs was investigated and a functional [DmR] motif was discovered that if present in a tRNA bestows antagonistic properties unto it. Considering that G- and U-rich ssRNAs have been found to stimulate TLR7 (74) and the TLR7 agonist loxoribine is a guanosine analog, it is interesting to see that the [GmG] motif had the most pronounced TLR7 inhibitory effect. Understanding how modifications affect TLR7 recognition is important for many reasons. Invading pathogens may use modified RNA to avoid detection. If it is known how they do it, measures can be taken against it. The immune stimulatory potential of RNA has also to be considered for therapeutic approaches utilizing small interfering RNAs (siRNA). Here, the

incorporation of modified nucleotides can prevent unwanted side effects through TLR activation. On the other hand there are cases were both are wanted (132), the proinflammatory and the silencing activities of a siRNA for greater therapeutic benefits, for example in antiviral applications. Additionally, TLR7 plays a role in autoimmune diseases like systemic lupus erythematosus (SLE). Oligonucleotide-based inhibitors of TLR7 were shown to have therapeutic potential. They restored glucocorticoid sensitivity to pDCs *in vitro* thereby allowing treatment with smaller doses of corticosteroid drugs (133).

6 Material and Methods

6.1 Material

6.1.1 Instruments

Centrifuge 5810 R	Eppendorf (Hamburg, Germany)
Mixing Block MB-102	BIOER (Hangzhou, China)
NanoDrop 2000 Spectrophotometer	Thermo Scientific (Waltham, USA)
Quantum Model 3000 Gel Doc System	PEQLAB Biotechnologie GmbH (Erlangen, Germany)
Shaker DOS-10L	neoLab (Heidelberg, Germany)
Speedvac Concentrator plus	Eppendorf
Thermocycler	Biometra (Goettingen, Germany)
Thermomixer comfort	Eppendorf
Typhoon 9400 variable mode imager	GE Healthcare (Buckinghamshire, UK)
Wallac 1409 liquid scintillation counter	PerkinElmer (Waltham, USA)

6.1.2 Chemicals and Reagents

[^{3}H]-*S*-adenosyl methionine (1 µCi/µL, 80 Ci/ mmol)	Hartmann Analytic (Braunschweig, Germany)
1-Propanol	Merck (Darmstadt, Germany)
2'-Deoxy-5-methylcytidine	Berry & Associates (Dexter, USA)
2'-Deoxyadenosine	Sigma Aldrich (St. Louis, USA)
2'-Deoxycytidine	Sigma Aldrich

2'-Deoxyguanosine	Sigma Aldrich
5-Methylcytidine	Sigma Aldrich
Acetone >99.5%	Sigma Aldrich
Adenosine	Sigma Aldrich
AdoEnYn	Elmar Weinhold (Aachen, Germany)
AlexaFluor 594 azide	Invitrogen (Carlsbad, USA)
Ammonium Acetate	Roth (Karlsruhe, Germany)
Ammonium peroxydisulfate	Roth
Bromphenol blue	Merck
Chloroform	Sigma Aldrich
Cytidine	Sigma Aldrich
Dichlorodimethylsilane	Sigma Aldrich
Dithiothreitol (DTT)	Fermentas (St. Leon-Rot, Germany)
DNA loading dye 6x	Fermentas
dNTPs (for PCR)	Rapidozym (Berlin, Germany)
Ethanol >99.5%	Roth
Ethidium bromide	AppliChem (Darmstadt, Germany)
Ethylendiaminetetraacetic acid (EDTA)	Roth
Fluka Analytical Ammonium hydroxide solution > 25% in H_2O	Sigma Aldrich
Formamide	Roth
GelRed 3x	Biotium (Hayward, USA)
GenRuler 100 bp plus DNA ladder	Fermentas

Glycerol	Sigma Aldrich
Guanosine	Sigma Aldrich
Hydrochloric acid 37%	Grüssing (Filsum, Germany)
Isobutyric acid >99%	Sigma Aldrich
Lithium perchlorate, battery grade, dry	Sigma Aldrich
Magnesium chloride	Roth
NTPs (for IVT)	Sigma Aldrich
Roti-Phenol ph 7.5 – 8.0	Roth
Rotiphorese 10x TBE buffer	Roth
Rotiphorese Gel 40 (19:1)	Roth
Rotiphorese sequencing gel buffer concentrate	Roth
Rotiphorese sequencing gel concentrate	Roth
Rotiphorese sequencing gel diluent	Roth
S-adenosyl methionine	NEB (Frankfurt a. M., Germany)
SeAdoYn	Elmar Weinhold (Aachen, Germany)
SeaKem LE Agarose	Lonza (Basel, Switzerland)
Sodium acetate	VWR (Radnor, USA)
Sodium chloride	VWR
SYBR Gold	Invitrogen
TAMRA-Azide-Biotin	Jena Bioscience (Jena, Germany)
TEMED	Roth
Thymidine	Sigma Aldrich

Trichloroacetic acid	Roth
Tris	Roth
Tris-HCl	Roth
TritonX-100	Sigma Aldrich
Uridine	Sigma Aldrich

6.1.3 Disposables

Whatman filter paper	Roth
TLC plastic sheets 20x20 cm cellulose	Merck
TLC plastic sheets 20x20 cm silica gel	Merck
DyeEx 2.0 Spin Kit	Qiagen (Hilden, Germany)
Nanosep MF Centrifugal Devices 0.45 µM	Pall (New York, USA)
MicroSpin G50 size-exclusion columns	GE Healthcare (Buckinghamshire, UK)
Scintillation counting vials	Roth

6.1.4 Buffers

PCR buffer	67 mM Tris-HCl (pH 8.8), 16 mM $(NH_4)_2SO_4$, 0.01 % Tween-20
Strasbourg buffer	40 mM Tris-HCl (pH 8.8), 1 mM spermidine, 5 mM DTT, 0.01 % Triton X-100
TBE buffer	100 mM Tris (pH8.3), 90 mM boric acid, 1 mM EDTA
PAGE loading buffer (denaturing)	90 % (v/v) formamide, 9.9 % 10x TBE 0.1 % bromphenol blue

PAGE loading buffer (non-denaturing)	90 % (v/v) 1x TBE, 10 % glycerin
Elution buffer	0.3 M sodium acetate, Tris-HCl (pH 5.5)
KL buffer	50 mM Tris-HCL (pH 7.4), 10 mM $MgCl_2$
Methylation assay buffer	100 mM Tris-HCl (pH 8.0), 100 mM NH_4OAc; 0.1 mM EDTA, 10 mM $MgCl_2$
PUS buffer	100 mM Tris–HCl (pH 8.0), 100 mM NH_4OAc, 0.1 mM EDTA 10 mM $MgCl_2$, 0.5 mM DTT
Nuclease buffer	30 mM NH_4OAc (pH 5.0), 20 µM $ZnCl_2$
TLC running buffer I	isobutyric acid : concentrated ammonia : H_2O (50:1.1:28.9 [v:v:v])
TLC running buffer II	isopropanol : concentrated HCl : H_2O (68:18:14 [v:v:v])

6.1.5 Enzymes

Taq DNA polymerase	5 u/µl	Rapidozym
MvaI (BstNI)	10 u/µl	Fermentas
DNase I	50 u/µl	Fermentas
T4 polynucleotide kinase	10 u/µl	Fermentas
T4 DNA ligase	30 u/µl	Fermentas
T4 RNA ligase 1	10 u/µl	Fermentas
T4 RNA ligase 2		expressed and purified in our lab
T7 RNA Polymerase		expressed and purified in our lab
hDnmt2		expressed and purified in our lab or in the lab of Albert Jeltsch

Nuclease P1	Sigma Aldrich
FastAP thermosensitive alkaline phosphatase	Fermentas
Snake venom phosphodiesterase	Worthington (Lakewood, USA)

6.1.6 Native tRNAs

total *E. coli* tRNA	Roche Diagnostics (Mannheim, Germany)
E. coli tRNA^{Tyr}	Sigma Aldrich (Steinheim, Germany)
S. cerevisiae tRNA^{Phe}	Gérard Keith (Strasbourg, France)

6.1.7 Oligonucleotides

Ribonucleotides are indicated by plain letters, deoxyribonucleotides are indicated as dC, dT, dA, dG, or dm^{5}C, except for template DNA, primers and ligation splints which are presented in small letters. Underlined letters indicate a modification and/or mutation.

Table 1: Oligonucleotides used for mouse/human tRNA^{Asp} and its derived constructs.

Oligo name	Category	sequence (5'-3' orientation)	Supplier
MH 117	PCR template	tggctccccgtcggggaatcgaaccccggtctcccgcgtgacaggcggggatactcacca ctatactaacgaggagacggtaccgggtaccgtttcgtcctcacggactcatcagtcctcgtt atctccctatagtgagtcgtatt	IBA (Göttingen)
MH 53	forward primer	cgcgcgaagcttaatacgactcactata	IBA (Göttingen)
MH 118	reverse primer	tggctccccgtcggggaatcg	IBA (Göttingen)
MH 570	splint	ggaatcgaaccccggtctcccgcgtgacaggcggggatactcaccactatac	IBA (Göttingen)
MH 629	Splint 2	Aggcggggatactcaccactatactaacgaggatggctccccgtcggggaatcgaaccc cggtct	IBA (Göttingen)
MH 565	fragment 1	UCCUCGUUAGUAUAGUGGUGAGUAUCCCCGCCU	IBA (Göttingen)
MH 586	fragment 1	UCCUCGUUAGUAUAGUGGUGAGUAUCdCdCdCdGdCdCdT	Purimex (Grebenstein)
MH 646	fragment 1	UCCUCGUUAGUAUAGUGGUGAGUAUCCCCGCCU<u>AUAUC</u>	IBA (Göttingen)
MH 648	fragment 1	<u>UGGC</u>UCCUCGUUAGUAUAGUGGUGAGUAUCCCCGCCU	IBA (Göttingen)

MH 567	fragment 1	UCCUCGUUAdGdUdAdUdAdGdUdGdGdUdGdAdGdUdAdUCCC CGCCU	IBA (Göttingen)
MH 660	fragment 1	dTdCdCdCdGdTdCdCdCdGdCdCdT	IBA (Göttingen)
MH 566	fragment 2	GUCACGCGGGAGACCGGGGUUCGAUUCCCCGACGGGGAGC CA	IBA (Göttingen)
MH 568	fragment 2	GUCACGCGGGAGACdCdGdGdGdGdUdUdCdGdAdUdUdCdCd CdCdGACGGGGAGCCA	IBA (Göttingen)
MH 569	fragment 2	GUCAd<u>m⁵C</u>GCGGGAGACCGGGGUUCGAUUCCCCGACGGGG AGCCA	IBA (Göttingen)
MH 606	fragment 2	GUCA<u>m⁵C</u>GCGGGAGACCGGGGUUCGAUUCCCCGACGGGGA GCCA	IBA (Göttingen)
MH 571	fragment 2	GUCAdCGCGGGAGACCGGGGUUCGAUUCCCCGACGGGGAG CCA	IBA (Göttingen)
MH 584	fragment 2	GUCdAdCdGCGGGAGACCGGGGUUCGAUUCCCCGACGGGG AGCCA	IBA (Göttingen)
MH 585	fragment 2	GUdCdAdCdGdCGGGAGACCGGGGUUCGAUUCCCCGACGGG GAGCCA	IBA (Göttingen)
MH 587	fragment 2	dGdTdCdAdCdGdCdGdGdGAGACCGGGGUUCGAUUCCCCGA CGGGGAGCCA	Purimex (Grebenstein)
MH 623	fragment 2	dGdTdCdAdCdGdCdGdGdGdAdGdACCGGGGUUCGAUUCCCC GACGGGGAGCCA	IBA (Göttingen)
MH 642	fragment 2	dGdTdCdAdCdGdCdGdGdGdAdGdAdCdCdGdGGGUUCGAUUC CCCGACGGGGAGCCA	IBA (Göttingen)
MH 619	fragment 2	<u>dCdCdCdC</u>dCGCGGGAGACCGGGGUUCGAUUCCCCGACGGG GAGCCA	IBA (Göttingen)
MH 638	fragment 2	<u>dCdCdCdC</u>dCdGdCdGdGdGAGACCGGGGUUCGAUUCCCCGA CGGGGAGCCA	IBA (Göttingen)
MH 643	fragment 2	dGdAdTdAdTdCdCdCdCdCdGdCdGdGdGAGACCGGGGUUCGA UUCCCCGACG	IBA (Göttingen)
MH 647	fragment 2	dGdAdTdAdTdCdCdCdCdCdGdCdGdGdGdGdAdGdAdCdCdGdGG GUUCGAUUCCCCGACGGGGAGCCA	IBA (Göttingen)
MH 624	fragment 2	dGdTdCdAdCdGdCdGdGdG	IBA (Göttingen)
MH 639	fragment 2	dGdTdCdAdCdGdCdGdGdGdGdAdGdA	IBA (Göttingen)
MH 640	fragment 2	<u>dCdCdCdC</u>dCdGdCdGdGdGdGdAdGdA	IBA (Göttingen)
MH 650	fragment 2	<u>dGdAdTdAdTdCdCdCdC</u>dCdGdCdGdGdGdGdAdGdAdCdCdGdG	IBA (Göttingen)
MH 696	fragment 2	<u>dGdAdTdAdTdCdCdCdC</u>dCdGdCdGdGdGdGdAdGdAdCdCd<u>dT</u>dG	IBA (Göttingen)
MH 659	fragment 2	dGdTdCdAdCdGdCdGdGdGdGdAdCdGdGdGdGdA	IBA (Göttingen)
MH 674	fragment 2	dCdCdCdCdGdCdGdGdGdGdAdCdGdGdGdGdA	IBA (Göttingen)
MH625	fragment 3	AGACCGGGGUUCGAUUCCCCGACGGGGAGCCA	IBA (Göttingen)
MH641	fragment 3	CCGGGGUUCGAUUCCCCGACGGGGAGCCA	IBA (Göttingen)
MH649	fragment 3	GGUUCGAUUCCCCGACGGGGAGCCA	IBA (Göttingen)
MH695	fragment 3	<u>UGUUCGAUUCAC</u>AGACGGGGAGCCA	IBA (Göttingen)

Table 2: Oligonucleotides used for *E. coli* tRNA^{Tyr}.

Oligo name	Category	sequence (5'-3' orientation)	Supplier
MH 375	PCR template	tggtggtgggggaaggattcgaaccttcgaagtctgtgacggcagatttacagtctgctccct ttggccgctcgggaaccccaccgacggtaccgggtaccgtttcgtcctcacggactcatca gggtggggtttctccctatagtgagtcgtatt	IBA (Göttingen)
MH 53	forward primer	cgcgcgaagcttaatacgactcactata	IBA (Göttingen)
MH 376	reverse primer	tggtggtggggg	IBA (Göttingen)
MH 510	splint	tggtggtgggggaaggattcgaaccttcgaagtctgtgacggcagatttacagtctgctccct ttggccgctcgggaaccccacc	IBA (Göttingen)
MH 515	fragment 1	GGUGGGGUUCCCGAGCGGCCAAAG	IBA (Göttingen)
MH 490	fragment 1	GGUGGGGUUCCCGAGC<u>Gm</u>GCCAAAG	Dharmacon (Chicago)
MH 563	fragment 1	GGUGGGG<u>C</u>UCCCGAGC<u>Gm</u>GCCAAAG	IBA (Göttingen)
MH 627	fragment 1	GGUGGGGUUCCCGAGC<u>Gm</u><u>C</u>CCAAAG	IBA (Göttingen)
MH 680	fragment 1	GGUGGGGUUCCCGAGC<u>Gm</u><u>A</u>CCAAAG	IBA (Göttingen)
MH 679	fragment 1	GGUGGGGUUCCCGAGC<u>Gm</u><u>U</u>CCAAAG	IBA (Göttingen)
MH 617	fragment 1	GGUGGGGUUCCCGAGG<u>Gm</u><u>C</u>CCAAAG	Biomers (Ulm)
MH 681	fragment 1	GGUGGGGUUCCCGAGC<u>Am</u>GCCAAAG	IBA (Göttingen)
MH 616	fragment 1	GGUGGGGUUCCCGAGC<u>Um</u>GCCAAAG	Biomers (Ulm)
MH 682	fragment 1	GGUGGGGUUCCCGAGC<u>Cm</u>GCCAAAG	IBA (Göttingen)
MH 532	fragment 1	GGUGGGGUUCCCGAGCG<u>Gm</u>CCAAAG	IBA (Göttingen)
MH 628	fragment 1	GGUGGGGUUCCCGAGCG<u>Gm</u>GCAAAG	IBA (Göttingen)
MH 508	fragment 2	GGAGCAGACUGUAAAUCUGCCGUCACAG	IBA (Göttingen)
MH 516	fragment 2	GGAGCAGACU<u>Gm</u>UAAAUCUGCCGUCACAG	IBA (Göttingen)
MH 683	fragment 2	GGAGCAGACU<u>Gm</u>AAAAUCUGCCGUCACAG	IBA (Göttingen)
MH 684	fragment 2	GGAGCAGACU<u>Gm</u>GAAAUCUGCCGUCACAG	IBA (Göttingen)
MH 685	fragment 2	GGAGCAGACU<u>Gm</u><u>C</u>AAAUCUGCCGUCACAG	IBA (Göttingen)
MH 509	fragment 3	ACUUCGAAGGUUCGAAUCCUUCCCCCACCACCA	IBA (Göttingen)
MH 517	fragment 3	ACUUCGAAGGUUC<u>Gm</u>AAUCCUUCCCCCACCACCA	IBA (Göttingen)
MH 531	fragment 3	ACUUCGAAGGUU<u>GG</u>AAUCCUUCCCCCACCACCA	Eurofins (Ebersberg)
MH 564	fragment 3	ACUUCGAAGGU<u>GG</u>GAAUCCUUCCCCCACCACCA	IBA (Göttingen)
MH 686	fragment 3	ACUUCGAAGGUUC<u>Gm</u><u>G</u>AUCCUUCCCCCACCACCA	IBA (Göttingen)
MH 687	fragment 3	ACUUCGAAGGUUC<u>Gm</u><u>U</u>AUCCUUCCCCCACCACCA	IBA (Göttingen)
MH 688	fragment 3	ACUUCGAAGGUUC<u>Gm</u><u>C</u>AUCCUUCCCCCACCACCA	IBA (Göttingen)

Table 3: Oligonucleotides used for *S. cerevisiae* tRNA^{Phe}.

Oligo name	Category	sequence (5'-3' orientation)	Supplier
MH 216	splint	tggtgcgaattctgtggatcgaacacaggacctccagatcttcagtctggcgctctcccaa ctgagctaaatccgc	IBA (Göttingen)
MH 535	fragment 1	GCGGAUUUAGCUCAGUUGGGAGAGCGCCAGACU<u>Gm</u>AA	IBA (Göttingen)
MH 498	fragment 2	GAUCUGGAGGUCCUGU	Biomers (Ulm)
MH 499	fragment 3	GUUCGAUCCACAGAAUUCGCACCA	Biomers (Ulm)
MH 530	fragment 1a	GCGGAUUUAGCUCAGUU<u>Gm</u>GGAGAGCGCC	Eurofins (Ebersberg)
MH 450	fragment 2a	P-AGACUGAAGAUCUGGAGGUCCUG	Dharmacon (Chicago)
MH 215	fragment 3a	P-UGUUCGAUCCACAGAAUUCGCACC A	IBA (Göttingen)

6.2 Methods

6.2.1 Polymerase chain reaction

50 µl reactions were performed in PCR buffer supplemented with 3 mM $MgCl_2$, dNTPs 1.2 mM each, 1 µM DNA template, 5 µM of each primer and 0.1 u/µl Taq DNA polymerase. The template was a reverse complement of the target tRNA with a hammerhead (hh) ribozyme and a T7 promotor.

The PCR programme consisted of a denaturation step (2 min at 92°C), 25 cycles of annealing (20 sec at 57°C), elongation (45 sec at 72°C) and denaturation (15 sec at 92°C), and a final elongation step of 10 min at 72°C.

The products were stored at -20°C until used for *in vitro* transcription.

6.2.2 Agarose gel electorphoresis

An aliquot of the PCR reaction mixture after the PCR and an aliquot of the mixture before the addition of the enzyme were mixed with 1/6 vol of 6x DNA loading dye and run on a 2% agarose gel, prestained with ethidium bromide, in 1x TBE at 150 V for 45 min. The PCR product was visualized by fluorescence with the gel doc.

6.2.3 *In vitro* transcription

1 ml transcription reactions were performed with 100 µl of non-purified PCR product or, in case of *S. cerevisiae* tRNA^{Phe}, 8 µg MvaI (BstNI)-linearized tRNA coding plasmid in Strasbourg buffer supplied with 30 mM $MgCl_2$, 10 mM DTT, 2 ng/µl BSA, NTPs 4 mM each and 50 ng/µl T7 RNA polymerase for 4 h at 37°C. Under these reaction conditions the generated hammerhead-tRNA-transcripts were autocatalyticly cleaved by the hh-ribozyme leading to tRNAs with a free hydroxyl group at the 5' end. During the reaction, the formation of a white precipitate of magnesium pyrophosphate indicated the success of the reaction.

6.2.4 Denaturing polyacrylamide gel electrophoresis (PAGE)

For analysis and purification of reactions containing RNA, the reaction mixture was mixed with 1 vol of PAGE loading buffer, loaded on a 10% denaturing polyacrylamide

gel and run in 1x TBE buffer for 100 min at 18 W. For 100 ml of PAGE, 400 µl of 10% APS solution and 80 µl of TEMED were used. The gels were poured using standard glas plates (20 x 20 cm) coated with dichlorodimethylsilane and 1 mm wide spacers. Pockets were formed by sticking in combs of the appropriate size. After polymerization the comb was removed, the pockets were rinsed with 1x TBE, and the gel fitted into the gel running apparatus.

6.2.5 Visualization of RNA after PAGE

PAGE gels loaded with higher amounts of nucleic acids like transcription and ligation mixtures were analyzed by UV-shadowing. The gel was placed on a fluorescent TLC plate and irradiated with a UV-lamp at 256 nm. As nucleic acids absorb light at this wavelength, dark bands could be seen in contrast to the background of the green fluorescing TLC plate.

Analytical PAGE gels and gels loaded with not enough amounts of nucleic acids for UV-shadowing were stained with GelRed or SYBR Gold and visualized by fluorescence with the gel doc or the Typhoon scanner.

6.2.6 Elution and precipitation of gel purified RNA

The PAGE gel bands containing the desired product were excised from the gel, cut into small pieces and crushed with a scalpel, split into 1.5 ml reaction tubes and eluted in 450 µl elution buffer over night at 20°C and shaking with 550 rpm. The solution was seperated from gel residues with Nanosep 0.45 µm membrane filters by centrifugation at 2500 rcf for 1 min. The reaction tube containing the gel was rinsed with an additional 100 µl of elution buffer. The solution was filtered through the same Nanosep and united with the other part. The RNA was precipitated by addition of 2.5 vol of -80°C cold 100% Ethanol. The sample was vortexed and stored at -20°C for at least 2 h. After vortexing again the RNA was peleted by centrifugation at 16 000 rcf for 90 – 120 min. The supernatant was removed and the pellet was dried in an Eppendorf speedvac. Finally the pellet was resuspended in Millipore water and the RNA concentration was determined with a Nanodrop spectrophotometer.

6.2.7 Splinted ligation of tRNA fragments to full-length tRNAs

Splinted ligation was performed as described previously, by annealing two (for tRNA^{Asp} RNA:DNA hybrid constructs) or three (for tRNA^{Tyr} and tRNA^{Phe} modivariants) synthetic fragments of RNA or DNA:RNA hybrids, corresponding in sequence to the desired tRNA onto a 52 nt long (for tRNA^{Asp}) or full-length (for tRNA^{Tyr} and tRNA^{Phe}) reverse complementary oligodeoxynucleotide (134,135). Appropriate fragments (4 nmol) were 5'-phosphorylated by incubating in KL buffer supplemented with 5 mM ATP, 5 mM DTT and 0.75 u/µl T4 polynucleotide kinase (PNK, Fermentas, Germany) in a final volume of 150 µl in the thermomixer at 37°C for 1 h. To the phosphorylation reaction mixture(s) an equimolar amount of the 5'-fragment and the DNA splint were added, as well as KL buffer, ATP (5 mM) and DTT (5 mM) leading to a final volume of 500 µl and a 8 µM concentration of each fragment. The RNA fragments were hybridized to the DNA splint by heating to 75°C in the thermomixer for 4 min and letting the reaction mixture cool down to room temperature for 15 min. Then T4 DNA ligase (1.5 u/µl; Fermentas) and T4 RNA ligase 2 (22 ng/µl) were added and the ligation was performed in the thermomixer at 16°C over night. Splint DNA, in tRNA$^{Asp}_{dC38}$ and all-ribo tRNA^{Asp} constructs and in the tRNA^{Tyr} and tRNA^{Phe} modivariants, was removed by addition of 1.5 u/µL DNase I (Fermentas), followed by 1 h of incubation at 37°C. The DNase digestion was omitted for hybrids containing DNA stretches of 3 nucleotides in length or more. All tRNA and tRNA hybrids were purified from ligation mixtures by denaturing PAGE, excised and eluted from the gel, and precipitated with ethanol. Concentrations were calculated from absorption at 254 nm, as determined on a Nanodrop ND-2000 spectrometer.

6.2.8 Dnmt2 protein preparation

Cloning, expression and purification by IMAC (immobilized metal ion affinity chromatography) of the human DNMT2-His6 fusion protein was performed as described before (14,19). Expression was done in *E. coli* (DE3) Rosetta2 pLysS cells. The protein expression was induced at OD$_{(600\,nm)}$ = 0.6 with 1 mM IPTG and the cells were harvested 3 h after induction.

6.2.9 Tritium incorporation assay of *in vitro* methylation

In vitro methylation was done essentially as described (136). The *in vitro* methylation assay measures the transfer of a tritiated methyl group from its donor [^{3}H]-*S*-adenosyl methionine (^{3}H-SAM , 1 µCi/µL, 80 Ci/ mmol, from Hartmann Analytics, Braunschweig, Germany) onto the target tRNA, which is catalyzed by m^{5}C-methyltransferases. The tRNA is precipitated on small filters and the radioactive signal counted in a scintillation counter. The standard reaction volume was 40 µl. Unless stated otherwise, 120 pmol tRNA were diluted in water and heated to 65 °C for 2 min. tRNA-MT-assay buffer and DTT were added immediately to final concentrations of 100 mM Tris-HCl pH 8.0; 100 mM NH$_4$OAc; 0.1 mM EDTA, 10 mM MgCl$_2$ and 10 mM DTT. ^{3}H-SAM-Stock solution (10x; containing cold and ^{3}H-SAM) was added to a final concentration of 0.9 µM SAM and 1 µCi per sample. The enzyme was added to final concentrations of 1 µM and mixed well by pipetting. At various time points 8 µL aliquots were spotted onto small Whatman filters and precipitated in 5 % ice-cold TCA, followed by two washes at room temperature for 20 min and 10 min, respectively in 5 % TCA. Then the filters were swirled in EtOH. After drying, the Whatman filters were transferred into scintillation vials and 3 ml of Ultima Gold MV liquid scintillation cocktail (PerkinElmer, Waltham, USA) were added into each vial. The incorporated tritium was measured by liquid scintillation counting with a Wallac 1409 liquid scintillation counter (PerkinElmer, Waltham, USA). Measuring duration was 60 sec per sample. 1 µL of the 10x SAM-stock solution was spotted in duplicate as a standard for specific activity. Initial reaction rates were extracted from methylation kinetics (Figure 11) by linear regression after background correction. From the initial rates, K_m and V_{max} values were obtained by a non-linear two component least square fit, and k_{cat} was calculated from V_{max}.

Thin-layer chromatography

For the RgD Experiments the concentration of nucleic acid and enzyme was doubled and the ratio of hot to cold SAM was increased (2.3 µCi per sample). The total reaction volume was 50 µl. At two time points after reaction start (15 and 120 minutes), aliquots were spotted on a whatman filter paper and measured with the Cherenkov counter. The remaining portion of the sample was subjected to a nucleic acid precipitation with LiClO$_4$ in acetone to purify the nucleic acids. The precipitation

with perchlorate and acetone was chosen over standard EtOH precipitation, as it is more suited to precipitate small oligonucleotides. The pellet was then resuspended in H_2O and further purified with a MicroSpin G50 size-exclusion column (GE Healthcare, Solingen, Germany). The purified oligonucleotides were enzymatically hydrolyzed to nucleosides with nuclease P1, snake venom phosphodiesterase and shrimp alkaline phosphatase. After the addition of commercially available nucleosides as standards(all Sigma-Aldrich, Missouri, US, except dm[5]C, Berry & Associates, Dexter, USA), the samples were concentrated and spotted on a 10 cm x 10 cm cellulose TLC plate (Merck ref#1.05577.000, Darmstadt, Germany) and subjected to two-dimensional thin-layer chromatography. For the first dimension the solvent was isobutyric acid : concentrated ammonia : H_2O (50:1.1:28.9 [v:v:v]) and for the second dimension isopropanol : concentrated HCl : H_2O (68:18:14 [v:v:v]). After each run the TLC plate was dried for several hours in a fume hood. The nucleoside spots were visualized with a UV-lamp (256 nm), marked with a pencil, and the cellulose corresponding to a spot was scraped off with a scalpel and transferred to areaction tube. The nucleosides were extracted with water and subjected to liquid scintillation counting.

6.2.10 Reaction with AdoEnYn or SeAdoYn

In 40 µl total reaction volume 320 pmol *in vitro*-transcribed tRNA[Asp] were incubated together with 320 pmol Dnmt2 in the presence of either 50 µM AdoEnYn or 50 µM SeAdoYn in PUS buffer for 2 h at 37°C. After the reaction, the tRNA was purified by phenol/$CHCl_3$ extraction followed by EtOH precipitation and resuspended in 5 µl H_2O.

Then, the purified, alkynylated tRNA was subjected to a CuAAC click reaction. It was incubated in phosphate buffer (100 mM, pH 8) supplied with 2.5 mM TPTA (tris-[4-(3-hydroxypropyl)-(1,2,3)triazolyl-1-methyl)amine) ligand, 5 mM sodium ascorbate, 0.5 mM $CuSO_4$ and either 50 µM Alexa 594 azide or 50 µM TAMRA-Azide-Biotin for 3 h at 25°C. The total reaction volume was 10 µl. Excess dye was removed with a DyeEx column after increasing the volume to 30 µl with H_2O. Afterwards the tRNA was run on a denaturing gel and the gel analyzed for fluorescently labeled tRNAs with the Typhoon scanner.

6.2.11 HPLC-MS/MS Analysis

The LC-MS/MS experiment was performed by Dr. Stefanie Kellner.

0.5 µg of either Dnmt2 treated or untreated tRNA was dissolved in 20 mM NH_4OAc pH 5.3 and digested to nucleosides as described before (137). Additionally the commercial oligomer MH569 containing deoxy-5-methyl-cytidine was digested and used as a reference sample for MS fragmentation experiments. For ribo-5-methyl-cytidine a commercial nucleoside was used (Sigma-Aldrich, St. Louis, US).

The digested RNA was analyzed on an Agilent 1260 series equipped with a diode array detector (DAD) and Triple Quadrupol mass spectrometer Agilent 6460. A Synergy Fusion RP column (4 µm particle size, 80 Å pore size, 250 mm length, 2 mm inner diameter) from Phenomenex (Aschaffenburg, Germany) was used at 35 °C. The solvents consisted of 5 mM ammonium acetate buffer adjusted to pH 5.3 using acetic acid (solvent A) and pure acetonitrile (solvent B). The elution started with 100% solvent A followed by a linear gradient to 20% solvent B at 10 min. Initial conditions were regenerated by rinsing with 100% solvent A for 7 minutes. The flow rate was 0.5 mL/min.

The effluent from the column was first measured photometrical at 254 nm by the DAD followed by the mass spectrometer equipped with an electrospray ion source (Agilent Jet Stream). ESI parameters were as follows: gas temperature 300°C, Gas flow 5 L/min, Nebulizer pressure 35 psi, Sheath gas temperature 350°C, Sheath gas flow 12 L/min, capillary voltage 3500 V. The MS was operated in positive ion mode monitoring multiple fragmentation reactions (MRM mode) at previously optimized conditions. The transitions and retention times used for identification of nucleosides can be found in Table 4.

Table 4: Mass transition for MRM and retention times in LC-MS analysis.

Nucleoside	Precursor ion [m/z]	Product ion [m/z]	Retention time [min]
ribocytidine (C)	244	112	2.8
ribouridine	245.2	113	3.7
deoxycytidine (dC)	228	112	4.0
ribomethylcytidine (rm^{5}C)	258.1	126.1	5.1
deoxymethylcytidine (dm^{5}C)	242	126.1	6.0
adenosine	268	136	7.5

6.2.12 Immunostimulation and hINF-α-ELISA

The following experiments were carried out by the group of Prof. Dr. A. Dalpke at the Hygiene Institute, University of Heidelberg.

Human PBMCs were isolated from heparinized blood of healthy donors by standard Ficoll-Hypaque density-gradient centrifugation (Bicoll 1.078 g/ml). PBMCs were filtered through a 100 µm cell strainer and resuspended in complete medium prepared of RPMI 1640 supplemented with heat-inactivated (1h, 56°C) 2% autologous serum. Cells were plated at $4x10^5$cells/well in a 96-well flat bottom plate. 1 µgtRNA sample was diluted in a volume of 5 µl. The RNA was encapsulated with 2.5 µl of 1 mg/ml DOTAP (*N*-[1-(2, 3-dioleoyloxy)propyl]-*N*, *N*, *N*-trimethylammoniummethylsulfate) by mixing with serum-free medium and incubation for 10 min. PBMCs were stimulated in a humidified 5% CO_2atmosphere at 37°C for 16 h. As internal positive control PBMCs were stimulated with the TLR9-specific stimulus CpG2216 (1 µM). Cell-free supernatant was analyzed for secretion of IFN-α using a sandwich ELISA (Bender MedSystems, Vienna, Austria).

Statistical analysis

Data were analyzed by GraphPad Prism 5 program. Significant differences were assessed by analysis of variance (ANOVA) to compare groups followed by Bonferroni post-tests. In all figures the p-value is indicated by * for $p < 0.05$, ** for $p < 0.01$ and *** for $p < 0.001$.

7 References

1.   Hoagland, M.B., Stephenson, M.L., Scott, J.F., Hecht, L.I. and Zamecnik, P.C. (1958) A soluble ribonucleic acid intermediate in protein synthesis. *The Journal of biological chemistry*, **231**, 241-257.

2.   Holley, R.W., Apgar, J., Everett, G.A., Madison, J.T., Marquisee, M., Merrill, S.H., Penswick, J.R. and Zamir, A. (1965) Structure of a Ribonucleic Acid. *Science*, **147**, 1462-1465.

3.   Giegé, R. and Frugier, M. (2009) Transfer RNA structure and identity. *Madame Curie Bioscience Database [Internet]*.

4.   Dirnheimer, G., Keith, G., Dumas, P. and Westhof, E. (1995) In Söll, D. and RajBhandary, U. L. (eds.), *tRNA: Structure, biosynthesis and function*. American Society for Microbiology, Washington, DC, pp. 93-126.

5.   Grosjean, H. (ed.) (2005) *Fine-Tuning of RNA Functions by Modification and Editing*. Springer-Verlag, Berlin Heidelberg.

6.   Machnicka, M.A., Milanowska, K., Osman Oglou, O., Purta, E., Kurkowska, M., Olchowik, A., Januszewski, W., Kalinowski, S., Dunin-Horkawicz, S., Rother, K.M. *et al.* (2013) MODOMICS: a database of RNA modification pathways--2013 update. *Nucleic acids research*, **41**, D262-267.

7.   Davis, D.R. (1998) In Grosjean, H. and Benne, R. (eds.), *Modification and Editing of RNA*. ASM Press, Washington, D.C.

8.   Helm, M. (2006) Post-transcriptional nucleotide modification and alternative folding of RNA. *Nucleic acids research*, **34**, 721-733.

9.   Motorin, Y. and Helm, M. (2010) tRNA stabilization by modified nucleotides. *Biochemistry*, **49**, 4934-4944.

10.   Yoder, J.A. and Bestor, T.H. (1998) A candidate mammalian DNA methyltransferase related to pmt1p of fission yeast. *Human molecular genetics*, **7**, 279-284.

11.   Goll, M.G. and Bestor, T.H. (2005) Eukaryotic cytosine methyltransferases. *Annual review of biochemistry*, **74**, 481-514.

12.   Okano, M., Xie, S. and Li, E. (1998) Dnmt2 is not required for de novo and maintenance methylation of viral DNA in embryonic stem cells. *Nucleic acids research*, **26**, 2536-2540.

13.   Goll, M.G., Kirpekar, F., Maggert, K.A., Yoder, J.A., Hsieh, C.L., Zhang, X., Golic, K.G., Jacobsen, S.E. and Bestor, T.H. (2006) Methylation of tRNAAsp by the DNA methyltransferase homolog Dnmt2. *Science*, **311**, 395-398.

14.   Hermann, A., Schmitt, S. and Jeltsch, A. (2003) The human Dnmt2 has residual DNA-(cytosine-C5) methyltransferase activity. *The Journal of biological chemistry*, **278**, 31717-31721.

15.   Raddatz, G., Guzzardo, P.M., Olova, N., Fantappie, M.R., Rampp, M., Schaefer, M., Reik, W., Hannon, G.J. and Lyko, F. (2013) Dnmt2-dependent methylomes lack defined DNA methylation patterns. *Proceedings of the National Academy of Sciences of the United States of America*, **110**, 8627-8631.

16.   Phalke, S., Nickel, O., Walluscheck, D., Hortig, F., Onorati, M.C. and Reuter, G. (2009) Retrotransposon silencing and telomere integrity in somatic cells of Drosophila depends on the cytosine-5 methyltransferase DNMT2. *Nature genetics*, **41**, 696-702.

17. Schaefer, M. and Lyko, F. (2010) Lack of evidence for DNA methylation of Invader4 retroelements in Drosophila and implications for Dnmt2-mediated epigenetic regulation. *Nature genetics*, **42**, 920-921; author reply 921.

18. Rai, K., Chidester, S., Zavala, C.V., Manos, E.J., James, S.R., Karpf, A.R., Jones, D.A. and Cairns, B.R. (2007) Dnmt2 functions in the cytoplasm to promote liver, brain, and retina development in zebrafish. *Genes & development*, **21**, 261-266.

19. Jurkowski, T.P., Meusburger, M., Phalke, S., Helm, M., Nellen, W., Reuter, G. and Jeltsch, A. (2008) Human DNMT2 methylates tRNA(Asp) molecules using a DNA methyltransferase-like catalytic mechanism. *Rna*, **14**, 1663-1670.

20. Jeltsch, A., Nellen, W. and Lyko, F. (2006) Two substrates are better than one: dual specificities for Dnmt2 methyltransferases. *Trends in biochemical sciences*, **31**, 306-308.

21. Bujnicki, J.M., Feder, M., Ayres, C.L. and Redman, K.L. (2004) Sequence-structure-function studies of tRNA:m5C methyltransferase Trm4p and its relationship to DNA:m5C and RNA:m5U methyltransferases. *Nucleic acids research*, **32**, 2453-2463.

22. Tuorto, F., Liebers, R., Musch, T., Schaefer, M., Hofmann, S., Kellner, S., Frye, M., Helm, M., Stoecklin, G. and Lyko, F. (2012) RNA cytosine methylation by Dnmt2 and NSun2 promotes tRNA stability and protein synthesis. *Nature structural & molecular biology*, **19**, 900-905.

23. Becker, M., Muller, S., Nellen, W., Jurkowski, T.P., Jeltsch, A. and Ehrenhofer-Murray, A.E. (2012) Pmt1, a Dnmt2 homolog in Schizosaccharomyces pombe, mediates tRNA methylation in response to nutrient signaling. *Nucleic acids research*, **40**, 11648-11658.

24. Muller, S., Windhof, I.M., Maximov, V., Jurkowski, T., Jeltsch, A., Forstner, K.U., Sharma, C.M., Graf, R. and Nellen, W. (2013) Target recognition, RNA methylation activity and transcriptional regulation of the Dictyostelium discoideum Dnmt2-homologue (DnmA). *Nucleic acids research*, **41**, 8615-8627.

25. Schaefer, M., Pollex, T., Hanna, K. and Lyko, F. (2009) RNA cytosine methylation analysis by bisulfite sequencing. *Nucleic acids research*, **37**, e12.

26. Schaefer, M., Pollex, T., Hanna, K., Tuorto, F., Meusburger, M., Helm, M. and Lyko, F. (2010) RNA methylation by Dnmt2 protects transfer RNAs against stress-induced cleavage. *Genes & development*, **24**, 1590-1595.

27. Shanmugam, R., Aklujkar, M., Schafer, M., Reinhardt, R., Nickel, O., Reuter, G., Lovley, D.R., Ehrenhofer-Murray, A., Nellen, W., Ankri, S. *et al.* (2014) The Dnmt2 RNA methyltransferase homolog of Geobacter sulfurreducens specifically methylates tRNA-Glu. *Nucleic acids research*, **42**, 6487-6496.

28. Burgess, A.L., David, R. and Searle, I.R. (2015) Conservation of tRNA and rRNA 5-methylcytosine in the kingdom Plantae. *BMC plant biology*, **15**, 199.

29. Persson, B.C., Jager, G. and Gustafsson, C. (1997) The spoU gene of Escherichia coli, the fourth gene of the spoT operon, is essential for tRNA (Gm18) 2'-O-methyltransferase activity. *Nucleic acids research*, **25**, 4093-4097.

30. Hori, H., Yamazaki, N., Matsumoto, T., Watanabe, Y., Ueda, T., Nishikawa, K., Kumagai, I. and Watanabe, K. (1998) Substrate recognition of tRNA (Guanosine-2'-)-methyltransferase from Thermus thermophilus HB27. *The Journal of biological chemistry*, **273**, 25721-25727.

31. Hori, H., Kubota, S., Watanabe, K., Kim, J.M., Ogasawara, T., Sawasaki, T. and Endo, Y. (2003) Aquifex aeolicus tRNA (Gm18) methyltransferase has

unique substrate specificity. TRNA recognition mechanism of the enzyme. *The Journal of biological chemistry*, **278**, 25081-25090.

32. Cavaille, J., Chetouani, F. and Bachellerie, J.P. (1999) The yeast Saccharomyces cerevisiae YDL112w ORF encodes the putative 2'-O-ribose methyltransferase catalyzing the formation of Gm18 in tRNAs. *Rna*, **5**, 66-81.

33. Juhling, F., Morl, M., Hartmann, R.K., Sprinzl, M., Stadler, P.F. and Putz, J. (2009) tRNAdb 2009: compilation of tRNA sequences and tRNA genes. *Nucleic acids research*, **37**, D159-162.

34. Gehrig, S., Eberle, M.E., Botschen, F., Rimbach, K., Eberle, F., Eigenbrod, T., Kaiser, S., Holmes, W.M., Erdmann, V.A., Sprinzl, M. *et al.* (2012) Identification of modifications in microbial, native tRNA that suppress immunostimulatory activity. *The Journal of experimental medicine*, **209**, 225-233.

35. Akira, S., Uematsu, S. and Takeuchi, O. (2006) Pathogen recognition and innate immunity. *Cell*, **124**, 783-801.

36. Janeway, C.A., Jr. (1989) Approaching the asymptote? Evolution and revolution in immunology. *Cold Spring Harbor symposia on quantitative biology*, **54 Pt 1**, 1-13.

37. Akira, S., Takeda, K. and Kaisho, T. (2001) Toll-like receptors: critical proteins linking innate and acquired immunity. *Nature immunology*, **2**, 675-680.

38. Takeda, K., Kaisho, T. and Akira, S. (2003) Toll-like receptors. *Annual review of immunology*, **21**, 335-376.

39. Takeda, K. and Akira, S. (2005) Toll-like receptors in innate immunity. *International immunology*, **17**, 1-14.

40. Theofilopoulos, A.N., Baccala, R., Beutler, B. and Kono, D.H. (2005) Type I interferons (alpha/beta) in immunity and autoimmunity. *Annual review of immunology*, **23**, 307-336.

41. Anderson, K.V., Jurgens, G. and Nusslein-Volhard, C. (1985) Establishment of dorsal-ventral polarity in the Drosophila embryo: genetic studies on the role of the Toll gene product. *Cell*, **42**, 779-789.

42. Anderson, K.V., Bokla, L. and Nusslein-Volhard, C. (1985) Establishment of dorsal-ventral polarity in the Drosophila embryo: the induction of polarity by the Toll gene product. *Cell*, **42**, 791-798.

43. Morisato, D. and Anderson, K.V. (1994) The spatzle gene encodes a component of the extracellular signaling pathway establishing the dorsal-ventral pattern of the Drosophila embryo. *Cell*, **76**, 677-688.

44. Lemaitre, B., Nicolas, E., Michaut, L., Reichhart, J.M. and Hoffmann, J.A. (1996) The dorsoventral regulatory gene cassette spatzle/Toll/cactus controls the potent antifungal response in Drosophila adults. *Cell*, **86**, 973-983.

45. Medzhitov, R., Preston-Hurlburt, P. and Janeway, C.A., Jr. (1997) A human homologue of the Drosophila Toll protein signals activation of adaptive immunity. *Nature*, **388**, 394-397.

46. O'Neill, L.A., Golenbock, D. and Bowie, A.G. (2013) The history of Toll-like receptors - redefining innate immunity. *Nature reviews. Immunology*, **13**, 453-460.

47. Kawai, T. and Akira, S. (2010) The role of pattern-recognition receptors in innate immunity: update on Toll-like receptors. *Nature immunology*, **11**, 373-384.

48. Ozinsky, A., Underhill, D.M., Fontenot, J.D., Hajjar, A.M., Smith, K.D., Wilson, C.B., Schroeder, L. and Aderem, A. (2000) The repertoire for pattern recognition of pathogens by the innate immune system is defined by

cooperation between toll-like receptors. *Proceedings of the National Academy of Sciences of the United States of America*, **97**, 13766-13771.

49. Takeuchi, O., Sato, S., Horiuchi, T., Hoshino, K., Takeda, K., Dong, Z., Modlin, R.L. and Akira, S. (2002) Cutting edge: role of Toll-like receptor 1 in mediating immune response to microbial lipoproteins. *Journal of immunology*, **169**, 10-14.

50. Jin, M.S., Kim, S.E., Heo, J.Y., Lee, M.E., Kim, H.M., Paik, S.G., Lee, H. and Lee, J.O. (2007) Crystal structure of the TLR1-TLR2 heterodimer induced by binding of a tri-acylated lipopeptide. *Cell*, **130**, 1071-1082.

51. Takeuchi, O., Kawai, T., Muhlradt, P.F., Morr, M., Radolf, J.D., Zychlinsky, A., Takeda, K. and Akira, S. (2001) Discrimination of bacterial lipoproteins by Toll-like receptor 6. *International immunology*, **13**, 933-940.

52. Kang, J.Y., Nan, X., Jin, M.S., Youn, S.J., Ryu, Y.H., Mah, S., Han, S.H., Lee, H., Paik, S.G. and Lee, J.O. (2009) Recognition of lipopeptide patterns by Toll-like receptor 2-Toll-like receptor 6 heterodimer. *Immunity*, **31**, 873-884.

53. Poltorak, A., He, X., Smirnova, I., Liu, M.Y., Van Huffel, C., Du, X., Birdwell, D., Alejos, E., Silva, M., Galanos, C. *et al.* (1998) Defective LPS signaling in C3H/HeJ and C57BL/10ScCr mice: mutations in Tlr4 gene. *Science*, **282**, 2085-2088.

54. Hoshino, K., Takeuchi, O., Kawai, T., Sanjo, H., Ogawa, T., Takeda, Y., Takeda, K. and Akira, S. (1999) Cutting edge: Toll-like receptor 4 (TLR4)-deficient mice are hyporesponsive to lipopolysaccharide: evidence for TLR4 as the Lps gene product. *Journal of immunology*, **162**, 3749-3752.

55. Qureshi, S.T., Lariviere, L., Leveque, G., Clermont, S., Moore, K.J., Gros, P. and Malo, D. (1999) Endotoxin-tolerant mice have mutations in Toll-like receptor 4 (Tlr4). *The Journal of experimental medicine*, **189**, 615-625.

56. Shimazu, R., Akashi, S., Ogata, H., Nagai, Y., Fukudome, K., Miyake, K. and Kimoto, M. (1999) MD-2, a molecule that confers lipopolysaccharide responsiveness on Toll-like receptor 4. *The Journal of experimental medicine*, **189**, 1777-1782.

57. Schromm, A.B., Lien, E., Henneke, P., Chow, J.C., Yoshimura, A., Heine, H., Latz, E., Monks, B.G., Schwartz, D.A., Miyake, K. *et al.* (2001) Molecular genetic analysis of an endotoxin nonresponder mutant cell line: a point mutation in a conserved region of MD-2 abolishes endotoxin-induced signaling. *The Journal of experimental medicine*, **194**, 79-88.

58. Park, B.S., Song, D.H., Kim, H.M., Choi, B.S., Lee, H. and Lee, J.O. (2009) The structural basis of lipopolysaccharide recognition by the TLR4-MD-2 complex. *Nature*, **458**, 1191-1195.

59. Ohto, U., Fukase, K., Miyake, K. and Shimizu, T. (2012) Structural basis of species-specific endotoxin sensing by innate immune receptor TLR4/MD-2. *Proceedings of the National Academy of Sciences of the United States of America*, **109**, 7421-7426.

60. Hayashi, F., Smith, K.D., Ozinsky, A., Hawn, T.R., Yi, E.C., Goodlett, D.R., Eng, J.K., Akira, S., Underhill, D.M. and Aderem, A. (2001) The innate immune response to bacterial flagellin is mediated by Toll-like receptor 5. *Nature*, **410**, 1099-1103.

61. Uematsu, S., Jang, M.H., Chevrier, N., Guo, Z., Kumagai, Y., Yamamoto, M., Kato, H., Sougawa, N., Matsui, H., Kuwata, H. *et al.* (2006) Detection of pathogenic intestinal bacteria by Toll-like receptor 5 on intestinal CD11c+ lamina propria cells. *Nature immunology*, **7**, 868-874.

62. Uematsu, S., Fujimoto, K., Jang, M.H., Yang, B.G., Jung, Y.J., Nishiyama, M., Sato, S., Tsujimura, T., Yamamoto, M., Yokota, Y. *et al.* (2008) Regulation of humoral and cellular gut immunity by lamina propria dendritic cells expressing Toll-like receptor 5. *Nature immunology*, **9**, 769-776.

63. Yoon, S.I., Kurnasov, O., Natarajan, V., Hong, M., Gudkov, A.V., Osterman, A.L. and Wilson, I.A. (2012) Structural basis of TLR5-flagellin recognition and signaling. *Science*, **335**, 859-864.

64. Hasan, U., Chaffois, C., Gaillard, C., Saulnier, V., Merck, E., Tancredi, S., Guiet, C., Briere, F., Vlach, J., Lebecque, S. *et al.* (2005) Human TLR10 is a functional receptor, expressed by B cells and plasmacytoid dendritic cells, which activates gene transcription through MyD88. *Journal of immunology*, **174**, 2942-2950.

65. Zhang, D., Zhang, G., Hayden, M.S., Greenblatt, M.B., Bussey, C., Flavell, R.A. and Ghosh, S. (2004) A toll-like receptor that prevents infection by uropathogenic bacteria. *Science*, **303**, 1522-1526.

66. Yarovinsky, F., Zhang, D., Andersen, J.F., Bannenberg, G.L., Serhan, C.N., Hayden, M.S., Hieny, S., Sutterwala, F.S., Flavell, R.A., Ghosh, S. *et al.* (2005) TLR11 activation of dendritic cells by a protozoan profilin-like protein. *Science*, **308**, 1626-1629.

67. Andrade, W.A., Souza Mdo, C., Ramos-Martinez, E., Nagpal, K., Dutra, M.S., Melo, M.B., Bartholomeu, D.C., Ghosh, S., Golenbock, D.T. and Gazzinelli, R.T. (2013) Combined action of nucleic acid-sensing Toll-like receptors and TLR11/TLR12 heterodimers imparts resistance to Toxoplasma gondii in mice. *Cell host & microbe*, **13**, 42-53.

68. Koblansky, A.A., Jankovic, D., Oh, H., Hieny, S., Sungnak, W., Mathur, R., Hayden, M.S., Akira, S., Sher, A. and Ghosh, S. (2013) Recognition of profilin by Toll-like receptor 12 is critical for host resistance to Toxoplasma gondii. *Immunity*, **38**, 119-130.

69. Alexopoulou, L., Holt, A.C., Medzhitov, R. and Flavell, R.A. (2001) Recognition of double-stranded RNA and activation of NF-kappaB by Toll-like receptor 3. *Nature*, **413**, 732-738.

70. Choe, J., Kelker, M.S. and Wilson, I.A. (2005) Crystal structure of human toll-like receptor 3 (TLR3) ectodomain. *Science*, **309**, 581-585.

71. Bell, J.K., Askins, J., Hall, P.R., Davies, D.R. and Segal, D.M. (2006) The dsRNA binding site of human Toll-like receptor 3. *Proceedings of the National Academy of Sciences of the United States of America*, **103**, 8792-8797.

72. Liu, L., Botos, I., Wang, Y., Leonard, J.N., Shiloach, J., Segal, D.M. and Davies, D.R. (2008) Structural basis of toll-like receptor 3 signaling with double-stranded RNA. *Science*, **320**, 379-381.

73. Diebold, S.S., Kaisho, T., Hemmi, H., Akira, S. and Reis e Sousa, C. (2004) Innate antiviral responses by means of TLR7-mediated recognition of single-stranded RNA. *Science*, **303**, 1529-1531.

74. Heil, F., Hemmi, H., Hochrein, H., Ampenberger, F., Kirschning, C., Akira, S., Lipford, G., Wagner, H. and Bauer, S. (2004) Species-specific recognition of single-stranded RNA via toll-like receptor 7 and 8. *Science*, **303**, 1526-1529.

75. Lund, J.M., Alexopoulou, L., Sato, A., Karow, M., Adams, N.C., Gale, N.W., Iwasaki, A. and Flavell, R.A. (2004) Recognition of single-stranded RNA viruses by Toll-like receptor 7. *Proceedings of the National Academy of Sciences of the United States of America*, **101**, 5598-5603.

76. Hornung, V., Guenthner-Biller, M., Bourquin, C., Ablasser, A., Schlee, M., Uematsu, S., Noronha, A., Manoharan, M., Akira, S., de Fougerolles, A. *et al.*

(2005) Sequence-specific potent induction of IFN-alpha by short interfering RNA in plasmacytoid dendritic cells through TLR7. *Nature medicine*, **11**, 263-270.

77. Lee, H.K., Lund, J.M., Ramanathan, B., Mizushima, N. and Iwasaki, A. (2007) Autophagy-dependent viral recognition by plasmacytoid dendritic cells. *Science*, **315**, 1398-1401.

78. Mancuso, G., Gambuzza, M., Midiri, A., Biondo, C., Papasergi, S., Akira, S., Teti, G. and Beninati, C. (2009) Bacterial recognition by TLR7 in the lysosomes of conventional dendritic cells. *Nature immunology*, **10**, 587-594.

79. Hemmi, H., Takeuchi, O., Kawai, T., Kaisho, T., Sato, S., Sanjo, H., Matsumoto, M., Hoshino, K., Wagner, H., Takeda, K. *et al.* (2000) A Toll-like receptor recognizes bacterial DNA. *Nature*, **408**, 740-745.

80. Lund, J., Sato, A., Akira, S., Medzhitov, R. and Iwasaki, A. (2003) Toll-like receptor 9-mediated recognition of Herpes simplex virus-2 by plasmacytoid dendritic cells. *The Journal of experimental medicine*, **198**, 513-520.

81. Krug, A., French, A.R., Barchet, W., Fischer, J.A., Dzionek, A., Pingel, J.T., Orihuela, M.M., Akira, S., Yokoyama, W.M. and Colonna, M. (2004) TLR9-dependent recognition of MCMV by IPC and DC generates coordinated cytokine responses that activate antiviral NK cell function. *Immunity*, **21**, 107-119.

82. Krug, A., Luker, G.D., Barchet, W., Leib, D.A., Akira, S. and Colonna, M. (2004) Herpes simplex virus type 1 activates murine natural interferon-producing cells through toll-like receptor 9. *Blood*, **103**, 1433-1437.

83. Oldenburg, M., Kruger, A., Ferstl, R., Kaufmann, A., Nees, G., Sigmund, A., Bathke, B., Lauterbach, H., Suter, M., Dreher, S. *et al.* (2012) TLR13 recognizes bacterial 23S rRNA devoid of erythromycin resistance-forming modification. *Science*, **337**, 1111-1115.

84. Hidmark, A., von Saint Paul, A. and Dalpke, A.H. (2012) Cutting edge: TLR13 is a receptor for bacterial RNA. *Journal of immunology*, **189**, 2717-2721.

85. Li, X.D. and Chen, Z.J. (2012) Sequence specific detection of bacterial 23S ribosomal RNA by TLR13. *eLife*, **1**, e00102.

86. Kawai, T. and Akira, S. (2007) Signaling to NF-kappaB by Toll-like receptors. *Trends in molecular medicine*, **13**, 460-469.

87. Gay, N.J. and Keith, F.J. (1991) Drosophila Toll and IL-1 receptor. *Nature*, **351**, 355-356.

88. Bowie, A. and O'Neill, L.A. (2000) The interleukin-1 receptor/Toll-like receptor superfamily: signal generators for pro-inflammatory interleukins and microbial products. *Journal of leukocyte biology*, **67**, 508-514.

89. McKenna, K., Beignon, A.S. and Bhardwaj, N. (2005) Plasmacytoid dendritic cells: linking innate and adaptive immunity. *Journal of virology*, **79**, 17-27.

90. Colonna, M., Trinchieri, G. and Liu, Y.J. (2004) Plasmacytoid dendritic cells in immunity. *Nature immunology*, **5**, 1219-1226.

91. Liu, Y.J. (2005) IPC: professional type 1 interferon-producing cells and plasmacytoid dendritic cell precursors. *Annual review of immunology*, **23**, 275-306.

92. Hemmi, H., Kaisho, T., Takeuchi, O., Sato, S., Sanjo, H., Hoshino, K., Horiuchi, T., Tomizawa, H., Takeda, K. and Akira, S. (2002) Small anti-viral compounds activate immune cells via the TLR7 MyD88-dependent signaling pathway. *Nature immunology*, **3**, 196-200.

93. Jurk, M., Heil, F., Vollmer, J., Schetter, C., Krieg, A.M., Wagner, H., Lipford, G. and Bauer, S. (2002) Human TLR7 or TLR8 independently confer responsiveness to the antiviral compound R-848. *Nature immunology*, **3**, 499.

94. Heil, F., Ahmad-Nejad, P., Hemmi, H., Hochrein, H., Ampenberger, F., Gellert, T., Dietrich, H., Lipford, G., Takeda, K., Akira, S. *et al.* (2003) The Toll-like receptor 7 (TLR7)-specific stimulus loxoribine uncovers a strong relationship within the TLR7, 8 and 9 subfamily. *European journal of immunology*, **33**, 2987-2997.

95. Lee, J., Chuang, T.H., Redecke, V., She, L., Pitha, P.M., Carson, D.A., Raz, E. and Cottam, H.B. (2003) Molecular basis for the immunostimulatory activity of guanine nucleoside analogs: activation of Toll-like receptor 7. *Proceedings of the National Academy of Sciences of the United States of America*, **100**, 6646-6651.

96. Colak, E., Leslie, A., Zausmer, K., Khatamzas, E., Kubarenko, A.V., Pichulik, T., Klimosch, S.N., Mayer, A., Siggs, O., Hector, A. *et al.* (2014) RNA and imidazoquinolines are sensed by distinct TLR7/8 ectodomain sites resulting in functionally disparate signaling events. *Journal of immunology*, **192**, 5963-5973.

97. Akira, S. and Takeda, K. (2004) Toll-like receptor signalling. *Nature reviews. Immunology*, **4**, 499-511.

98. Li, S., Strelow, A., Fontana, E.J. and Wesche, H. (2002) IRAK-4: a novel member of the IRAK family with the properties of an IRAK-kinase. *Proceedings of the National Academy of Sciences of the United States of America*, **99**, 5567-5572.

99. Deng, L., Wang, C., Spencer, E., Yang, L., Braun, A., You, J., Slaughter, C., Pickart, C. and Chen, Z.J. (2000) Activation of the IkappaB kinase complex by TRAF6 requires a dimeric ubiquitin-conjugating enzyme complex and a unique polyubiquitin chain. *Cell*, **103**, 351-361.

100. Bradley, J.R. and Pober, J.S. (2001) Tumor necrosis factor receptor-associated factors (TRAFs). *Oncogene*, **20**, 6482-6491.

101. Adhikari, A., Xu, M. and Chen, Z.J. (2007) Ubiquitin-mediated activation of TAK1 and IKK. *Oncogene*, **26**, 3214-3226.

102. Chen, F., Bhatia, D., Chang, Q. and Castranova, V. (2006) Finding NEMO by K63-linked polyubiquitin chain. *Cell death and differentiation*, **13**, 1835-1838.

103. Yamaguchi, K., Shirakabe, K., Shibuya, H., Irie, K., Oishi, I., Ueno, N., Taniguchi, T., Nishida, E. and Matsumoto, K. (1995) Identification of a member of the MAPKKK family as a potential mediator of TGF-beta signal transduction. *Science*, **270**, 2008-2011.

104. Shibuya, H., Yamaguchi, K., Shirakabe, K., Tonegawa, A., Gotoh, Y., Ueno, N., Irie, K., Nishida, E. and Matsumoto, K. (1996) TAB1: an activator of the TAK1 MAPKKK in TGF-beta signal transduction. *Science*, **272**, 1179-1182.

105. Takaesu, G., Kishida, S., Hiyama, A., Yamaguchi, K., Shibuya, H., Irie, K., Ninomiya-Tsuji, J. and Matsumoto, K. (2000) TAB2, a novel adaptor protein, mediates activation of TAK1 MAPKKK by linking TAK1 to TRAF6 in the IL-1 signal transduction pathway. *Molecular cell*, **5**, 649-658.

106. Ishitani, T., Takaesu, G., Ninomiya-Tsuji, J., Shibuya, H., Gaynor, R.B. and Matsumoto, K. (2003) Role of the TAB2-related protein TAB3 in IL-1 and TNF signaling. *The EMBO journal*, **22**, 6277-6288.

107. Cheung, P.C., Nebreda, A.R. and Cohen, P. (2004) TAB3, a new binding partner of the protein kinase TAK1. *The Biochemical journal*, **378**, 27-34.

108. Wang, C., Deng, L., Hong, M., Akkaraju, G.R., Inoue, J. and Chen, Z.J. (2001) TAK1 is a ubiquitin-dependent kinase of MKK and IKK. *Nature*, **412**, 346-351.

109. Hayden, M.S., West, A.P. and Ghosh, S. (2006) NF-kappaB and the immune response. *Oncogene*, **25**, 6758-6780.

110. Honda, K., Yanai, H., Mizutani, T., Negishi, H., Shimada, N., Suzuki, N., Ohba, Y., Takaoka, A., Yeh, W.C. and Taniguchi, T. (2004) Role of a transductional-transcriptional processor complex involving MyD88 and IRF-7 in Toll-like receptor signaling. *Proceedings of the National Academy of Sciences of the United States of America*, **101**, 15416-15421.

111. Kawai, T., Sato, S., Ishii, K.J., Coban, C., Hemmi, H., Yamamoto, M., Terai, K., Matsuda, M., Inoue, J., Uematsu, S. *et al.* (2004) Interferon-alpha induction through Toll-like receptors involves a direct interaction of IRF7 with MyD88 and TRAF6. *Nature immunology*, **5**, 1061-1068.

112. Uematsu, S., Sato, S., Yamamoto, M., Hirotani, T., Kato, H., Takeshita, F., Matsuda, M., Coban, C., Ishii, K.J., Kawai, T. *et al.* (2005) Interleukin-1 receptor-associated kinase-1 plays an essential role for Toll-like receptor (TLR)7- and TLR9-mediated interferon-{alpha} induction. *The Journal of experimental medicine*, **201**, 915-923.

113. Hoshino, K., Sugiyama, T., Matsumoto, M., Tanaka, T., Saito, M., Hemmi, H., Ohara, O., Akira, S. and Kaisho, T. (2006) IkappaB kinase-alpha is critical for interferon-alpha production induced by Toll-like receptors 7 and 9. *Nature*, **440**, 949-953.

114. Hacker, H., Redecke, V., Blagoev, B., Kratchmarova, I., Hsu, L.C., Wang, G.G., Kamps, M.P., Raz, E., Wagner, H., Hacker, G. *et al.* (2006) Specificity in Toll-like receptor signalling through distinct effector functions of TRAF3 and TRAF6. *Nature*, **439**, 204-207.

115. Oganesyan, G., Saha, S.K., Guo, B., He, J.Q., Shahangian, A., Zarnegar, B., Perry, A. and Cheng, G. (2006) Critical role of TRAF3 in the Toll-like receptor-dependent and -independent antiviral response. *Nature*, **439**, 208-211.

116. Koski, G.K., Kariko, K., Xu, S., Weissman, D., Cohen, P.A. and Czerniecki, B.J. (2004) Cutting edge: innate immune system discriminates between RNA containing bacterial versus eukaryotic structural features that prime for high-level IL-12 secretion by dendritic cells. *Journal of immunology*, **172**, 3989-3993.

117. Kariko, K., Buckstein, M., Ni, H. and Weissman, D. (2005) Suppression of RNA recognition by Toll-like receptors: the impact of nucleoside modification and the evolutionary origin of RNA. *Immunity*, **23**, 165-175.

118. Eberle, F., Giessler, K., Deck, C., Heeg, K., Peter, M., Richert, C. and Dalpke, A.H. (2008) Modifications in small interfering RNA that separate immunostimulation from RNA interference. *Journal of immunology*, **180**, 3229-3237.

119. Hamm, S., Latz, E., Hangel, D., Muller, T., Yu, P., Golenbock, D., Sparwasser, T., Wagner, H. and Bauer, S. (2010) Alternating 2'-O-ribose methylation is a universal approach for generating non-stimulatory siRNA by acting as TLR7 antagonist. *Immunobiology*, **215**, 559-569.

120. Robbins, M., Judge, A., Liang, L., McClintock, K., Yaworski, E. and MacLachlan, I. (2007) 2'-O-methyl-modified RNAs act as TLR7 antagonists. *Molecular therapy : the journal of the American Society of Gene Therapy*, **15**, 1663-1669.

121. Sioud, M., Furset, G. and Cekaite, L. (2007) Suppression of immunostimulatory siRNA-driven innate immune activation by 2'-modified RNAs. *Biochemical and biophysical research communications*, **361**, 122-126.

122. Schmid, K., Thuring, K., Keller, P., Ochel, A., Kellner, S. and Helm, M. (2015) Variable presence of 5-methylcytosine in commercial RNA and DNA. *RNA biology*, **12**, 1152-1158.

123. Jurkowski, T.P., Shanmugam, R., Helm, M. and Jeltsch, A. (2012) Mapping the tRNA binding site on the surface of human DNMT2 methyltransferase. *Biochemistry*, **51**, 4438-4444.

124. Motorin, Y., Burhenne, J., Teimer, R., Koynov, K., Willnow, S., Weinhold, E. and Helm, M. (2011) Expanding the chemical scope of RNA:methyltransferases to site-specific alkynylation of RNA for click labeling. *Nucleic acids research*, **39**, 1943-1952.

125. Willnow, S., Martin, M., Luscher, B. and Weinhold, E. (2012) A selenium-based click AdoMet analogue for versatile substrate labeling with wild-type protein methyltransferases. *Chembiochem : a European journal of chemical biology*, **13**, 1167-1173.

126. Tomkuviene, M., Clouet-d'Orval, B., Cerniauskas, I., Weinhold, E. and Klimasauskas, S. (2012) Programmable sequence-specific click-labeling of RNA using archaeal box C/D RNP methyltransferases. *Nucleic acids research*, **40**, 6765-6773.

127. Kim, S.H., Suddath, F.L., Quigley, G.J., McPherson, A., Sussman, J.L., Wang, A.H., Seeman, N.C. and Rich, A. (1974) Three-dimensional tertiary structure of yeast phenylalanine transfer RNA. *Science*, **185**, 435-440.

128. Kaiser, S., Rimbach, K., Eigenbrod, T., Dalpke, A.H. and Helm, M. (2014) A modified dinucleotide motif specifies tRNA recognition by TLR7. *Rna*, **20**, 1351-1355.

129. Jurkowski, T.P. and Jeltsch, A. (2011) On the evolutionary origin of eukaryotic DNA methyltransferases and Dnmt2. *PloS one*, **6**, e28104.

130. Yamasaki, S., Ivanov, P., Hu, G.F. and Anderson, P. (2009) Angiogenin cleaves tRNA and promotes stress-induced translational repression. *The Journal of cell biology*, **185**, 35-42.

131. Muller, M., Hartmann, M., Schuster, I., Bender, S., Thuring, K.L., Helm, M., Katze, J.R., Nellen, W., Lyko, F. and Ehrenhofer-Murray, A.E. (2015) Dynamic modulation of Dnmt2-dependent tRNA methylation by the micronutrient queuine. *Nucleic acids research*.

132. Gantier, M.P., Tong, S., Behlke, M.A., Irving, A.T., Lappas, M., Nilsson, U.W., Latz, E., McMillan, N.A. and Williams, B.R. (2010) Rational design of immunostimulatory siRNAs. *Molecular therapy : the journal of the American Society of Gene Therapy*, **18**, 785-795.

133. Guiducci, C., Gong, M., Xu, Z., Gill, M., Chaussabel, D., Meeker, T., Chan, J.H., Wright, T., Punaro, M., Bolland, S. *et al.* (2010) TLR recognition of self nucleic acids hampers glucocorticoid activity in lupus. *Nature*, **465**, 937-941.

134. Hengesbach, M., Meusburger, M., Lyko, F. and Helm, M. (2008) Use of DNAzymes for site-specific analysis of ribonucleotide modifications. *Rna*, **14**, 180-187.

135. Eigenbrod, T., Keller, P., Kaiser, S., Rimbach, K., Dalpke, A.H. and Helm, M. (2015) Recognition of Specified RNA Modifications by the Innate Immune System. *Methods in enzymology*, **560**, 73-89.

136. Tovy, A., Hofmann, B., Helm, M. and Ankri, S. (2010) In vitro tRNA methylation assay with the Entamoeba histolytica DNA and tRNA

methyltransferase Dnmt2 (Ehmeth) enzyme. *Journal of visualized experiments : JoVE*.

137. Kellner, S., Seidu-Larry, S., Burhenne, J., Motorin, Y. and Helm, M. (2011) A multifunctional bioconjugate module for versatile photoaffinity labeling and click chemistry of RNA. *Nucleic acids research*, **39**, 7348-7360.

List of Publications

Identification of modifications in microbial, native tRNA that suppress immunostimulatory activity.

Gehrig S, Eberle ME, Botschen F, Rimbach K, Eberle F, Eigenbrod T, Kaiser S, Holmes WM, Erdmann VA, Sprinzl M, Bec G, Keith G, Dalpke AH, Helm M.

J. Exp. Med., 2012.

A modified dinucleotide motif specifies tRNA recognition by TLR7.

Steffen Kaiser, Katharina Rimbach, Tatjana Eigenbrod, Alexander H. Dalpke and Mark Helm

RNA, 2014

2'-O-Methylation within Bacterial RNA Acts as Suppressor of TLR7/TLR8 Activation in Human Innate Immune Cells

Katharina Rimbach, Steffen Kaiser, Mark Helm, Alexander H. Dalpke and Tatjana Eigenbrod

J. Innate Immun., 2015

Recognition of Specified RNA Modifications by the Innate Immune System.

Eigenbrod T, Keller P, Kaiser S, Rimbach K, Dalpke AH, Helm M.

Methods Enzymol., 2015

Cytosine methylation of tRNA-Asp by DNMT2 has a role in translation of proteins containing poly-Asp sequences.

Raghuvaran Shanmugam, Jacob Fierer, Steffen Kaiser, Mark Helm, Tomasz P Jurkowski & Albert Jeltsch

Cell Discovery, 2015

Curriculum Vitae